IMPLICATIONS OF HETEROZYGOUS LOSS-OF-FUNCTION OF PAX6 IN THE BRAIN: A CROSS-SPECIES EVALUATION OF NEUROANATOMY

by

MADISON K. GRANT

(Under the Direction of James D. Lauderdale)

ABSTRACT

The paired-box 6 (*PAX6*) gene encodes a highly-conserved transcription factor necessary for normal development of both the eye and the central nervous system. PAX6 has been implicated in aspects of central nervous system development such as patterning, regionalization, and the formation of neural circuits; however, PAX6's role in the adult brain has yet to be described. Heterozygous loss-of-function mutations to *PAX6* result in a disorder called aniridia in humans and the *Small eye* phenotype in mice. Aniridia is a congenital and progressive disorder most well-known for its ocular phenotypes including absence or hypoplasia of the iris, for which it is named. Although the disorder is best-known for its ocular phenotypes, the condition has a several other abnormalities, which are only recently emerging as prominent features of the disorder. These include neural, sensory, cognitive, and auditory processing abnormalities. These abnormalities are likely caused by either developmental deficits within the brain or maintenance related problems in the adult brain. There has been little homogeneity within brain-related aniridia research, and a wide-variety of structural changes with much variation across the population have been described. The work presented here aimed to investigate the structural abnormalities in the brains of both aniridia patients and our mouse model of the disorder using

high-resolution structural MRI. Through analysis of a new cohort of aniridia patients, representing a variety of aniridia-causing mutations, we showed that the structural changes to the aniridia brains are highly variable and less severe than previously reported. We also investigated structural changes in the brain of our mouse model of the disorder, *Small eye* (*Pax6*$^{SeyNeu/+}$), and found similar results using structural MRI and histology. Our mice had strikingly normal brains with all structures still present and only slight reductions in volume and commissure thickness. We did, however, discover an age-related change in the plasticity of the *Pax6*$^{SeyNeu/+}$ brains, suggesting a role of Pax6 during adult brain neurogenesis and maintenance. Together, these studies contribute to our understanding of the role of PAX6 in both normal development and maintenance of the adult mammalian brain, and aid in understanding the neurological phenotypes of aniridia patients.

INDEX WORDS: PAX6, MRI, *Small Eye* mouse, neuroanatomy

IMPLICATIONS OF HETEROZYGOUS LOSS-OF-FUNCTION OF PAX6 IN THE BRAIN: A CROSS-SPECIES EVALUATION OF NEUROANATOMY

by

MADISON K. GRANT

BS, Florida State University, 2012

A Dissertation Submitted to the Graduate Faculty of The University of Georgia in Partial Fulfillment of the Requirements for the Degree

DOCTOR OF PHILOSOPHY

ATHENS, GEORGIA

2019

© 2019

Madison K. Grant

All Rights Reserved

IMPLICATIONS OF HETEROZYGOUS LOSS-OF-FUNCTION OF PAX6 IN THE BRAIN: A CROSS-SPECIES EVALUATION OF NEUROANATOMY

by

MADISON K. GRANT

Major Professor:	James D. Lauderdale
Committee:	Scott T. Dougan Douglas B. Menke Peter Kner

Electronic Version Approved:

Suzanne Barbour
Dean of the Graduate School
The University of Georgia
August, 2019

DEDICATION

This dissertation is dedicated to my family and to my friend, Anastasia Bobilev. Without them this would not have been possible. I would like to especially thank my wonderful mother, Janet Grant, and my perfect sister, Kinsey Grant, for everything they have done for me in my life.

ACKNOWLEDGEMENTS

I would like to thank my major professor, Dr. James D. Lauderdale, for his mentorship and guidance through my graduate school career. He has fostered my independence as a scientist, and I truly appreciate his willingness to let me follow my curiosity. I would also like to thank my undergraduate mentor, Dr. James M. Fadool, who is the reason I fell in love with research and the reason I came to graduate school. He made me the curious, enduring, independent researcher I am today, and none of this would have happened without him.

I would like to thank my wonderful committee members for their unending support and help during graduate school. Thank you, Dr. Scott Dougan for always having wonderful ideas about my research and pushing me to think outside the box. Thank you, Dr. Doug Menke for always being there when I have questions. And thank you, Dr. Peter Kner for sharing in microscopy enthusiasm throughout my time as a graduate student during so many different projects. I would also like to thank Dr. Jonathan Eggenschwiler for his constructive and kind feedback during our group lab meetings.

Finally, I would like to thank the wonderful members of the Lauderdale lab who have become family to me. Thank you to past members Dr. Linsey Beebe, Dr. Kenji Johnson and Dr. Ariel VanLeuven for their friendship and advice in the lab. A special thank you to Dr. Anastasia Bobilev, who gave me a chance as a first-year graduate student, and without whom I would not have made it through. Thank you to our wonderful lab technician, Rebecca Ball, who is the sole reason our lab works and has become a wonderful friend during these years. Thank you to my current lab members, Karl Kudyba, Ashley Rasys, Chelsea Gunderson, and Christina Sabin, for

your willingness to help whenever I need it and your friendship. Thank you to my wonderful undergraduate students, Branson Byers and Hannah Schriever. And thank you to Tyler Miyawaki for always listening to me and helping me during the last five years. It has been such a joy to work with you all over the years.

TABLE OF CONTENTS

LIST OF TABLES

Page

LIST OF FIGURES

Page

CHAPTER 1:

INTRODUCTION AND LITERATURE REVIEW

1.1 Introduction to PAX6 and imaging in aniridia

1.1.1 Introduction

An overarching goal of neuroscience is to elucidate the relationships between the structural organization of the brain and its regional and global functioning. Advances in neuroimaging technologies now allow for investigation of both structure and function of the human brain with high resolution; however, most studies are only able to identify correlative rather than causal relationships. Studies in model organisms clearly demonstrate that the structural organization of the brain begins by the appropriate specification of precursor cells in developing germ layers, which expand and differentiate into the many specific cell types required by each brain region. These processes are tightly regulated in time and space by gene regulatory networks composed of large-scale sets of protein interactions acting in concert to convey specific spatial coordinates, instruct identity, and direct appropriate wiring. How these processes ultimately coalesce to knit cells and structures into ensembles and circuits is less clear. Among the most important players in these networks are early transcription factors (TFs) and the networks in which they operate. While much work has been done to identify the pathways, interactions, and target genes of individual brain-specific TFs, most studies address single TFs in isolation. To understand how complex processing circuits can emerge from separate parts, it is necessary to integrate our understanding of TFs into a system-level framework emphasizing

pathways rather than individual proteins. Towards this end, a promising approach is to assess TFs that regulate multiple processes.

While some transcription factors have limited, specific roles in dictating individual developmental programs, others such as the members of the PAX gene family regulate many developmental processes simultaneously. The paired-box 6 (PAX6) gene encodes a highly conserved and essential transcription factor, whose region-specific expression boundaries are key to the establishment of anterior-posterior and dorsal-ventral brain axes. Reduced or altered efficiency of PAX6 function leads to widespread abnormalities in neural organization in addition to ocular, olfactory, and brain-related phenotypes [1–4]. The molecular interactions [5–7], cellular mechanisms [6, 8–10], and developmental roles [6, 11–16] of PAX6 have been reviewed extensively. However, while it is known to act as a master regulatory TF, the networks of genes coordinated by PAX6 in the context of functional neuroanatomy remain poorly understood.

1.1.2 PAX6 gene structure and products

The PAX6 gene spans approximately 22kb located on chromosome 11p13 in humans and chromosome 2 in mice [17, 18]. The PAX6 protein sequence is highly conserved from *Drosophila* to frogs, fish, birds, mice and humans, and also demonstrates high conservation of regulatory and enhancer sequences in vertebrates [9, 19–22]. PAX6 includes 16 exons and three promoter regions (P0, P1, and Pα), which give rise to three isoforms of the PAX6 protein known as canonical PAX6, PAX6(5a), and PAX6(ΔPD) [23, 24]. The canonical isoform contains four functional domains: two DNA binding domains (paired domain and homeodomain) joined by a linker domain, and a proline-serine-threonine rich (PTS) transactivation domain [25–27]. The PAX6 5a isoform contains an additional alternatively spliced 5a exon inserted into the paired domain, which alters DNA binding activity [28]. The last isoform, PAX6(ΔPD), or the paired-

less isoform, is a product of an alternative start site found in the linker domain sequence and lacks the paired domain present in the other two isoforms [29]. The three isoforms are a result of different transcriptional and post-transcriptional regulation and all have distinct DNA binding activities and unique spatiotemporal expression and regulatory profiles during development [23, 28, 30]. The complete understanding of these unique isoform expression profiles and functional properties, especially within the brain, during both development and tissue maintenance are yet to be fully understood and have rarely been studied.

1.1.3 Expression and role of PAX6 in the brain

The highly-conserved transcription factor, *PAX6,* is necessary for normal eye and brain development, and is expressed at high levels during embryonic development within the eye, brain, spinal cord, and pancreas [29]. The regulatory role of PAX6 during development of these structures has been extensively characterized using the mouse model and *Drosophila*, however the functional role of PAX6 during adult brain maintenance and neurogenesis has not been studied to the same extent [8, 31–33]. For the remainder of this body of work I will be using two different versions of the PAX6 nomenclature: *PAX6* and PAX6 represents the human form of the gene and protein respectively, while *Pax6* and Pax6 represents the mouse form of the gene and protein respectively.

During brain development in the mouse, Pax6 is expressed as early as embryonic day 8 (E8) in the ventricular zone of the basal and medial neural tube, with continued expression through development and adulthood [34, 35]. Pax6 expression corresponds highly to boundary formation within the developing brain, and as development continues it is broadly expressed in the mitotic germinal zone, followed by the telencephalon, diencephalon, mesencephalon, and hindbrain [34, 36]. At E11.5 Pax6 is highly expressed in the neuroepithelia of the ventricular

zone within the forebrain and hindbrain and the mesencephalic reticular formation and floor of the midbrain [35]. By E13 Pax6 is expressed in the dorsal forebrain in a rostral to caudal gradient, which creates a boundary at the posterior commissure [36]. Pax6 expression is restricted to the forebrain and hindbrain and absent throughout the midbrain at E12, E14, and postnatal day 1 (P1) [35]. In adulthood Pax6 expression persists in discreet regions, mainly the olfactory bulb, cerebellum, and parts of the cortex although at much lower levels within the tissue than in the developing brain [35]. Pax6 plays an integral role in boundary formation and regionalization within the brain, as evidenced by the strict expression zones within the developing brain.

Although localization of Pax6 expression gives us some understanding of its role during development, we have learned most from loss-of-function, gain-of-function, and transgenic experiments in the mouse model. These genetic tools have uncovered the mechanisms by which Pax6 regulates development and cell-type specification within the brain. Studies using homozygous Pax6 mutant mice showed not only a reduction in the size of the cortical plate, but also showed widespread disruptions to dorso-ventral patterning in the telencephalon and cortical forebrain [14, 37, 38]. These data demonstrate the necessity of Pax6 for patterning and specification of brain regions. The normal distribution of Pax6 within a wild-type developing mouse brain is restricted in a rostral-caudal and dorso-ventral manner, and in homozygous Pax6 mutants this regionalization of expression is disrupted leading to decreased boundary delineation in addition to improper posterior commissure formation [39]. Cells taken from homozygous mutant embryos and transplanted into wild-type embryos also show an inability to properly differentiate into dopaminergic perigloumlar or superficial granule cells [40]. These data taken

together show Pax6 is necessary for boundary formation, regional specification, and cell-specific specification within the developing mouse brain.

At the cellular level, there is evidence for a role of PAX6 in cortical neural progenitor cell division and initial cell fate decisions during early brain development, as well as maintenance of neuron subtypes [36, 41]. Loss-of-function studies have shown that Pax6 plays an important role in cell proliferation, specification of dorsal neurogenic cell fates, and appropriate migration of these neurons within the cortex [42–45]. Pax6's role during corticogenesis has been shown through over-expression and conditional knock-out experiments. Within the cortex, overexpression of Pax6 increases the cell cycle length in apical progenitors and leads to increased neurogenesis [3]. These increases are specific to late stage corticogenesis, during which time the superficial layers of neurons are generated and where Pax6 is most highly expressed. Additionally, the total number of superficial layer neurons is reduced in postnatal mice in the over expression model [3]. Conditional deletion of *Pax6* in the cortex during corticogenesis affects both numbers and specification of late-born neurons in the superficial layers of the cortex [3]. Additionally, conditional cortex-specific knock-out of Pax6 during the onset of neurogenesis showed premature cell cycle exit of early progenitors leading to an increase in early born neuron subsets in the marginal zone and lower layers of the cortex with an almost complete absence of upper layer neurons [2]. Knock-out of Pax6 after the lower layer of neurons of the cortex formed did not show an effect on specification or number of late-born neurons, suggesting that layering defects in Pax6-deficient animals can be attributed to a depletion of the progenitor pool available [2]. Additionally, these cortex knockout mice showed deficits in sensorimotor information integration, hippocampus-dependent short term memory processes, and cortical-dependent long term memory processes [2]. Finally, in cortex-specific

Pax6 knockouts, mice show decreased overall brain volume, olfactory bulb volume, and cortical thickness in addition to disorganization of interhemispheric fiber tracts [46]. These cortex-specific experiments highlight the importance of dosage of Pax6 during cortical development, specifically for the superficial layers, and the necessity of Pax6 for organization of fiber tracts.

In the developing hindbrain Pax6 is expressed in the rhobomeric lip, eventually contributing to the granule cells in the cerebellum [47–49]. Experiments using heterozygous Pax6 mutant mice with a *lacZ* reporter suggest that Pax6 is a regulator of genes necessary for hindbrain identity and segmentation [50]. In homozygous Pax6 mutant mice three of the five precerebellar nuclei do not form correctly, the granule cell layer of the cerebellum is absent, and some of the granule cells are found in ectopic regions within the inferior colliculus [49]. These results demonstrate the necessity of Pax6 within the developing cerebellum for normal organization and neuronal migration, similar to the role Pax6 plays throughout the developing brain.

In humans, PAX6 has been implicated in cell fate decisions for both pyramidal cortical cells (projection neurons) and interneuron differentiation [51]. Additionally, PAX6 plays a role in axon guidance and neural circuitry formation in both local and inter-hemispheric cortico-cortical and cortico-thalamic networks [52–54]. In humans, the functional components of the auditory processing pathway in the brain overlap greatly with the neuronal subtypes and regional connectivity which are dependent on PAX6, though this has not been directly/experimentally determined. Further, mammalian PAX6 expression persists throughout the lifespan in a restricted manner localized to the olfactory bulb, cortex, mitotic sub-ventricular zone and cerebellum [35]. These findings suggest that, through developmental and maintenance

mechanisms, PAX6 plays a critical role in establishing and maintaining normal cognitive and sensory processing circuitry in the brain, including the auditory processing stream.

1.1.4 PAX6-mediated aniridia

PAX6 is a necessary transcription factor for normal eye and brain development in mammals, and heterozygous loss-of-function mutations in PAX6 are causal for the disorder known as aniridia. Aniridia is panocular, congenital, and progressive disorder with an occurrence of approximately 1 in 83,000 live births [55, 56]. Aniridia is best characterized by the lack of or hypoplasia of the iris, for which it is named, in addition to a variety of other ocular abnormalities which culminate in reduced visual acuity [57]. Due to the progressive nature of the disease, individuals usually develop multiple ocular abnormalities such as keratopathy, corneal vascularization and opacification, glaucoma, anterior chamber fibrosis, and cataracts [58–61].

A majority of the mutations to PAX6 associated with aniridia are nonsense mutations, which give rise to a premature termination codon (PTC) [55]. These mutated transcripts are believed to be degraded through nonsense-mediated decay, and therefore lead to PAX6 haploinsufficiency; however, this has yet to be directly tested [62]. Although the majority of research has focused on the eye phenotypes associated with aniridia, recent research has begun to focus on the brain-related changes that occur with the disorder. Within the last few years multiple studies have sought to understand the consequences of losing one functional copy of PAX6 on both brain development and maintenance. These studies include both structural and functional assays such as structural MRI, functional MRI, EEG, and DTI on both the aniridia patient population and the mouse model of the disorder, *Small eye* [63–72].

1.1.5 Animal models

To gain a deeper understanding of the structural and molecular consequences of heterozygous loss-of-function to the PAX6 gene, researchers have turned to the mouse model of aniridia, *Small eye*, for which there are multiple variants. The spontaneously derived *Small eye* (*Sey*) allele consists of a single point mutation, specifically a G>T transversion at c.194 which causes a premature termination codon (PTC) in exon 5 [73–75]. The *Small eye Neuherberg* allele (Sey^{Neu}) is also a single point mutation which was established by an ENU (*N*-ethyl-*N*-nitrosourea) mutagenesis screen [76]. This mutation is also a G>T transversion at the +1 position of intron 10, and causes a splice junction disruption, which leads to an additional 116 nucleotide extension and ultimately a PTC found in the intronic sequence [75]. The *Dickie's Small eye* allele (Sey^{Dey}) is a spontaneous large deletion on chromosome 2 which encompasses *Pax6* and the neighboring *Wt1* locus, originally discovered in 1964 by Dr. Margaret Dickie and later phenotypically characterized [77]. Another large chromosomal deletion of Pax6 is seen in the Sey^{H} allele, which was radiation induced [75, 78]. The Sey^{H} and Sey^{Dey} alleles present the most devastating phenotypic outcomes compared to other *Pax6* mutation strains likely because of the deletion of neighboring coding and regulatory genetic sequence. Homozygous mutants from all three lines do not survive past postnatal day 1 (P1) and demonstrate severe craniofacial and nasal underdevelopment, while heterozygous mutants display the characteristic reduced eye size [31, 75, 79].

By combining brain imaging of aniridia patients and the powerful *Small eye* mouse model, we have begun to understand the structural and functional consequences of heterozygous loss-of-function mutations to the *PAX6* gene. The focus of this review is to highlight recent work regarding neuroanatomical and functional consequences of *PAX6* mutations in humans and model organisms, and to present the study of *PAX6* as a unique opportunity to bridge the gap

between molecular genetic changes and our understanding of their impact on human brain anatomy and physiology on a systems scale.

1.2 Neuroanatomical abnormalities associated with *PAX6* mutations

1.2.1 Neuroanatomical findings in PAX6-mediated aniridia

The primary feature of aniridia is a hypoplastic or absent iris, and persons with aniridia exhibit a number of other ocular as well as pancreatic symptoms which characterize the disorder [80–83]. As mentioned previously, the majority of research within the aniridia field has focused on the eye phenotypes; however, patients report multiple sensory-related phenotypes that are likely due to changes within the central nervous system as a result of loss of functional copy of PAX6. Because of these patient reports, phenotypes associated with the brain are currently a topic of great interest and are becoming a central component in understanding the composite symptoms of aniridia. Structural MRI studies have identified abnormalities in specific brain structures, white matter tracts, and whole neuroanatomical regions in persons with PAX6-mediated aniridia. Pronounced abnormalities in interhemispheric white matter tracts have been observed, including hypoplasia or absence of the anterior commissure, reduction of the posterior commissure, agenesis of the corpus callosum, and atrophy of the optic chiasm [63, 66, 67, 69, 70, 84]. The potential impairment of interhemispheric transfer from the alterations in white matter tracts has been implicated in cognitive processing deficits in working memory and auditory processing [63, 67, 85]. Additionally, discreet structures within the brain have been found to be altered across studies. These include an absence or hypoplasia of the pineal gland, an endocrine gland involved in the regulation of circadian rhythm, reductions to and reduced function of the olfactory bulb, and unilateral polymicrogyria [63, 69, 70, 84, 86]. The pineal

gland reduction or absence, combined with impaired ability to regulate light due to lack of iris, are the likely cause of disordered sleep reported by persons with aniridia [86–88].

Structural MRIs conducted on the aniridia patient population have shown varied changes to structures within the brain. This is in part due to use of both a 1.5-tesla magnet and a 3-testla magnet, with the 3T magnet having almost double the resolution of the 1.5T magnet. This allows for higher resolution imaging, especially of small commissures such as the ones often altered in the population. This resolution difference of the magnet could be a potential explanation for the differences in frequency of abnormality seen among the different studies. In addition to the differences in magnet strength, not all of the studies focused on the same structures, with most of them only focusing on one or two structural changes in the patients. This presents a challenge when comparing findings across studies. Finally, most of the studies reviewed here have examined vastly different aniridia patient populations, which all included many different types of PAX6 mutations. Although there has never been a significant genotype-phenotype correlation made with aniridia, this fact could still contribute to different findings from different groups, especially if modifier effects are a factor in the structural changes seen [89].

Structural MRI of the brain was conducted on 78 patients with ages ranging from 7 years old to 64 years old in 6 separate studies. There are 6 major structures are affected in the highest number of individuals: the anterior commissure, posterior commissure, pineal gland, corpus callosum, optic chiasm, and olfactory bulb. The anterior commissure was by far the most well studied structure with a majority of the studies in this review looking at structural changes to it. The anterior commissure was absent in 28 patients, reduced in 27 patients, normal in 21 patients, and could not be determined in 2 patients [63, 66, 67, 69, 70, 84]. The olfactory bulb was examined in 2 studies and in 38 individuals. It was found to be absent in 2 patients, reduced in 4

patients, and present in 32 patients [69, 70]. The olfactory bulb, which has also been shown to be reduced in the heterozygous and homozygous Pax6 mutant mouse, is connected to the rest of the brain through the olfactory peduncle, which contains the anterior olfactory nucleus [69, 90–92]. The anterior olfactory nucleus (AON) receives direct input from the OB through axons from the lateral olfactory tract, and is a relay point for information, including contacts with the anterior limb of the anterior commissure for regulation of the contralateral portions of the olfactory bulb [91]. Taken together, the reduction to the anterior commissure could be caused in part by a reduction of inputs from the olfactory bulbs. This, however, has yet to be tested experimentally.

The posterior commissure was also a commonly investigated structure with 3 of the studies looking for changes in aniridia patients compared to healthy individuals: a total of 39 patients were screened for abnormalities of the structure. The posterior commissure was absent in 1 individual screened, reduced in 5, normal in 9, and reported as "present" in 24 individuals [63, 70, 84]. Of all the major structures that had abnormalities, the pineal gland had the highest severity of abnormality, and was examined in 39 individuals in 3 studies. It was found absent in 18 patients, reduced in 17 patients, and normal in 4 patients [63, 70, 84]. The corpus callosum was examined in 38 individuals in 4 of the studies. A corpus callosum cyst was identified in 2 patients, it was reduced in 11 patients, and normal in 25 patients [63, 66, 67, 84]. The optic chiasm was also examined, however only in 15 patients in 2 studies. It was found to be reduced in 8 patients and normal in 7 patients [63, 84]. The Mitchell et al. 2003 paper also reported other abnormalities within the brain such as superior temporal polymicrogyria in 2/24 patients, bilateral hippocampal hypoplasia in 1/24 patients, hippocampal fornix hypoplasia in 1/24 patients, and small inferior cerebellar vermis in 2/24 patients [70].

1.2.2 Grey and white matter volumetric changes in patients with aniridia

In addition to discrete structural abnormalities surveyed on an individual level, multiple studies have focused on group-wise volumetric changes in patients with aniridia as compared to *PAX6*-normal individuals. Most of these studies utilized voxel-based morphometry (VBM) to assess volumetric changes on a group-wise level. VBM uses a computational approach to segment white matter and grey matter and compare volumes of both on a grouped basis. Similar to the structural studies discussed, the results in volumetric analyses are also varied across studies. In a quantitative VBM study of PAX6-mediated aniridia conducted by Free *et.al*, the corpus callosum was found to have varying degrees of changes to white matter and surrounding grey matter, specifically related to mutation type [72]. This research group considered the potential difference between truncating PAX6 mutations (haploinsufficiency group) and C-terminal extension mutations, which are thought to have more devastating effects due to the addition on the transactivation domain of the protein. They found an increase in grey matter below the spenium and below and slightly anterior to genu in the PAX6 haploinsufficient and C-terminal extension groups [72]. A decrease in white matter was seen in both the splenium and genu of the corpus callosum for the PAX6 haploinsufficient group, but the decrease was only seen in the genu for the C-terminal extension group [72]. Additionally, the C-terminal extension group had a large increase in white matter concentration above the corpus callosum in both hemispheres, which was not seen in the haploinsufficiency group or in the overall aniridia group analysis [72]. This study reported bilateral increases in cerebellar grey matter volume, increases in ventral occipital cortex volume, and abnormal sulcus orientations in the occipital lobe [72]. The researchers also report increases in grey matter concentration at the anterior and lateral edges of both cerebellar hemispheres for both groups; however, in the haploinsufficiency group

the region of grey matter increase was smaller and slightly more lateral than anterior [72]. Within the cerebellum they also found decreases in grey matter in the inferior cerebellar vermis for both groups [72]. These varying differences seem to indicate that changes in grey matter concentration could be due to a shift of grey matter tissue as a result of loss of white matter instead of increases in absolute grey matter volume or a potential artifact of the particular analysis.

Ellison-Wright *et al.* also used VBM analyses to investigate grey and white matter changes in aniridia patients. They examined seven members of the same family diagnosed with aniridia and cognitive deficits [93]. They showed an increase in grey matter volume to the mostly left side anterior and dorsal cingulate cortex, bilateral cerebellum, bilateral medial temporal lobe structures including hippocampus and parahippocampal gyrus, right ventral striatum, and the right insula [93]. White matter differences between aniridia patient group and healthy comparison group showed extensive bilateral deficits in the anterior and posterior corpus callosum, which extended anteriorly into the frontal lobes and posteriorly into the occipital and parietal lobes [93]. All subjects in this study were from one family, and although they all had clinically diagnosed aniridia, they also presented with cognitive deficits as compared to age and gender-matched controls, specifically significantly lower verbal IQ scores. It is possible that these deficits in IQ are due to changes in brain structure/organization dependent on heterozygous loss-of-function of PAX6; however, it is also possible that these deficits are unrelated, potentially due to other unfound mutations or modifier effects, and this should be considered when interpreting the results. Recently a study using a similar volumetric technique, surface based morphometry, found most strikingly, that there was an age related increase in cortical thinning in aniridia patients as compared to healthy comparisons [71]. The paper showed an

accelerated decrease in cortical thickness in the inferior parietal lobe, prefrontal areas, and premotor areas in both hemispheres [71]. A study using DTI assessed differences in white mater structural integrity in 11 aniridia patients compared to 11 age and gender matched controls and found changes in the aniridia population in the visual tracts and visual pathway [65]. An additional study investigated volume of the pineal gland in patients with PAX6 haploinsufficiency by using a volumetric approach found that PAX6-deficient patients had significantly lower pineal gland volume compared to healthy comparison [86]. However, this study will not be considered in our review of aniridia because 28/37 individuals with PAX6 mutations had WAGR syndrome (Wilms tumor, Aniridia, Genitourinary anomalies, and cognitive impairment), which is caused by a large deletion to chromosome 11 and likely reflects additive or synergistic effects associated with the deletion of other genes with roles in brain development in addition to the PAX6 mutation.

These group-wise comparison results raise the question of how and where PAX6 is involved in brain maintenance throughout the lifetime, and how different types of mutations can contribute to differing structural changes in the brain. These differences, along with the variation seen in individual affected structures, suggest that some neuroanatomical brain abnormalities in aniridia may be consistent in the population, while others may be associated with specific types of mutations. The investigation of this question demands closer inspection of human mutations at the molecular level, as well as the use of model organisms to dissociate conserved PAX6-dependent neuroanatomical abnormalities from mutation-specific or modifier effects that are unique to humans.

1.2.3 Findings from model organisms

Within the aniridia population there is a wide variety of mutations and a range of structural and functional changes within the brain. These changes are likely due to both a direct and an indirect result of loss of one functional copy of *PAX6.* To better understand the abnormalities seen in the human population, many groups have used rodent models of aniridia. Rodent models have long provided a way to study human disorders while having tighter genetic control over the system, and allow for a deeper mechanistic understanding of the consequences of heterozygous loss-of-function of *PAX6.*

The Stoykova group has done a tremendous amount of work studying cortex-specific *Pax6* knock-out mice (*Pax6cKO)* [1, 2, 46]. Using juvenile *Pax6cKO* they found that the KO mice had slightly enlarged caudal cortex areas, reductions to the rostral cortex, and a rostral shift of graded expression in markers of cell identity; however, area-specific thalamocortical and corticofugal projections appeared normal [1]. Their data suggests that knocking out *Pax6* expression in the cortex during neural development does not directly lead to altered thalamocortical or corticofugal area identity, but does however, lead to altered cortical layering [1]. The rostral shift in markers of cell identity fits nicely with the known graded expression of *Pax6* during neural development in which it is expressed in a high-rostral lateral to low-caudal medial expression gradient. Additionally, it was shown that the same mice have premature cell cycle exit of early progenitors, increases to early born neuron subsets in the marginal zone, and an almost complete absence of upper cortical layer neurons [2]. An imaging-based study of these *Pax6cKO* mice used structural MRI, manganese-enhanced MRI, and diffusion tensor imaging (DTI) to show that loss of cortical Pax6 leads to decreased volume of the entire brain, specifically to the olfactory bulb, in addition to major cortical layering defects [46]. DTI and

fiber bundle tracking showed a disorganization of corpus callosum fibers and a lack of interhemispheric connectivity [46]. Few studies have investigated the *Small eye* mutant rodent lines, which better mimic aniridia in humans because of their heterozygosity of the Pax6 mutation. One study used 7T structural MRI on the *rSey*^{2} rat to investigate volumetric changes as compared to wild-type rats [94]. This group employed deformation-based morphometry (DBM) and region-of-interest (ROI) analyses to show volumetric changes in the *rSey*^{2} rats [94]. They showed overall decreases to volume in these rats, specifically to the following brain regions: amygdala, anterior commissure, cingulum, fimbria, optic pathways, neocortex, corpus callosum, olfactory structures, hippocampal formation, diencephalon, and midbrain [94]. The anterior commissure seemed to show a sex-specific decrease with female *rSey*^{2} having a larger decrease in volume than the males [94]. There were no identified areas of increased volume, and the visual areas of the brain showed the largest volume decreases overall [94].

A study from our lab investigated volumetric and structural changes to the *Sey*^{Neu} mouse model of aniridia using structural MRI and histological analysis. The study employed the use of a 7T MRI as well, however whole area volumes were determined using ROI masking for the collected scans. This study also used two different age groups for the mice, a 4-5 month "younger" group and a 12-13 month "older" group of *Sey*^{Neu} mice to investigate age related changes in the mouse model of the disease that could be similar to the age-related effects seen in the human study. Whole-brain analysis using brain weight and volume found no significant changes between *Sey*^{Neu} and wild-type mice across genotype; however, whole brain weight decreased as a result of age in both groups but whole brain volume stayed consistent. This suggests that aging plays a role in density of the brain rather than total volume. Region of interest analysis was conducted for the eyes, olfactory bulbs, cortex, and cerebellum using the

3D MRI scans. Not surprisingly, there was a very significant decrease in eye volume in the *Sey*^{Neu} mice compared to wild-type in both age groups. Additionally, there was a significant decrease in olfactory bulb volume across genotype with the *Sey*^{Neu} mice having a significantly smaller OB volume overall compared to wildtype. Interestingly though, in the wild-type mice, there was an age-related increase in OB volume from the younger age group to the older age group; however, this significant increase was not seen in the *Sey*^{Neu} mice comparing the age groups, with the two *Sey*^{Neu} age groups having virtually identical means. The age-related increase in olfactory bulb volume with age was also seen in another study conducted on olfactory bulb volume in Pax6-deficient mice, and within this paper they too see less of an increase in the *Sey* mouse as it ages compared to wild-type [92]. There was no significant change in cortex volume across genotypes or age for the groups of mice examined. Cerebellum volume showed no significant change in volume between genotypes. Age did seem to be significant to cerebellum volume though, with the wild-type older cohort having significantly smaller total cerebellum volumes than the younger wild-type cohort. Similar to the olfactory bulb data from this study, the *Sey*^{Neu} mice did not show this age-related decrease in volume, with mean volume for the *Sey*^{Neu} mice young and old group being almost identical. The findings in the olfactory bulb and cerebellum suggest that the *Sey*^{Neu} mice may not have the neural plasticity that the wild-type mice do, potentially shedding light on a new role of Pax6 in the adult mouse brain.

Histological measurement analysis from this study examine 5 structures for differences across genotype and age: the optic chiasm, the corpus callosum (anterior, mid, and posterior), the anterior commissure, the posterior commissure, and the dorsal hippocampal commissure. Within the corpus callosum, there are only changes in the anterior portion, not in the middle or posterior corpus callosum. Consistent with other studies and the reduced visual inputs the eye is receiving

as a product of reduced visual acuity, the optic chiasm is significantly thinner in the *Sey*^{Neu} mice compared to wild-type. This change is exacerbated with age. Age plays a role in the thickness of the anterior corpus callosum, with the older wild-type mice having significantly thicker anterior corpus callosum than the younger wild-type mice. This increase in thickness as a result of age is not seen in the *Sey*^{Neu} mice, suggesting that genotype plays a role in the ability to create white matter tracts or maintaining integrity as a function of age. At the younger age group and at the older age group there are significant differences in the anterior corpus callosum when comparing *Sey*^{Neu} to wild-type mice. At 4-5 months of age the *Sey*^{Neu} anterior corpus callosum is actually thicker than the wild-type, with this switching at 12 months with the wild-type having a thicker anterior corpus callosum. Both the middle and posterior corpus callosum show no age or genotype-related changes between the groups. The anterior commissure also had genotype-related changes within this study. At the younger age group, the wild-type and *Sey*^{Neu} mice had virtually identical thickness of the anterior commissure; however, at the older age group the *Sey*^{Neu} anterior commissure was significantly thinner than the wild-type comparison. The posterior commissure and dorsal hippocampal commissure showed no genotype-related changes; however, the dorsal hippocampal commissure did show an age-related increase for both genotypes. These data suggest that the most severe genotype-related changes occur in the more rostral or anterior part of the brain while the more posterior structures are not changed in the *Sey*^{Neu} mice. This fits with our knowledge of the rostral-caudal high-low expression gradient of Pax6 in the developing brain, and could suggest that the changes we see are at least in part due to the developmental reduction in Pax6 protein.

1.3 Functional neuro-abnormalities

Although multiple studies have examined neuroanatomical abnormalities in aniridia, there have been very few that have sought to understand the functional link between these changes and cognitive and sensory processing deficits. Additionally, those that have studied it have been largely correlative in nature. One of the first investigations of functional changes in aniridia patients was a test of olfactory function. The olfactory bulb is a brain region that is highly affected in persons with *PAX6* mutations. Sisodiya and colleagues showed that persons with aniridia had a higher level of hyposmia, or a reduced ability to smell, consistent with reductions in olfactory bulb volume [69]. The Ellison-Wright study from 2004 used functional MRI to test cognitive ability in aniridia patients [93]. They conducted a sentence completion test for both aniridia patients and healthy comparisons which showed a marked difference and attenuation in brain region activated for aniridia patients [93]. In addition to the sentence completion test, the group also used a verbal fluency test to identify differences in brain activation in aniridia patients. For this test they also found a broad attenuation of response in the aniridia group in the left premotor cortex, left dorsal anterior cingulate gyrus, right inferior parietal lobe, right anterior insula, right putamen and caudate nucleus, bilateral thalamus, and midline cerebellum with no areas showing an increase in function [93]. These regions are thought to correspond most consistently with structural abnormalities seen in the left dorsal cingulate gyrus. In two studies, Bamiou and colleagues showed auditory interhemispheric transfer deficits both in children and adults with *PAX6* mutations [66, 67]. Central auditory tests in adults with aniridia showed abnormalities within the aniridia group compared to PAX6-normal comparisons with both increases and decreases observed [66]. The same group conducted similar auditory tests in children and found that children with aniridia had trouble

understanding speech while other noises were occurring as compared to their healthy controls [67]. These auditory processing deficits, despite normal audiograms, seen in the pediatric group of aniridia patients could be due to a decrease in commissure volume such as the decreases seen in the anterior commissure and the corpus callosum or to a difference in structural organization within the brain.

Pierce *et al.* presented a functional assessment of neural activity in the aniridia population using functional MRI (fMRI). This study showed that in resting state functional networks, increases in connectivity representing recruitment of non-traditional neuroanatomical areas were present in persons with aniridia relative to subject-matched controls in the executive control, primary visual and default mode networks [64]. These findings were the first to directly examine brain activity in aniridia, and likely capture the functional consequences of gross neuroanatomical findings and neuronal circuit disruptions, which are not detectable by structural MRI. Prior to the current work, functional neuroimaging measures in the context of cognitive or sensory processing applied to this population remained entirely unexplored.

Electroencephalography (EEG) provides a direct measure of neural activity with incredible temporal sensitivity, and can be implemented in conjunction with stimuli, which selectively target cognitive or sensory processes. A recently published paper employed this technology to investigate the auditory processing deficits seen in the previous aniridia studies (Bobilev,2019). The study provided direct assessment of neural activity related to auditory processing in aniridia. Subjects were presented with tones designed to elicit an auditory steady-state response (aSSR) at 22 Hz, 40 Hz, and 84 Hz, and infrequent broadband target tones to maintain attention during electroencephalography (EEG) recording (Bobilev, 2019). Persons with aniridia showed increased early cortical responses (P50 AEP) in response to all tones and

increased high-frequency oscillatory entrainment (84 Hz aSSR) (Bobilev, 2016). In contrast, the aniridia group showed a decreased cortical integration response (P300 AEP to target tones) and reduced neural entrainment to cortical beta-band stimuli (22 Hz aSSR) (Bobilev, 2019). Collectively, the results suggest that early, subcortical auditory processing is augmented in aniridia, while functional cortical integration of auditory information is deficient in this population, suggesting more wide-spread organizational changes within the brain of aniridia patients compared to non-aniridia comparisons (Bobilev, 2019).

Functional neuroimaging such as fMRI and EEG can provide perspective on neurocognitive processes that can greatly advance our understanding of extraocular phenotypes in PAX6-mediated aniridia. Combining the functional imaging techniques with molecular and neuroanatomic techniques allows for a deeper understanding of aniridia and start to allow for clinicians to take a more holistic approach when treating the disorder and helping patients understand their symptomology.

This dissertation will provide evidence for the role of the transcription factor, PAX6 in development and maintenance of the central nervous system. Structural MRI analysis of aniridia patients show reductions in discreet structures within the brain, although at a much lower frequency and with less severity than previously reported. Structural MRI in the mouse model of the disorder, *Small eye*, revealed similar findings in which the structural changes in the brain are much less severe than originally thought. Together, these studies provide insights into the role of PAX6 in the adult brain, which is only just now receiving more attention.

1.4 References

1. Piñon MC, Tuoc TC, Ashery-Padan R, et al (2008) Altered molecular regionalization and normal thalamocortical connections in cortex-specific Pax6 knock-out mice. J Neurosci 28:8724–34. https://doi.org/10.1523/JNEUROSCI.2565-08.2008
2. Tuoc TC, Radyushkin K, Tonchev AB, et al (2009) Selective cortical layering abnormalities and behavioral deficits in cortex-specific Pax6 knock-out mice. J Neurosci 29:8335–49. https://doi.org/10.1523/JNEUROSCI.5669-08.2009
3. Georgala PA, Manuel M, Price DJ (2011) The generation of superficial cortical layers is regulated by levels of the transcription factor Pax6. Cereb Cortex 21:81–94. https://doi.org/10.1093/cercor/bhq061
4. Azuma N, Yamaguchi Y, Handa H, et al (2003) Mutations of the PAX6 gene detected in patients with a variety of optic-nerve malformations. Am J Hum Genet 72:1565–70. https://doi.org/10.1086/375555
5. Shaham O, Menuchin Y, Farhy C, Ashery-Padan R (2012) Pax6: A multi-level regulator of ocular development. Prog Retin Eye Res 31:351–376. https://doi.org/10.1016/j.preteyeres.2012.04.002
6. Cvekl A, Callaerts P (2017) PAX6: 25th anniversary and more to learn. Exp Eye Res 156:10–21. https://doi.org/10.1016/J.EXER.2016.04.017
7. Haubst N, Berger J, Radjendirane V, et al (2004) Molecular dissection of Pax6 function: the specific roles of the paired domain and homeodomain in brain development. Development 131:6131–40. https://doi.org/10.1242/dev.01524
8. Ashery-Padan R, Gruss P (2001) Pax6 lights-up the way for eye development. Curr Opin Cell Biol 13:706–714

9. Glaser T, Walton DS, Maas RL (1992) Genomic structure, evolutionary conservation and aniridia mutations in the human PAX6 gene. Nat Genet 2:232–239. https://doi.org/10.1038/ng1192-232

10. Prosser J, van Heyningen V (1998) PAX6 mutations reviewed. Hum Mutat 11:93–108. https://doi.org/10.1002/(SICI)1098-1004(1998)11:2<93::AID-HUMU1>3.0.CO;2-M

11. Osumi N, Shinohara H, Numayama-Tsuruta K, Maekawa M (2008) Concise Review: Pax6 Transcription Factor Contributes to both Embryonic and Adult Neurogenesis as a Multifunctional Regulator. Stem Cells 26:1663–1672. https://doi.org/10.1634/stemcells.2007-0884

12. Heins N, Malatesta P, Cecconi F, et al (2002) Glial cells generate neurons: the role of the transcription factor Pax6. Nat Neurosci 5:308–315. https://doi.org/10.1038/nn828

13. Kikkawa T, Casingal CR, Chun SH, et al (2018) The role of Pax6 in brain development and its impact on pathogenesis of autism spectrum disorder. Brain Res. https://doi.org/10.1016/J.BRAINRES.2018.02.041

14. Manuel M, Price DJ (2005) Role of Pax6 in forebrain regionalization. Brain Res Bull 66:387–393. https://doi.org/10.1016/j.brainresbull.2005.02.006

15. Simpson TI, Price DJ (2002) Pax6; a pleiotropic player in development. Bioessays 24:1041–1051. https://doi.org/10.1002/bies.10174

16. van Heyningen V (2002) PAX6 in sensory development. Hum Mol Genet 11:1161–1167. https://doi.org/10.1093/hmg/11.10.1161

17. Siracusa LD, Abbott CM (1992) Mouse Chromosome 2. Mamm Genome 3:S20–S43. https://doi.org/10.1007/BF00648420

18. Walther C, Guenet J-L, Simon D, et al (1991) Pax: A murine multigene family of paired

box-containing genes. Genomics 11:424–434. https://doi.org/10.1016/0888-7543(91)90151-4

19. Kleinjan DA, Seawright A, Childs AJ, van Heyningen V (2004) Conserved elements in Pax6 intron 7 involved in (auto)regulation and alternative transcription. Dev Biol 265:462–477

20. Morgan R (2004) Conservation of sequence and function in the Pax6 regulatory elements. Trends Genet 20:283–7. https://doi.org/10.1016/j.tig.2004.04.009

21. Plessy C, Dickmeis T, Chalmel F, Strähle U (2005) Enhancer sequence conservation between vertebrates is favoured in developmental regulator genes. Trends Genet 21:207–10. https://doi.org/10.1016/j.tig.2005.02.006

22. Quiring R, Walldorf U, Kloter U, Gehring W (1994) Homology of the eyeless gene of Drosophila to the Small eye gene in mice and Aniridia in humans. Science (80-) 265:785–789. https://doi.org/10.1126/science.7914031

23. Kammandel B, Chowdhury K, Stoykova A, et al (1999) Distinct cis-essential modules direct the time-space pattern of the Pax6 gene activity. Dev Biol 205:79–97. https://doi.org/10.1006/dbio.1998.9128

24. Carriere C, Plaza S, Martin P, et al (1993) Characterization of quail Pax-6 (Pax-QNR) proteins expressed in the neuroretina. Mol Cell Biol 13:7257–7266

25. Epstein JA, Glaser T, Cai J, et al (1994) Two independent and interactive DNA-binding subdomains of the Pax6 paired domain are regulated by alternative splicing. Genes Dev 8:2022–2034

26. Tang HK, Singh S, Saunders GF (1998) Dissection of the transactivation function of the transcription factor encoded by the eye developmental gene PAX6. J Biol Chem

273:7210–7221

27. Xu PX, Zhang X, Heaney S, et al (1999) Regulation of Pax6 expression is conserved between mice and flies. Development 126:

28. Chauhan BK (2004) Functional Properties of Natural Human PAX6 and PAX6(5a) Mutants. Invest Ophthalmol Vis Sci 45:385–392. https://doi.org/10.1167/iovs.03-0968

29. Kim J, Lauderdale JD (2006) Analysis of Pax6 expression using a BAC transgene reveals the presence of a paired-less isoform of Pax6 in the eye and olfactory bulb. Dev Biol 292:486–505. https://doi.org/10.1016/j.ydbio.2005.12.041

30. Anderson TR, Hedlund E, Carpenter EM (2002) Differential Pax6 promoter activity and transcript expression during forebrain development

31. Grindley JC, Davidson DR, Hill RE (1995) The role of Pax-6 in eye and nasal development. Development 121:1433–42

32. Halder G, Callaerts P, Gehring W (1995) Induction of ectopic eyes by targeted expression of the eyeless gene in Drosophila. Science (80-) 267:1788–1792. https://doi.org/10.1126/science.7892602

33. Jang C-C (2003) Two Pax genes, eye gone and eyeless, act cooperatively in promoting Drosophila eye development. Development 130:2939–2951. https://doi.org/10.1242/dev.00522

34. Walther C, Gruss P (1991) Pax-6, a murine paired box gene, is expressed in the developing CNS. Development 113:

35. Duan D, Fu Y, Paxinos G, Watson C (2013) Spatiotemporal expression patterns of Pax6 in the brain of embryonic, newborn, and adult mice. Brain Struct Funct 218:353–372. https://doi.org/10.1007/s00429-012-0397-2

36. Stoykova A, Gruss P (1994) Roles of Pax-genes in developing and adult brain as suggested by expression patterns. J Neurosci 14:1395–1412

37. Stoykova A, Fritsch R, Walther C, Gruss P (1996) Forebrain patterning defects in Small eye mutant mice. Development 122:3453–65

38. Stoykova A, Treichel D, Hallonet M, Gruss P (2000) Pax6 modulates the dorsoventral patterning of the mammalian telencephalon. J Neurosci 20:8042–50. https://doi.org/10.1523/JNEUROSCI.20-21-08042.2000

39. Grindley JC, Hargett LK, Hill RE, et al (1997) Disruption of PAX6 function in mice homozygous for the Pax6Sey-1Neu mutation produces abnormalities in the early development and regionalization of the diencephalon. Mech Dev 64:111–26

40. Kohwi M, Osumi N, Rubenstein JL, Alvarez-Buylla A (2005) Pax6 is required for making specific subpopulations of granule and periglomerular neurons in the olfactory bulb. J Neurosci 25:6997–7003. https://doi.org/10.1523/JNEUROSCI.1435-05.2005

41. Asami M, Pilz GA, Ninkovic J, et al (2011) The role of Pax6 in regulating the orientation and mode of cell division of progenitors in the mouse cerebral cortex. Development 138:5067–5078. https://doi.org/10.1242/dev.074591

42. Gotz M, Stoykova A, Gruss P (1998) Pax6 controls radial glia differentiation in the cerebral cortex. Neuron 21:1031–1044

43. Osumi N (2001) The role of Pax6 in brain patterning. Tohoku J Exp Med 193:163–174

44. Warren N (1999) The Transcription Factor, Pax6, is Required for Cell Proliferation and Differentiation in the Developing Cerebral Cortex. Cereb Cortex 9:627–635. https://doi.org/10.1093/cercor/9.6.627

45. Schmahl W, Knoedlseder M, Favor J, Davidson D (1993) Defects of neuronal migration

and the pathogenesis of cortical malformations are associated with Small eye (Sey) in the mouse, a point mutation at the Pax-6-locus. Acta Neuropathol 86:126–135. https://doi.org/10.1007/BF00334879

46. Boretius S, Michaelis T, Tammer R, et al (2009) In vivo MRI of altered brain anatomy and fiber connectivity in adult pax6 deficient mice. Cereb Cortex 19:2838–2847. https://doi.org/10.1093/cercor/bhp057

47. Altman J, Bayer SA (1987) Development of the precerebellar nuclei in the rat: I. The precerebellar neuroepithelium of the rhombencephalon. J Comp Neurol 257:477–89. https://doi.org/10.1002/cne.902570402

48. Zhang L, Goldman JE (1996) Developmental fates and migratory pathways of dividing progenitors in the postnatal rat cerebellum. J Comp Neurol 370:536–50. https://doi.org/10.1002/(SICI)1096-9861(19960708)370:4<536::AID-CNE9>3.0.CO;2-5

49. Engelkamp D, Rashbass P, Seawright A, van Heyningen V (1999) Role of Pax6 in development of the cerebellar system. Development 126:3585–96.

50. Kayam G, Kohl A, Magen Z, et al (2013) A novel role for Pax6 in the segmental organization of the hindbrain. Development 140:2190–202. https://doi.org/10.1242/dev.089136

51. Mo Z, Zecevic N (2008) Is Pax6 critical for neurogenesis in the human fetal brain? Cereb Cortex 18:1455–65. https://doi.org/10.1093/cercor/bhm181

52. Hevner RF, Miyashita-Lin E, Rubenstein JLR (2002) Cortical and thalamic axon pathfinding defects in Tbr1, Gbx2, and Pax6 mutant mice: evidence that cortical and thalamic axons interact and guide each other. J Comp Neurol 447:8–17.

https://doi.org/10.1002/cne.10219

53. Jones L, Lopez-Bendito G, Gruss P, et al (2002) Pax6 is required for the normal development of the forebrain axonal connections. Development 129:5041–5052

54. Mastick GS, Davis NM, Andrew GL, Easter Jr. SS (1997) Pax-6 functions in boundary formation and axon guidance in the embryonic mouse forebrain. Development 124:1985–1997

55. Hanson IM, Seawright A, Hardman K, et al (1993) PAX6 mutations in aniridia. Hum Mol Genet 2:915–920

56. Grønskov K, Olsen JH, Sand A, et al (2014) Population-based risk estimates of Wilms tumor in sporadic aniridia. Hum Genet 109:11–18. https://doi.org/10.1007/s004390100529

57. Nelson LB, Spaeth GL, Nowinski TS, et al Aniridia. A review. Surv Ophthalmol 28:621–42

58. Grant WM, Walton DS (1974) Progressive changes in the angle in congenital aniridia, with development of glaucoma. Am J Ophthalmol 78:842–847

59. McCulley TJ, Mayer K, Dahr SS, et al (2005) Aniridia and optic nerve hypoplasia. Eye 19:762–764. https://doi.org/10.1038/sj.eye.6701642

60. Nishida K, Kinoshita S, Ohashi Y, et al (1995) Ocular surface abnormalities in aniridia. Am J Ophthalmol 120:368–375

61. Tsai JH, Freeman JM, Chan CC, et al (2005) A progressive anterior fibrosis syndrome in patients with postsurgical congenital aniridia. Am J Ophthalmol 140:1075–1079. https://doi.org/10.1016/j.ajo.2005.07.035

62. Tzoulaki I, White IM, Hanson IM (2005) PAX6 mutations: genotype-phenotype

correlations. BMC Genet 6:27. https://doi.org/10.1186/1471-2156-6-27

63. Grant MK, Bobilev AM, Pierce JE, et al (2017) Structural brain abnormalities in 12 persons with aniridia. F1000Research 6:255. https://doi.org/10.12688/f1000research.11063.2

64. Pierce JE, Krafft CE, Rodrigue AL, et al (2014) Increased functional connectivity in intrinsic neural networks in individuals with aniridia. Front Hum Neurosci 8:1013. https://doi.org/10.3389/fnhum.2014.01013

65. Burton CR, Schaeffer DJ, Bobilev AM, et al (2018) Microstructural differences in visual white matter tracts in people with aniridia. Neuroreport 1. https://doi.org/10.1097/WNR.0000000000001135

66. Bamiou DE, Musiek FE, Sisodiya SM, et al (2004) Deficient auditory interhemispheric transfer in patients with PAX6 mutations. Ann Neurol 56:503–509. https://doi.org/10.1002/ana.20227

67. Bamiou DE, Free SL, Sisodiya SM, et al (2007) Auditory interhemispheric transfer deficits, hearing difficulties, and brain magnetic resonance imaging abnormalities in children with congenital aniridia due to PAX6 mutations. Arch Pediatr Adolesc Med 161:463–469. https://doi.org/10.1001/archpedi.161.5.463

68. Mitchell TN, Stevens JM, Free SL, et al (2002) Anterior commissure absence without callosal agenesis: a new brain malformation. Neurology 58:1297–9

69. Sisodiya SM, Free SL, Williamson KA, et al (2001) PAX6 haploinsufficiency causes cerebral malformation and olfactory dysfunction in humans. Nat Genet 28:214–216. https://doi.org/10.1038/90042

70. Mitchell TN, Free SL, Williamson KA, et al (2003) Polymicrogyria and absence of pineal

gland due to PAX6 mutation. Ann Neurol 53:658–663. https://doi.org/10.1002/ana.10576

71. Yogarajah M, Matarin M, Vollmar C, et al (2016) PAX6 , brain structure and function in human adults: advanced MRI in aniridia. Ann Clin Transl Neurol. https://doi.org/10.1002/acn3.297

72. Free SL, Mitchell TN, Williamson KA, et al (2003) Quantitative MR image analysis in subjects with defects in the PAX6 gene. Neuroimage 20:2281–2290

73. Roberts RC (1967) Small eyes—a new dominant eye mutant in the mouse. Genet Res 9:121. https://doi.org/10.1017/S0016672300010387

74. Hogan BLM, Horsburgh G, Cohen J, et al (1986) Small eyes (Sey): a homozygous lethal mutation on chromosome 2 which affects the differentiation of both lens and nasal placodes in the mouse. 97:95–110

75. Hill RE, Favor J, Hogan BL, et al (1991) Mouse small eye results from mutations in a paired-like homeobox-containing gene. Nature 354:522–525. https://doi.org/10.1038/354522a0

76. Favor J, Neuhäuser-Klaus A, Ehling UH (1988) The effect of dose fractionation on the frequency of ethylnitrosourea-induced dominant cataract and recessive specific locus mutations in germ cells of the mouse. Mutat Res Mol Mech Mutagen 198:269–275. https://doi.org/10.1016/0027-5107(88)90003-6

77. Theiler K, Varnum DS, Stevens LC (1979) Development of Dickie's small eye, a mutation in the house mouse. Anat Embryol (Berl) 155:81–86. https://doi.org/10.1007/BF00315732

78. Lyon MF, Searle AG (1989) Genetic variants and strains of the laboratory mouse.

79. Hogan BLM, Hirst EMA, Horsburgh G, Hetherington CM (1988) Small eye (Sey): a

mouse model for the genetic analysis of craniofacial abnormalities. Development 103:115–119

80. Hingorani M, Williamson KA, Moore AT, van Heyningen V (2009) Detailed ophthalmologic evaluation of 43 individuals with PAX6 mutations. Invest Ophthalmol Vis Sci 50:2581–90. https://doi.org/10.1167/iovs.08-2827

81. Peter NM, Leyland M, Mudhar HS, et al (2013) PAX6 mutation in association with ptosis, cataract, iris hypoplasia, corneal opacification and diabetes: a new variant of familial aniridia? Clin Exp Ophthalmol 41:835–841. https://doi.org/10.1111/ceo.12109

82. Jordan T, Hanson I, Zaletayev D, et al (1992) The human PAX6 gene is mutated in two patients with aniridia. Nat Genet 1:328–32. https://doi.org/10.1038/ng0892-328

83. Nishi M, Sasahara M, Shono T, et al (2005) A case of novel de novo paired box gene 6 (PAX6) mutation with early-onset diabetes mellitus and aniridia. Diabet Med 22:641–644. https://doi.org/10.1111/j.1464-5491.2005.01469.x

84. Abouzeid H, Youssef MA, ElShakankiri N, et al (2009) PAX6 aniridia and interhemispheric brain anomalies. Mol Vis 15:2074–83

85. Thompson PJ, Mitchell TN, Free SL, et al (2004) Cognitive functioning in humans with mutations of the PAX6 gene. Neurology 62:1216–1218

86. Hanish AE, Butman JA, Thomas F, et al (2015) Pineal hypoplasia, reduced melatonin and sleep disturbance in patients with PAX6 haploinsufficiency. J Sleep Res. https://doi.org/10.1111/jsr.12345

87. Ross RD (1998) Is Perception of Light Useful to the Blind Patient? Arch Ophthalmol 116:236–238. https://doi.org/10.1001/archopht.116.2.236

88. Wee R, Van Gelder RN (2004) Sleep disturbances in young subjects with visual

dysfunction. Ophthalmology 111:297-302; discussion 302–3. https://doi.org/10.1016/j.ophtha.2003.05.014

89. Gupta SK, De Becker I, Tremblay F, et al (1998) Genotype/phenotype correlations in aniridia. Am J Ophthalmol 126:203–210

90. Van Alphen HA (1969) The anterior commissure of the rabbit. Acta Anat Suppl (Basel) 57:1–112

91. Brunjes PC (2012) The mouse olfactory peduncle. 2.The anterior limb of the anterior commissure. Front Neuroanat 6:51. https://doi.org/10.3389/fnana.2012.00051

92. Dellovade TL, Pfaff DW, Schwanzel-Fukuda M (1998) Olfactory bulb development is altered in small-eye (Sey) mice. J Comp Neurol 402:402–18

93. Ellison-Wright Z, Heyman I, Frampton I, et al (2004) Heterozygous PAX6 mutation, adult brain structure and fronto-striato-thalamic function in a human family. Eur J Neurosci 19:1505–12. https://doi.org/10.1111/j.1460-9568.2004.03236.x

94. Hiraoka K, Sumiyoshi A, Nonaka H, et al (2016) Regional Volume Decreases in the Brain of Pax6 Heterozygous Mutant Rats: MRI Deformation-Based Morphometry. PLoS One 11:e0158153. https://doi.org/10.1371/journal.pone.0158153

CHAPTER 2:

STRUCTURAL BRAIN ABNORMALITIES IN 12 PERSONS WITH ANIRIDIA[1]

[1] Grant, M.K., Bobilev, A.M., Pierce, J.E., DeWitte, J., Lauderdale, J.D. 2017. *F1000Research*. Reprinted here with permission of the publisher.

Abstract

Background: Aniridia is a disorder predominately caused by heterozygous loss-of-function mutations of the *PAX6* gene, which is a transcriptional regulator necessary for normal eye and brain development. The ocular abnormalities of aniridia have been well characterized, but mounting evidence has implicated brain-related phenotypes as a prominent feature of this disorder as well. Investigations using neuroimaging in aniridia patients have shown reductions in discrete brain structures and changes in global grey and white matter. However, limited sample sizes and substantive heterogeneity of structural phenotypes in the brain remain a challenge.

Methods: Here, we examined brain structure in a new population sample in an effort to add to the collective understanding of anatomical abnormalities in aniridia. The current study used 3T magnetic resonance imaging to acquire high-resolution structural data in 12 persons with aniridia and 12 healthy demographically matched comparison subjects.

Results: We examined five major structures: the anterior commissure, the posterior commissure, the pineal gland, the corpus callosum, and the optic chiasm. The most consistent reductions were found in the anterior commissure and the pineal gland; however, abnormalities in all of the other structures examined were present in at least one individual.

Conclusions: Our results indicate that the anatomical abnormalities in aniridia are variable and largely individual-specific. These findings suggest that future studies investigate this heterogeneity further, and that normal population variation should be considered when evaluating structural abnormalities.

Keywords: MRI, PAX6, neuroanatomy

2.1 Introduction

Aniridia is panocular, congenital, and progressive disorder with an occurrence of approximately 1 in 83,000 live births [1, 2]. Aniridia is best characterized by the lack of or hypoplasia of the iris (for which it is named), in addition to several other ocular abnormalities, which culminate in reduced visual acuity [3]. Due to the progressive nature of the disease, individuals usually develop multiple ocular abnormalities, such as keratopathy, corneal vascularization and opacification, glaucoma, anterior chamber fibrosis, and cataracts [4–7]. Although aniridia is most well-known for its ocular phenotypes, the condition has a number of other abnormalities, including sensory, neural, cognitive, and auditory processing abnormalities [8, 9].

The development of aniridia in humans is linked to heterozygous loss-of-function mutations to the *PAX6* gene, which encodes a highly conserved transcription factor critical for normal eye and neural development [1]. The vast majority of aniridia cases (≥80%) are associated with mutations in *PAX6* [2, 10]. Functional mutations in this gene can be either sporadic or familial, and causal mutations in aniridia encompass a large number of variants. The majority of these variants are nonsense mutations, which lead to a premature termination codon, and are found across the *PAX6* locus [10, 11]. *PAX6* is expressed in the developing eye, brain, and spinal cord, and is required for aspects of anatomical and functional development of the central nervous system (CNS) and visual system [12]. Within the CNS, *PAX6* is involved in patterning, regionalization, and the formation of neural circuits [13–16]. Previous studies of patients with aniridia using structural magnetic resonance imaging (MRI) have shown abnormalities in major fiber tracts and subcortical structures of the brain, including the anterior commissure [9, 17–20], posterior commissure [18, 20], corpus callosum [9, 19, 20], pineal gland

[18, 20], optic chiasm [20], and olfactory bulb [17, 18]. The most consistently reported abnormalities are found in the anterior commissure, pineal gland, and optic chiasm; abnormalities in the posterior commissure, corpus callosum, and olfactory bulb are found in fewer than 35% of patients examined. Additionally, studies have shown conflicting results regarding grey matter volume differences in aniridia, with reports of both increases and decreases in whole brain grey matter [21, 22]. Most recently, it has been shown that there is an accelerated age-related increase in cortical thinning of the inferior parietal lobe and prefrontal/premotor areas in both brain hemispheres in aniridia compared to healthy patients [23].

While several previous studies have investigated structural brain abnormalities in patients with aniridia, the variance in brain structures affected and extent of anatomical abnormalities is high. The variance observed in the published literature may be interpreted as a result of genetic differences in patient samples, either directly related to disease-causing mutations or modifier effects caused by genomic differences across subjects. Most of the previous studies examining structural changes in the brain of aniridia patients have focused on a subset of the structures we examined, but only one other study has looked at all five together [20]. Additionally, we used a 3T magnet instead of a 1.5T, which allows for higher resolution structural images of small structures such as interhemispheric commissures, allowing us to more reliably identify subtle difference. The current study sought to investigate gross anatomical correlates of aniridia in a new population sample with varied *PAX6* mutations. Results from this study will serve as a comparison for previous studies, as well as contribute to what is known about the distribution of neuroanatomical phenotypes in the aniridia population as a whole. Overall, this will serve to clarify the extent of abnormalities in five brain structures in persons with aniridia with varied

mutations to the *PAX6* gene and contribute to our global understanding of the neuroanatomical characteristics of the disorder.

2.2 Methods

2.2.1 Subjects

A total of 14 individuals with aniridia and 15 healthy comparison individuals participated in the current study. Data from two participants with aniridia were excluded from analyses (due to a significant artifact and missing data). One healthy subject was excluded due to an anatomical abnormality, and two others were excluded because they did not match the demographic profile of an individual in the aniridia group included in the analysis. The remaining 12 individuals with aniridia (7 females; 3 left handed; mean age =36 years, SD=15) and 12 age- and gender-matched comparisons (7 females; 4 left handed; mean age= 35 years, SD=14) were included in the analyses (Table 1). Patients and healthy comparison subjects in this study were previously used in a study on functional connectivity [24]. Healthy comparison subjects were recruited through flyers posted in the community. Participants with aniridia were recruited through the Aniridia Foundation International Conference held in 2011 in Athens, Georgia and had been clinically diagnosed with aniridia. Exonic sequencing of the *PAX6* gene (11p13) (OMIM: 607108) was conducted at the University of Georgia, as previously described [10, 24]. All mutations, which can be found in Table 1, have been submitted to the Human *PAX6* Allelic Variant Database (http://lsdb.hgu.mrc.ac.uk/home.php?select_db=PAX6), as part of a previous genotype identification study [10]. Three of the participants with aniridia belonged to the same family, and all other participants included in the analyses were unrelated. After written informed consent was obtained and MRI safety screening was conducted, all participants completed an MRI session in which a high-resolution structural scan was obtained. The Institutional Review Board

of the University of Georgia approved all activities prior to subject recruitment, data collection, and data analysis (Project number: 2011-10862-1; STUDY00003122).

2.2.2 MRI data acquisition

All data were collected on a 3T GE Signa MRI (General Electric, Milwaukee, WI, USA) at the University of Georgia's Bio-Imaging Research Center. To obtain a high-resolution structural scan, images were acquired with a T1-weighted 3D FSPGR sequence [echo time (TE)=min full, flip angle=20°; field of view (FOV)=240 mm x 240 mm; matrix size=256 x 256, 150 axial slices; in-slice resolution=0.94 x 0.94 mm; slice thickness=1.2 mm].

2.2.3 MRI structural analysis

MR images were transferred to a DICOM image format and analyzed using two software programs, SPM run on MATLAB and OsiriX. For SPM analysis, DICOM files were converted to nifti format and analyzed using Statistical Parametric Mapping Software (SPM8; Wellcome Trust Centre for Neuroimaging; http://www.fil.ion.ucl.ac.uk/spm/) run on a MATLAB software platform (MATLAB Release 2015b; The Mathworks, Inc., Natick, MA, USA). SPM software was used to compare aniridia subjects to their demographically matched comparison subjects. DICOM files were additionally analyzed using Osirix Lite DICOM viewer (OsiriX v5.6,;Pixmeo SARL, Bernex, Switzerland) and all images generated using this software. All 24 individual subjects' data were visually inspected for gross anatomical abnormalities in two independent sessions by the first author (MG) and a radiologist (JDW). Regions of interest were determined by literature review to include the anterior commissure, posterior commissure, pineal gland, corpus callosum, and optic chiasm. The only structure that has been examined in the literature that we did not examine in our population was the olfactory bulb. This structure was excluded because both evaluators independently determined that the olfactory bulb could not be reliably

assessed in the current data set. The radiologist was blinded to patient status and genotype during visual examination of scans. No new regions of interest were determined during both the first and second examination of the scans.

2.2.4 Corpus callosum quantitative analysis

Following the approach of Free and colleagues (2003), the cross-sectional area of the corpus callosum was quantified at the mid-sagittal plane [21]. In order to align all MR images to the mid-sagittal plane, individual T1 images were reconstructed in AFNI software [25] and aligned manually using the anterior commissure, posterior commissure, and interhemispheric landmarks. On the mid-sagittal image, the corpus callosum was manually traced and the number of voxels within this delineation was counted. Additionally, the structural volumes were automatically segmented with FreeSurfer software (http://surfer.nmr.mgh.harvard.edu) to obtain estimates of total grey and white matter volume [26, 27]. The ratio of corpus callosum area to total cerebral volume was calculated to control for differences in overall brain size (see Supplementary Figure 1 "Ratio"). Supplementary Figure 1 graphs were created using GraphPad Prism 7 software (https://www.graphpad.com/).

2.3 Results

Whole brain visual inspection was used to identify major structural abnormalities in aniridia patients. All neuroanatomical results are reported in Table 1, which includes subject demographics and mutations. We analyzed five major brain structures that demonstrate clear anatomical abnormalities in aniridia patients. Our study showed that all 12 aniridia patients had a reduced anterior commissure when compared to their demographically matched healthy comparisons, as shown in Figure 1. The posterior commissure was reduced in 5/12 aniridia patients and normal in 7/12 of aniridia patients (Figure 1). Of the five aniridia patients with

reduced posterior commissures, one had a reduced commissure at the midline. The pineal gland was affected in all 12 aniridia patients: absent in two (Figure 1), highly reduced in one, and reduced in nine. The corpus callosum was slightly thinned in 3/12 aniridia patients and normal in 9/12 aniridia patients (Figure 2). The optic chiasm was reduced in 7/12 of patients (Figure 2) and normal in 5/12 patients.

In an effort to consider normal structural variation in the healthy population, we also evaluated healthy comparisons for structural brain abnormalities. We saw a reduced anterior commissure in two of the healthy comparisons and a reduced posterior commissure in one healthy comparison. The pineal gland showed the most variance within the healthy comparison group with one subject with no visible pineal gland, three healthy comparisons with slightly reduced to reduced pineal glands, and eight healthy comparisons with normal pineal glands. All healthy comparisons had normal corpus callosums and optic chiasms. A full description of which structures showed abnormalities in both the aniridia and healthy comparison groups are reported in Table 1. These findings provide context for asserting disease-related changes in the aniridia population, in the current study as well as others.

Additionally, we examined corpus callosum area at the mid-sagittal plane along with grey matter, white matter, and whole brain volume in our aniridia and healthy comparison groups. Grey matter volume and total brain volume averages are indistinguishable between aniridia and healthy comparison subjects. There is a slight reduction in the aniridia patients compared to healthy individuals in average corpus callosum area as well as white matter volume and ratio of corpus callosum area to whole brain volume. However, these are just trends and no measurement was statistically significant, which can also be explained by a high degree of variability within the aniridia population. Volumetric and area measurements along with

graphical representations of the data can be seen in Supplementary Table 1 and Supplementary Figure 1.

2.4 Discussion

The most commonly reported neuroanatomical abnormality in MRI studies of aniridia patients is the anterior commissure. Previous studies have reported changes in the anterior commissure with some cases described as reductions and others reported as complete absence of the structure [9, 17–19]. Consistent with these reports, our study identified a reduction in the anterior commissure in all 12 aniridia patients, but none of the patients lacked the structure. The posterior commissure has also been evaluated in previous studies: one study reports that it is present in all subjects while the other study presented evidence that one patient had an absent structure while the others had normal posterior commissures [18, 20]. We found no individuals lacking the posterior commissure, and fewer than half of our aniridia patients seemed to have an abnormal structure. Interestingly though, it seems as if one patient exhibited a reduction of the posterior commissure at the midline with thickened bundles adjacent to the midline suggesting that commissure formation was incomplete. PAX6 has a known role in formation of the posterior commissure in rodents, so it is likely that this phenotype in humans is a direct consequence of PAX6 deficiency [15]. In agreement with previous findings, we also see abnormal or absent pineal glands in our entire patient population. This finding is consistent with sleep regulation deficits in persons with aniridia reported in other studies [28]. The corpus callosum has also been a structure commonly evaluated in aniridia MRI studies, with many reporting reductions in corpus callosum thickness and severe agenesis [9, 19, 20]. However, we found very few patients present with a reduced or abnormal corpus callosum, and propose that the slight reduction we see in three of our patients falls within normal population variation. Unlike most previous studies,

we examined the optic chiasm, and found a reduction in the structure in more than half of our patients. This reduction could be a developmental consequence of the disorder or a progressive phenotype associated with reduced levels of PAX6. Anatomical abnormality findings seem to be highly dependent on population sample, and a larger collective sample in the literature will help us get closer to understanding common disease traits and variation.

As described above, we observed a reduction in the anterior commissure in every patient we evaluated and a reduction of the posterior commissure in five patients, but no individuals completely lacked either structure. Our study utilized a high resolution 3T MRI for data acquisition, while most other studies used a 1.5T MRI. Signal to noise ratio from 3T MRIs are almost double that of 1.5T MRIs, which will lead to an improved image quality and resolution from the 3T magnet [29]. We propose that the difference in observing a reduced versus absent anterior/posterior commissure may be due to a difference in scan resolution between images captured from a 3T versus 1.5T magnet. We see multiple patients in our group who have a severely reduced anterior commissure, and identifying this abnormality using a 1.5T magnet may be more difficult than when using a 3T. Additionally, the posterior commissure is smaller than the anterior commissure naturally, making it more difficult to distinguish between presence and absence in a scan. Lower scan resolution may not capture small structures such as these commissures, especially if they are reduced in size, leading to a false judgment of their absence.

A recent study has found an age component to cortical thickness in aniridia patients when compared to healthy individuals. The study found that in patients with aniridia there is an accelerated reduction in cortical thickness of the inferior parietal lobe and prefrontal/premotor areas in both brain hemispheres [23]. Adding to this age component seen in the Yogarajah (2016) study, there are also population differences in brain anatomy, even within healthy groups,

between younger subjects and older subjects [30]. Additionally, as we show in our study, there is anatomical variability even within healthy, unaffected participants. This makes it vitally important for careful selection of comparison subjects, and presents a caveat for interpreting differences we see in this and other clinical populations.

In addition to abnormal structural findings in patient populations with aniridia, multiple studies have assessed volumetric differences in grey and white matter in the brains of aniridia versus healthy comparisons. Similar to the findings in gross structural differences, much variation exists between reports on volumetric differences. Some studies show an increase in grey matter volume in aniridia patients compared to healthy control groups, while others find both increases and decreases depending on brain region [21, 22]. Changes in white matter findings follow the same suit, with some reports of reductions in white matter and others finding both reductions and increases [21, 22]. Even more interestingly, structures, such as the anterior commissure, posterior commissure, and pineal gland, show no deviation from healthy in these group-wise comparisons. This suggests that either the abnormalities seen in these structures are not as common among aniridia patients as previously thought, or that the characteristics of anatomical changes observed in aniridia patients have a high degree of variability within the population. Due to the consistency of abnormalities in structures like the anterior commissure in our study, as well as others, we predict the latter explains this discrepancy. This explanation is supported by the consistency of our results from volumetric and visual inspection of the corpus callosum in the current dataset. It is also possible that the differences observed across and within studies of these structures are a result of scan resolution and inconsistency of structure localization or plane of imaging to capture them given their small size and overall individual anatomical variation.

2.5 Conclusions

The current study investigated anatomical brain abnormalities correlated to aniridia in a new population sample in an effort to serve as a comparison to previous studies. Our aim was to contribute to what is known about the distribution of neuroanatomical phenotypes in the aniridia population as a whole. Although we found similar neuroanatomical abnormalities as previous studies, we find the severity is not as great as previously reported. The anterior commissure and pineal gland seem to be the structures most affected in the aniridia patients we examined, and we do see abnormalities in the posterior commissure, corpus callosum and the optic chiasm, albeit at lower frequency than previously reported. We believe the neuroanatomical abnormalities seen in aniridia populations have a high level of variability, and future studies should be aimed at collecting more patient MRI scans so that the breadth of abnormalities can be assessed.

2.6 Datasets

Dataset 1: Aniridia and healthy comparison MRI data: Structural MRI DICOM files for 12 aniridia and 12 healthy comparison individuals. Files are in DICOM format and labeled according to subject I.D. found in Table 1. These files can be opened using SPM software run in Matlab or OsiriX DICOM viewer (see Methods section).

Mutation information that has been presented here is also available through *PAX6* Allelic Variant Database (http://lsdb.hgu.mrc.ac.uk/home.php?select_db=PAX6).

2.7 References

1. Hanson IM, Seawright A, Hardman K, et al (1993) PAX6 mutations in aniridia. Hum Mol Genet 2:915–920.
2. Grønskov K, Olsen JH, Sand A, et al (2014) Population-based risk estimates of Wilms tumor in sporadic aniridia. Hum Genet 109:11–18. doi: 10.1007/s004390100529
3. Nelson LB, Spaeth GL, Nowinski TS, et al Aniridia. A review. Surv Ophthalmol 28:621–42.
4. Grant WM, Walton DS (1974) Progressive changes in the angle in congenital aniridia, with development of glaucoma. Am J Ophthalmol 78:842–847.
5. McCulley TJ, Mayer K, Dahr SS, et al (2005) Aniridia and optic nerve hypoplasia. Eye 19:762–764. doi: 10.1038/sj.eye.6701642
6. Nishida K, Kinoshita S, Ohashi Y, et al (1995) Ocular surface abnormalities in aniridia. Am J Ophthalmol 120:368–375.
7. Tsai JH, Freeman JM, Chan CC, et al (2005) A progressive anterior fibrosis syndrome in patients with postsurgical congenital aniridia. Am J Ophthalmol 140:1075–1079. doi: 10.1016/j.ajo.2005.07.035
8. Thompson PJ, Mitchell TN, Free SL, et al (2004) Cognitive functioning in humans with mutations of the PAX6 gene. Neurology 62:1216–1218.
9. Bamiou DE, Musiek FE, Sisodiya SM, et al (2004) Deficient auditory interhemispheric transfer in patients with PAX6 mutations. Ann Neurol 56:503–509. doi: 10.1002/ana.20227
10. Bobilev AM, McDougal ME, Taylor WL, et al (2015) Assessment of PAX6 alleles in 66 families with aniridia. Clin Genet. doi: 10.1111/cge.12708

11. Hingorani M, Williamson KA, Moore AT, van Heyningen V (2009) Detailed ophthalmologic evaluation of 43 individuals with PAX6 mutations. Invest Ophthalmol Vis Sci 50:2581–90. doi: 10.1167/iovs.08-2827

12. Kim J, Lauderdale JD (2006) Analysis of Pax6 expression using a BAC transgene reveals the presence of a paired-less isoform of Pax6 in the eye and olfactory bulb. Dev Biol 292:486–505. doi: 10.1016/j.ydbio.2005.12.041

13. Manuel M, Price DJ (2005) Role of Pax6 in forebrain regionalization. Brain Res Bull 66:387–393. doi: 10.1016/j.brainresbull.2005.02.006

14. Simpson TI, Price DJ (2002) Pax6; a pleiotropic player in development. Bioessays 24:1041–1051. doi: 10.1002/bies.10174

15. Mastick GS, Davis NM, Andrew GL, Easter Jr. SS (1997) Pax-6 functions in boundary formation and axon guidance in the embryonic mouse forebrain. Development 124:1985–1997.

16. Osumi N (2001) The role of Pax6 in brain patterning. Tohoku J Exp Med 193:163–174.

17. Sisodiya SM, Free SL, Williamson KA, et al (2001) PAX6 haploinsufficiency causes cerebral malformation and olfactory dysfunction in humans. Nat Genet 28:214–216. doi: 10.1038/90042

18. Mitchell TN, Free SL, Williamson KA, et al (2003) Polymicrogyria and absence of pineal gland due to PAX6 mutation. Ann Neurol 53:658–663. doi: 10.1002/ana.10576

19. Bamiou DE, Free SL, Sisodiya SM, et al (2007) Auditory interhemispheric transfer deficits, hearing difficulties, and brain magnetic resonance imaging abnormalities in children with congenital aniridia due to PAX6 mutations. Arch Pediatr Adolesc Med 161:463–469. doi: 10.1001/archpedi.161.5.463

20. Abouzeid H, Youssef MA, ElShakankiri N, et al (2009) PAX6 aniridia and interhemispheric brain anomalies. Mol Vis 15:2074–83.

21. Free SL, Mitchell TN, Williamson KA, et al (2003) Quantitative MR image analysis in subjects with defects in the PAX6 gene. Neuroimage 20:2281–2290.

22. Ellison-Wright Z, Heyman I, Frampton I, et al (2004) Heterozygous PAX6 mutation, adult brain structure and fronto-striato-thalamic function in a human family. Eur J Neurosci 19:1505–12. doi: 10.1111/j.1460-9568.2004.03236.x

23. Yogarajah M, Matarin M, Vollmar C, et al (2016) PAX6 , brain structure and function in human adults: advanced MRI in aniridia. Ann Clin Transl Neurol. doi: 10.1002/acn3.297

24. Pierce JE, Krafft CE, Rodrigue AL, et al (2014) Increased functional connectivity in intrinsic neural networks in individuals with aniridia. Front Hum Neurosci 8:1013. doi: 10.3389/fnhum.2014.01013

25. Cox RW (1996) AFNI: software for analysis and visualization of functional magnetic resonance neuroimages. Comput Biomed Res 29:162–73.

26. Dale AM, Fischl B, Sereno MI (1999) Cortical Surface-Based Analysis. Neuroimage 9:179–194. doi: 10.1006/nimg.1998.0395

27. Fischl B, Salat DH, Busa E, et al (2002) Whole brain segmentation: automated labeling of neuroanatomical structures in the human brain. Neuron 33:341–55.

28. Hanish AE, Butman JA, Thomas F, et al (2015) Pineal hypoplasia, reduced melatonin and sleep disturbance in patients with PAX6 haploinsufficiency. J Sleep Res. doi: 10.1111/jsr.12345

29. Wood R, Bassett K, Foerster V, et al PROS AND CONS OF 1.5 T MRI VERSUS 3.0 T MRI.

30. Coffey CE, Lucke JF, Saxton JA, et al (1998) Sex Differences in Brain Aging. Arch Neurol 55:169. doi: 10.1001/archneur.55.2.169

Table 2.1A: Subject demographics and structural abnormalities as seen in structural magnetic resonance images. Gender, age, handedness, mutation, and structural abnormalities of both aniridia subjects and healthy comparisons. Subject ID: Numbers are matched subjects, A refers to aniridia subjects, C refers to healthy comparisons. ND, not determined.

ANIRIDIA										
Subject ID	**Gender**	**Age**	**Handedness**	**Mutation**	**Predicted Mutation Effect**	**Anterior Commissure**	**Posterior Commissure**	**Pineal Gland**	**Corpus Callosum**	**Optic Chiasm**
1A	Male	18	Right	c.949C>T	Nonsense	Reduced	Normal	Reduced	Normal	Reduced
2A	Female	19	Ambidextrous	c.771delG	Frameshift deletion	Reduced	Normal	Reduced	Slightly reduced	Reduced
3A*	Male	20	Right	c.204delC	Frameshift deletion	Reduced	Normal	Reduced	Normal	Reduced
4A*	Female	24	Left	c.204delC	Frameshift deletion	Reduced	Reduced	Reduced	Normal	Reduced
5A	Female	25	Left	ND	ND	Reduced	Reduced center	Highly reduced	Normal	Reduced
6A	Female	28	Right	c.28C>T	Nonsense	Reduced	Normal	Absent	Slightly reduced	Normal
7A	Male	39	Right	c.482delG	Frameshift deletion	Reduced	Normal	Reduced	Normal	Normal
8A	Male	47	Right	ND	ND	Reduced	Normal	Reduced	Normal	Normal
9A*	Male	46	Left	c.204delC	Frameshift deletion	Reduced	Normal	Reduced	Normal	Reduced
10A	Female	51	Right	c.766-3C>G	Splice junction disruption	Reduced	Reduced	Absent	Normal	Normal
11A	Female	53	Right	ND	ND	Reduced	Reduced	Reduced	Normal	Normal
12A	Female	60	Ambidextrous	c.799A>T	Nonsense	Reduced	Reduced	Reduced	Slightly reduced	Reduced
* Indicates individuals from a single family										

Table 2.1B: Subject demographics and structural abnormalities as seen in structural magnetic resonance images. Gender, age, handedness, mutation, and structural abnormalities of both aniridia subjects and healthy comparisons. Subject ID: Numbers are matched subjects, A refers to aniridia subjects, C refers to healthy comparisons. ND, not determined.

PAX6 NORMAL										
Subject ID	**Gender**	**Age**	**Handedness**	**Mutation**	**Predicted Mutation Effect**	**Anterior Commissure**	**Posterior Commissure**	**Pineal Gland**	**Corpus Callosum**	**Optic Chiasm**
1C	Male	18	Right	*PAX6* Normal	N/A	Normal	Normal	Normal	Normal	Normal
2C	Female	20	Right	*PAX6* Normal	N/A	Normal	Normal	Normal	Normal	Normal
3C	Male	21	Right	*PAX6* Normal	N/A	Normal	Normal	Slightly Reduced	Normal	Normal
4C	Female	22	Left	*PAX6* Normal	N/A	Normal	Normal	Normal	Normal	Normal
5C	Female	23	Left	*PAX6* Normal	N/A	Normal	Normal	Normal	Normal	Normal
6C	Female	28	Left	*PAX6* Normal	N/A	Normal	Normal	Normal	Normal	Normal
7C	Male	37	Right	*PAX6* Normal	N/A	Normal	Normal	Normal	Normal	Normal
8C	Male	50	Right	*PAX6* Normal	N/A	Normal	Normal	Normal	Normal	Normal
9C	Male	50	Left	*PAX6* Normal	N/A	Reduced	Normal	Normal	Normal	Normal
10C	Female	48	Right	*PAX6* Normal	N/A	Reduced	Reduced	Absent	Normal	Normal
11C	Female	51	Right	*PAX6* Normal	N/A	Normal	Normal	Reduced	Normal	Normal
12C	Female	56	Right	*PAX6* Normal	N/A	Normal	Normal	Reduced	Normal	Normal

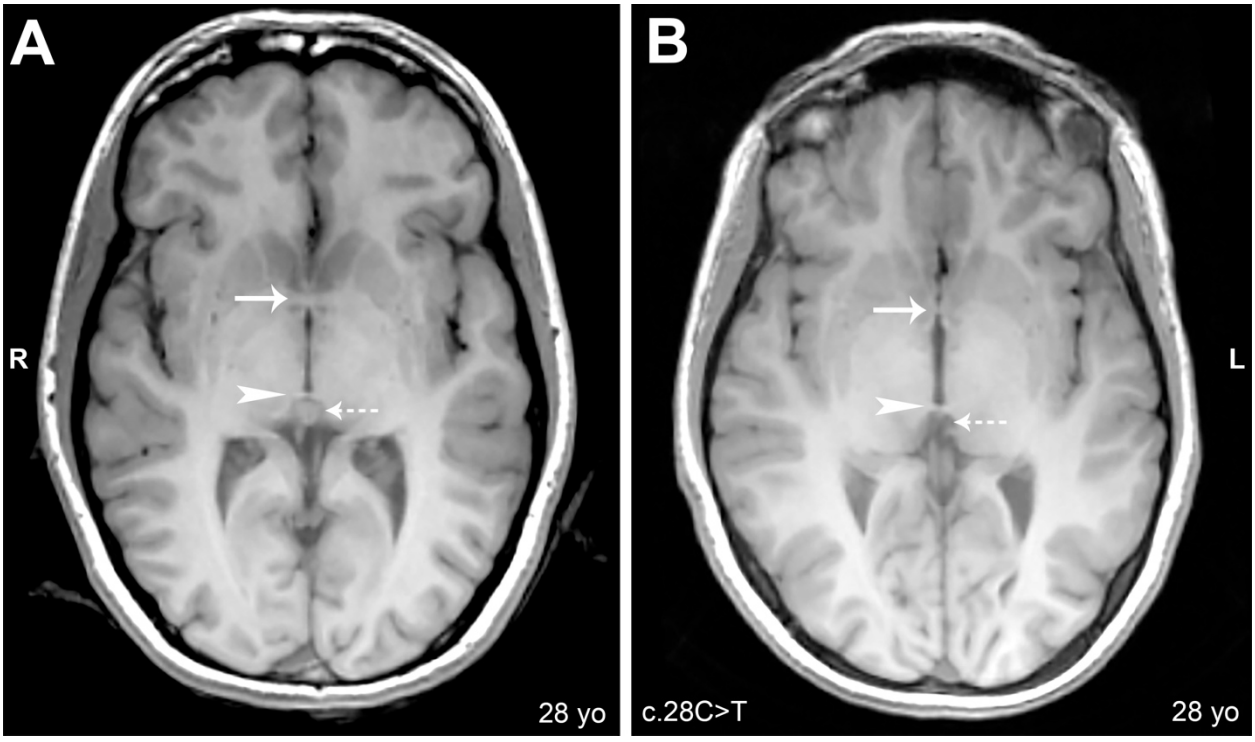

Figure 2.1: Anterior commissure, posterior commissure, and pineal gland. Axial cerebral T1-weighted magnetic resonance images, slice thickness 1.2mm. (**A**) Subject 6C: Arrow shows normal anterior commissure; arrowhead shows normal posterior commissure; dashed arrow shows normal pineal gland. (**B**) Subject 6A: Arrow shows reduced anterior commissure; arrowhead shows normal posterior commissure; dashed arrow shows absence of pineal gland.

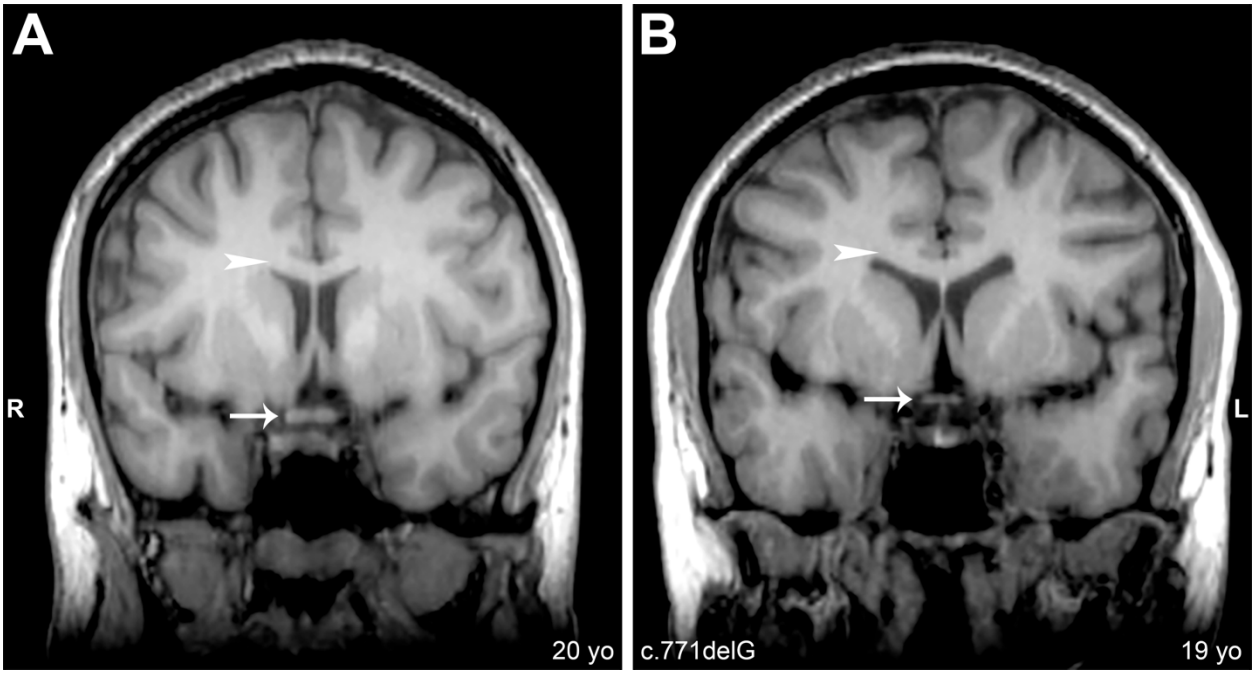

Figure 2.2: Optic chiasm and corpus callosum. Coronal cerebral T1-weighted magnetic resonance images, slice thickness 1.2mm. (**A**) Subject 2C: Arrow shows normal optic chiasm. (**B**) Subject 2A: Arrow shows reduced optic chiasm. Arrowheads in **A** and **B** denote normal corpus callosum.

Table 2.S.1: Subject corpus callosum area and brain volume measurements. Grey matter volume, white matter volume, total brain volume, and corpus callosum area of aniridia and matched subjects. Ratio refers to corpus callosum area/total brain volume. Subject ID: Numbers are matched subjects, A refers to aniridia subjects, C refers to healthy comparisons.

ANIRIDIA					
Subject ID	**Grey Matter Volume (mm^3)**	**White Matter Volume (mm^3)**	**Total Volume (mm^3)**	**Corpus Callosum Area (mm2)**	**Ratio: CC area/total volume**
1A	795957	654158	1450115	774	0.000534
2A	711626	604800	1316426	552	0.000419
3A*	683393	585559	1268952	712	0.000561
4A*	568045	505360	1073405	584	0.000544
5A	595209	573664	1168873	648	0.000554
6A	543481	496139	1039620	542	0.000521
7A	602438	545307	1147745	566	0.000493
8A	646003	616039	1262042	732	0.00058
9A*	621706	607971	1229677	684	0.000556
10A	533370	495092	1028462	713	0.000693
11A	623640	592662	1216302	652	0.000536
12A	528675	489748	1018423	555	0.000545
* Indicates individuals from a single family					

PAX6 NORMAL					
Subject ID	**Grey Matter Volume (mm^3)**	**White Matter Volume (mm^3)**	**Total Volume (mm^3)**	**Corpus Callosum Area (mm2)**	**Ratio: CC area/total volume**
1C	653601	568784	1222385	685	0.00056
2C	600216	547621	1147837	653	0.000569
3C	710079	668109	1378188	657	0.000477
4C	611409	542922	1154331	643	0.000557
5C	605760	545683	1151443	883	0.000767
6C	626978	587857	1214835	963	0.000793
7C	728278	734113	1462391	667	0.000456
8C	632857	647710	1280567	721	0.000563
9C	595440	613750	1209190	477	0.000394
10C	523144	484070	1007214	618	0.000614
11C	667226	616716	1283942	795	0.000619
12C	525662	540868	1066530	856	0.000803

Table 2.S.2: Subject ID. Subject ID used in this paper, MRI DICOM ID for DICOM file matching, and Person ID from *Bobilev et al. 2016* [10].

Subject ID	MRI DICOM ID	*Bobilev et al. 2016* Person ID
1A	50009	1001A316/sUGA
2A	50005	124A141/s-124
3A	50022	147A061/f-149
4A	50013	147A064/f-148
5A	50014	N/A
6A	50036	157A121/s-157
7A	50003	114A159/f-173
8A	50010	N/A
9A	50012	147A017/f-147
10A	50015	173A291/s-220
11A	50011	N/A
12A	50016	191A297/s-222
1C	1002	N/A
2C	50031	N/A
3C	1003	N/A
4C	50028	N/A
5C	50044	N/A
6C	50037	N/A
7C	50003 Match	N/A
8C	50034	N/A
9C	1017	N/A
10C	1070	N/A
11C	50032	N/A
12C	50064	N/A

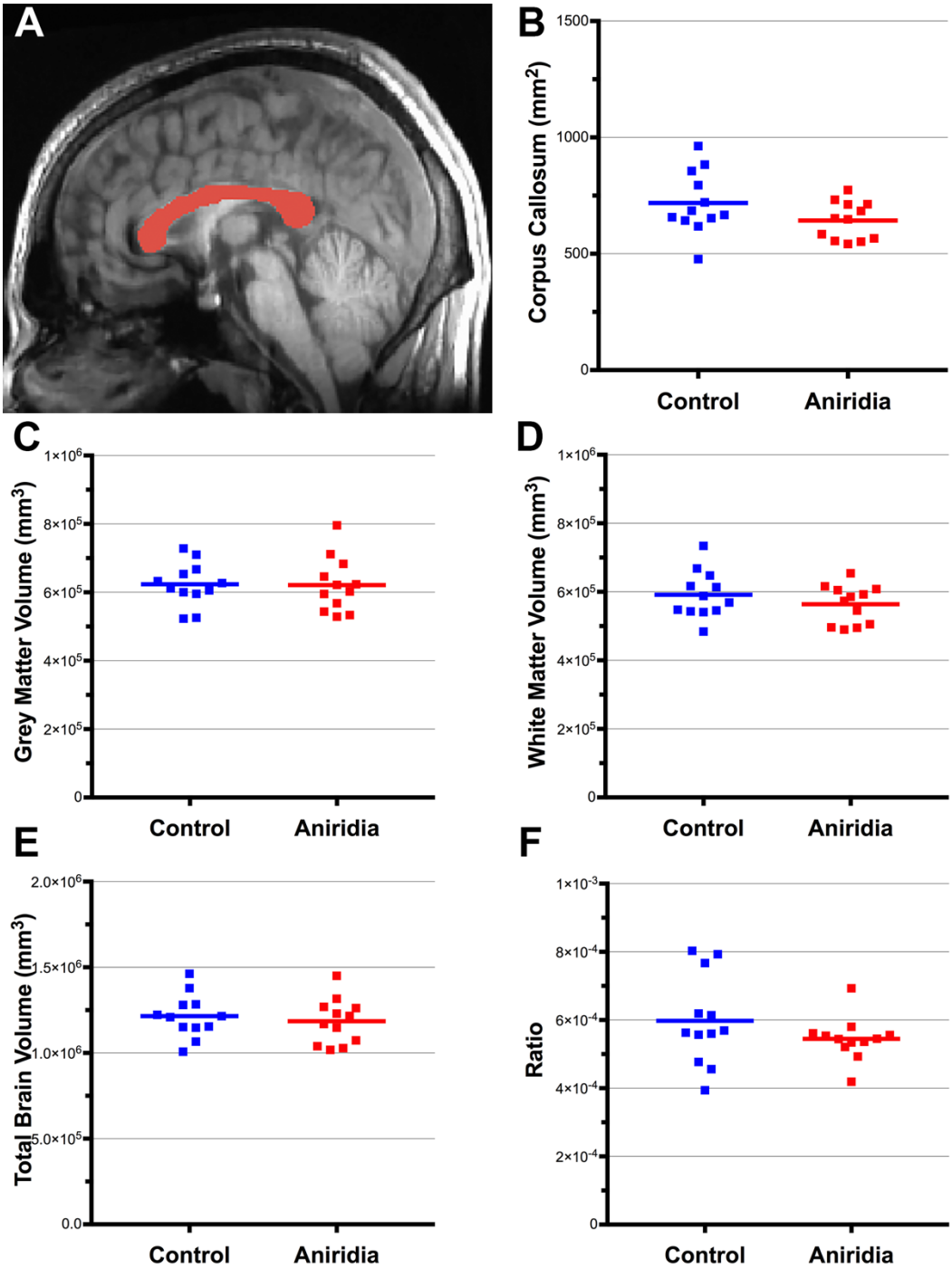
A
B
Corpus Callosum (mm²)
1500
1000
500
0
Control
Aniridia
C
Grey Matter Volume (mm³)
1×10⁶
8×10⁵
6×10⁵
4×10⁵
2×10⁵
0
Control
Aniridia
D
White Matter Volume (mm³)
1×10⁶
8×10⁵
6×10⁵
4×10⁵
2×10⁵
0
Control
Aniridia
E
Total Brain Volume (mm³)
2.0×10⁶
1.5×10⁶
1.0×10⁶
5.0×10⁵
0.0
Control
Aniridia
F
Ratio
1×10⁻³
8×10⁻⁴
6×10⁻⁴
4×10⁻⁴
2×10⁻⁴
0
Control
Aniridia

Figure 2.S.1: Corpus Callosum Cross-sectional area and brain volume comparisons. (**A**) Representation of manually traced corpus callosum in a mid-sagittal slice. (**B**) Corpus callosum area. (**C**) Grey matter volume. (**D**) White matter volume. (**E**) Total brain volume. (**F**) Ratio of corpus callosum area to total brain volume. Line in each graph represents average of group. No statistically significant differences were observed for any of the measurements depicted in this figure ($p < 0.05$).

CHAPTER 3:

GLOBAL AND AGE-RELATED NEUROANATOMICAL ABNORMALITIES IN A *PAX6*-DEFICIENT MOUSE MODEL OF ANIRIDIA SUGGESTS A ROLE FOR PAX6 IN ADULT NEUROPLASTICITY[2]

[2]Grant, M.K., Bobilev, A.M., Rasys, A.M., Byers, J.B., Schriever, H.C., Hekmatyar, K. & Lauderdale, J.D. 2019. *Submitted to Neurogenetics.*

Abstract

PAX6 encodes a highly conserved transcription factor necessary for normal development of the eyes and central nervous system. Heterozygous loss-of-function mutations in *PAX6* cause the disorder aniridia in humans and the *Small eye* trait in mice. Aniridia is a congenital and progressive disorder known for ocular phenotypes; however, recently, consequences of *PAX6* haploinsufficiency in the brains of aniridia patients have been identified. These findings span structural and functional abnormalities, including deficits in cognitive and sensory processing. Furthermore, some of these abnormalities are accelerated as aniridia patients age. Although some functional abnormalities may be explained by structural changes, variability of results remain, and the effects of PAX6 heterozygous loss-of-function mutations on neuroanatomy, particularly with regard to aging, have yet to be resolved. Our study used high-resolution magnetic resonance imaging (MRI) and histology to investigate structural consequences of such mutations in the adult brain of our aniridia mouse model, *Small eye* Neuherberg allele ($Pax6^{SeyNeu/+}$), at two adult age groups. Using both MRI and histology enables a direct comparison with human studies, while providing higher resolution for detection of more subtle changes. We show volumetric changes in olfactory bulbs, cerebellum, and eyes in the $Pax6^{SeyNeu/+}$ mouse. We also show alterations in thickness of major interhemispheric commissures, particularly those anteriorly located within the brain. In addition to the genotype-specific changes, we also show age-related differences in our $Pax6^{SeyNeu/+}$ and wild-type mice. Together, these genotype and age related changes to brain volumes and structures suggest a global decrease in adult brain plasticity in our $Pax6^{SeyNeu/+}$ mice.

Keywords: magnetic resonance imaging (MRI), ageing, plasticity, commissure, brain structure

3.1 Introduction

The development of the mammalian brain is directed by the precise and combinatorial effects of numerous gene products. Neuroanatomical structures and networks are directed and later maintained in the adult brain by the expression of many of these genes. One such gene is paired-box 6 (*PAX6* in humans, *Pax6* in rodents), which is expressed in the developing eye, brain, spinal cord, pancreas, and enteroendocrine cells of the small intestine [1–4]. PAX6 is a highly-conserved transcription factor that is critical for normal ocular, nasal, and neural development. During development, PAX6 is involved in brain patterning and regionalization as well as the formation of neural circuits, particularly in the forebrain [4–11]. Currently, the neuroanatomical implications of reduced functional expression of PAX6 in the brain have yet to be fully resolved.

Homozygous loss-of-function mutations of PAX6 lead to embryonic lethality, while heterozygous loss-of-function mutations produce a distinct ocular phenotype in rodents known as *Small eye,* and are causal for a condition known as aniridia in humans [12–18]. Aniridia is diagnosed by the absence or hypoplasia of the iris, for which it is named, and *PAX6*-mediated aniridia makes up ≥80% of all known cases [19, 20]. Although aniridia is primarily characterized by ocular defects, in recent years, evidence has emerged attributing both structural and functional brain-related phenotypes to the disorder. Structural changes within the brain of aniridia patients have been assessed in multiple studies. The most commonly reported structural changes in the brain of aniridia patients are those to major white matter tracts such as the corpus callosum, anterior commissure, posterior commissure, and optic chiasm [21–26]. Additionally, there are reports of discreet brain structures altered in aniridia patients such as reductions and absence of the pineal gland, reductions to the olfactory bulb, and unilateral polymicrogyria [21,

25–28]. Among the functional irregularities are deficits in auditory processing, olfactory dysfunction, and deficient pituitary function [23–25, 29]. It has also been shown that there is increased functional brain connectivity in resting state networks as measured by functional magnetic resonance imaging (fMRI) [30]. And in a recent electroencephalography (EEG) study, auditory information processing was shown to have reductions in lower frequency, longer-range activity and augmented higher frequency entrainment in aniridia compared to healthy comparison subjects in response to an auditory steady-state paradigm (unpublished). These phenotypic traits can likely be attributed to the reduction of functional *PAX6* during development and organization of the brain; however, these traits could also be a result of a reduction of functional *PAX6* during adult brain function and maintenance. Much research has been conducted on the developmental consequences of homozygous loss-of-function of PAX6 during development within the mouse model; however, this does not accurately depict the human disorder aniridia due to aniridia's heterozygosity of PAX6. Furthermore, research that has been conducting using the heterozygous mouse model, *Small eye*, has mainly focused on the developmental consequences in the eye and brain and most studies have not shown the effects in the adult brain. It is known though, that Pax6 is still expressed in adulthood, albeit at much lower levels, suggesting that its role potentially continues into adulthood [31].

Detailed investigation into the effects of *Pax6* heterozygous loss-of-function in the adult brain can be accomplished using rodent models. One group has employed MRI to assess phenotypic changes in brain structure associated with conditional removal of *Pax6* from *Emx1*-expressing neurons in the developing cortex [32]. These mutant animals exhibited several neuroanatomical changes, including reduced whole brain and olfactory bulb volume, decreased cortical thickness and decreased white matter tract connectivity. Further, these mice

demonstrated abnormalities in cortical layering and progenitor cell populations when *PAX6* was conditionally knocked out in the cortex during early and late neurogenesis [32–34].

While these studies show some abnormalities consistent with human patients, the genetic construct is not representative of a patient mutation because it is knocked out in selective cells and does not represent the global consequences of *Pax6* heterozygous loss-of-function throughout the lifespan. In an effort to better understand the consequences of heterozygous loss-of-function we have turned to the mouse model of aniridia, *Small eye*. The *Pax6* Neuherberg allele ($Pax6^{SeyNeu/+}$), used in this study, consists of a splice-junction mutation at the intersection of exon 10 and intron 10 which ultimately leads to a premature termination codon (PTC) in the intronic sequence [35]. The location and nature of this mutation putatively leads to haploinsufficient levels of Pax6 protein, and as such, is similar to a majority of human *PAX6*-mediated aniridia cases [19, 36].

The current study sought to identify differences in neuroanatomical structures between wild-type ($Pax6^{+/+}$) and *Pax6*-deficient ($Pax6^{SeyNeu/+}$) mice to gain a deeper understanding of the structural consequences of heterozygous loss-of-function of Pax6 in the adult mammalian brain. Because of recent insight on age-related increased cortical thinning in aniridia patients, our study examined two age groups: a younger (4-5M) cohort and an older (12-13M) cohort [37]. Our approach employed both high-resolution structural magnetic resonance imaging (MRI) and histological examination to show volumetric and structural changes in the *Small eye* mouse brain.

3.2 Methods

Animals

The mice used for this study were maintained as a *Pax6*$^{SeyNeu/+}$ colony on a CD-1 genetic background. Wild-type (*Pax6*$^{+/+}$) littermates were used as controls when possible, and *Pax6*$^{+/+}$ age- and sex-matched mice were used when littermates were not available. The genotype of each animal was determined by PCR as previously described [38]. All experiments involving mice were conducted in strict accordance with the National Institutes of Health Guide for the Care and Use of Laboratory Animals and were performed with approval and oversight of the University of Georgia Institutional Animal Care and Use Committee.

Magnetic Resonance Imaging (MRI) Data Collection

Sixteen mice (8 *Pax6*$^{SeyNeu/+}$, 8 *Pax6*$^{+/+}$) 4-5 months (P122-153) of age, 50% male for each genotype and sixteen mice (8 *Pax6*$^{SeyNeu/+}$, 8 *Pax6*$^{+/+}$) 12-13 months (P365-396) of age, 50% male for each genotype underwent 3D MRI imaging. This study employed high resolution MRI using a 7T Agilent system to acquire structural brain images using 3D T2-weighted fast spin echo sequences (3D: TR/TE 400/44 msec, nt=4, matrix size of 128 x 128 x 128). MRI data were collected with 0.1718 mm x 0.1718 x 0.1718 mm resolution along three different directions.

MRI Volumetric Analysis

3D T2-weighted fast spin echo sequences were originally saved in flexible data format (FDF), and were converted to NIFTI file format for viewing and masking along all three axes simultaneously. Images were converted, displayed, and masked using the open source MATLAB (R2016a) toolbox Aedes version 1.0 rev 219 (http://aedes.uef.fi). Masks were created by hand using a Wacom Intuos4 tablet by manually selecting the regions of interest in each cross-

sectional image along all three axes. The Allen Brain Atlas was used for reference in determining cross-sectional masks.

The masks were then saved to NIFTI format using the Aedes option Save ROI as Mask. Volumetric analysis was performed on the masks using ImageJ. The default "Huang Dark Thresholding" method within ImageJ allowed the masks to be outlined and measured by the "Analyze Particles" method within the software. The "Analyze Particles" method outlined objects in each slice of the masks one coronal section at a time and then computed the number of voxels contained by the outline. A boundary area between 100-16300 pixels was used to prevent the algorithm from outlining the entire frame of each coronal slice. The volume of holes in individual slices was excluded for brain regions (whole brain, olfactory bulb, cortex, cerebellum), and included for eye volumes. The cross-sectional areas were then summed to obtain the total number of voxels. The total number of voxels were converted to millimeters cubed by multiplying by 0.0051 mm^3, the volume of each voxel. Examples of masks on all structures in three axes can be seen in Supplementary Figure 1.

Histological examination

For histological analysis, mice were perfused with phosphate-buffered saline (PBS) then 4% paraformaldehyde in PBS. Brains were dissected and put in same fixative overnight at 4°C. Following fixation, brains were dehydrated in methanol solutions followed by xylene then embedded in paraffin blocks for sectioning. Tissue was sectioned serially and coronally at 10 μm and stored for staining. Paraffin was removed from sections before being stained using Luxol Fast Blue (Sigma) for myelinated structures and Cresyl-Violet for cell bodies (Sigma).

Histological images were taken using a Keyence BZ-X710 fluorescent microscope (https://www.keyence.com/ss/products/microscope/bz-x700/product/index.jsp) using bright field

4x magnification and automatic stitching. For structural measurements on histological sections a Zeiss SteREO Discovery.V12 (https://www.zeiss.com/microscopy/us/products/stereo-zoom-microscopes/stereo-discovery-v12.html) dissecting microscope was used. Images for histology measurements were taken at 15x zoom (FOV 15mm) for all structures measured. For each structure measured, the measurement was taken at midline of the brain (see Figure 3 for representative images of each structure).

For all histological measurement data, analysis of sex differences was conducted; however, because no sex differences could be seen, we combined male and female mice for each group. For every structure measured there was an equal number of male and female mice. All points on the graph for histology measurements are an average for that section for the specific group. The anterior commissure, middle corpus callosum, and optic chiasm measurements were taken on the same sections, which were determined in each animal by the first section in which the anterior commissure crossed the midline to the last section where the anterior commissure crossed the midline. The anterior corpus callosum measurements were taken on twenty sections starting from the first section where the corpus callosum crossed the midline and counting 20 sections posteriorly of that for all animals measured. The posterior corpus callosum measurements were conducted in a similar way, except the measurements were taken from the last section that the corpus callosum crossed the midline and counting 20 sections anteriorly from that section. Dorsal hippocampal commissure measurements were taken on the same sections as the posterior corpus callosum, but only on the sections in which we could determine the presence of the dorsal hippocampal commissure. Posterior commissure measurements were taken on the entirety of the structure starting at the first section in which the posterior commissure could be seen crossing the midline to the last section it crossed the midline. Because of the number of

sections that the posterior commissure encompassed, we have binned the data in to 5-section averages for this structure only. Each bin represents the average of 5 consecutive sections of the posterior commissure starting at the most anterior section and moving through the structure to the last and most posterior section that included it. All measurements were taken at midline for each structure measured, Supplementary Figure 2 shows representative images for each structure and a whole brain image for location of structural measurements. ImageJ software (https://imagej.net/Welcome) was used to take the histological section measurements, and statistical analysis and graph making was done using Prism Graphpad (https://www.graphpad.com/scientific-software/prism/). Unless explicitly stated otherwise, two-way ANOVAs were performed for all statistical analyses for both brain volume and histology measurements.

3.3 Results

Whole brain analysis

The first measures we used to compare *Pax6*$^{+/+}$ brains to *Pax6*$^{SeyNeu/+}$ brains were comparisons of whole-brain gross anatomy, weight, and volume. Figure 1A shows post-perfusion whole dissected brains of both *Pax6*$^{+/+}$and *Pax6*$^{SeyNeu/+}$ mice at both age groups. There were no gross anatomical changes between genotypes or age groups, with all four brains looking very similar in both size and basic structural organization. Our second assessment of whole-brain related changes between genotypes and ages was brain weight. Brains from *Pax6*$^{SeyNeu/+}$ and *Pax6*$^{+/+}$mice were taken post-perfusion for all animals. Normalized brain weight (brain weight in grams/mouse total body weight in grams) and total brain weight were both analyzed; however, because both normalized and total brain weight showed similar results, we used total brain weight in our analysis. At both the 4-5M and 12-13M group there is no significant change

between *Pax6*$^{+/+}$and *Pax6*$^{SeyNeu/+}$ (Figure 1B). Two-way ANOVA analysis revealed no main effect of genotype ($F_{1,58}$=0.2074, p=0.6505), but did reveal a significant main effect of age ($F_{1,58}$=8.07, p=0.0062) with the 12-13M group trending at a lower brain weight for both genotypes. Total brain volume was also analyzed for group-wise changes: Figure 1C shows the distribution of volumes for both genotypes in both age groups, demonstrating no visible change across groups. Two-way ANOVA confirmed that there is no difference in total brain volume and there was no main effect of genotype ($F_{1,31}$=0.336, p=0.5664) or age ($F_{1,31}$=0.02638, p=0.8702). Additionally, sex was used as a factor in analysis, but showed no significant changes between male (closed shapes) and female (open shapes). As previously mentioned, because we saw no sex-related differences in our populations, for the rest of this study we have chosen to combine male and female data for the remaining analyses.

Regional volumetric analysis of brain regions

Although whole-brain analysis comparing the age groups and genotypes did not result in any statistically significant differences between *Pax6*$^{+/+}$and *Pax6*$^{SeyNeu/+}$, we conducted manual region of interest (ROI) volume analysis using the MRI data on 3 major parts of the brain (olfactory bulbs, cortex, and cerebellum), as well as the eyes. Developmentally, Pax6 is necessary for specification and organization of these structures and there is evidence to show Pax6 expression persists through adulthood in these brain regions. Because of this, we elected to examine some of these regions more closely using our MRI data to investigate our hypothesis that these specific regions of the brain may be altered in our *Pax6*$^{SeyNeu/+}$ mice. Additionally, research on humans with aniridia has shown global reorganization of white matter and grey matter within the brain that might account for the absence of change seen in whole-brain volume

but a potential change in distinct regions, and the MRI data are most directly comparable to these human findings [37, 39, 40].

Patients with aniridia often present with mild to severe hyposmia, and the olfactory bulb has long been investigated in studies using Pax6 mutant mice due to the high concentration of PAX6-positive cells within the olfactory bulb. Here we examined total volume of the olfactory bulbs using 3D MRI data from our cohorts. Figure 2A shows that in both age groups, the $Pax6^{SeyNeu/+}$ mice have reduced volume compared to $Pax6^{+/+}$. Two-way ANOVA analysis revealed a significant main effect of both age ($F_{1,31}$=6.7, p=0.0144) and genotype ($F_{1,31}$=6.9, p=0.0129). Interestingly, the olfactory bulbs of the $Pax6^{+/+}$mice increased by a much greater degree from the 4-5M to the 12-13M age group than the $Pax6^{SeyNeu/+}$ mice (Figure 2A).

Aniridia's most predominate features, on which most research of the disorder has focused, are the eye phenotypes. Because of this reason, we decided to look at eye volume in addition to the brain volume. Figure 2B shows eye volumes for both genotypes at each age group. The $Pax6^{SeyNeu/+}$ volumes at both age groups show significantly smaller volumes than $Pax6^{+/+}$ animals. A two-way ANOVA analysis of eye volume showed a significant main effect of both age ($F_{1,31}$=5.374, p=0.0272) and genotype ($F_{1,31}$=83.59, p<0.0001); however, post-hoc analysis using Tukey's multiple comparison test indicated that there are no significant differences between 4-5M and 12-13M $Pax6^{+/+}$ (p=0.1722) or between 4-5M and 12-13M *Pax6SeyNeu/+* (p=0.6744) suggesting that the main effect of age is a result of sample size.

The cortex has distinct regions of Pax6 expression during development, and Pax6 has been shown to be critical for normal cortical cell specification and layer organization [34, 41]. Our MRI data show that within our *Pax6* heterozygous loss-of-function mouse, $Pax6^{SeyNeu/+}$, we do not see any differences in cortex volume as a function of age or genotype (Figure 2C). The

two-way ANOVA analysis confirmed this with no main effect of age ($F_{1,31}$=1.093, p=0.304) or genotype ($F_{1,31}$=0.009873, p=0.9215) present.

Pax6 is also necessary for hindbrain and cerebellum development, and Pax6 expression persists through adulthood in this structure [31, 42, 43]. We found that cerebellum volume decreases as a function of age in *Pax6*$^{+/+}$ mice, which agrees with a previous study on the cerebellum showing a significant decrease in size, particularly in the cerebellar purkinje cells [44]. Cerebellum volumetric changes are shown in Figure 2D, demonstrating that the *Pax6*$^{+/+}$ 12-13M age group is significantly less than its 4-5M comparison; interestingly this trend does not occur within the *Pax6*$^{SeyNeu/+}$ population. Two-way ANOVA analysis revealed an interaction ($F_{1,31}$=4.713, p=0.0377), a significant main effect of age ($F_{1,31}$=5.143, p=0.0305), but no significant main effect of genotype ($F_{1,31}$=0.01571, p=0.9011). Tukey's multiple comparison post-hoc analysis showed a significant decrease in *Pax6*$^{+/+}$ cerebellum volume in the 12-13M group compared to the 4-5M group (p=0.0249); however, this was not seen in the *Pax6*$^{SeyNeu/+}$ population comparing the two age groups (p=0.9999).

Histological examination

We next turned to a histological analysis of the two genotypes across the two age groups to assess the structural consequences within the brain of loss of one functional copy of *Pax6* at a higher magnification. We assessed six structures using luxol fast blue and cresyl violet staining of paraffin embedded brain sections: the olfactory bulbs, the corpus callosum (anterior, middle, posterior), the anterior commissure, the optic chiasm, the dorsal hippocampal commissure/dorsal fornix, and the posterior commissure. Differences in many of these structures have been observed in the brains of aniridia patients versus healthy comparison subjects. Figure 3 shows example sections from *Pax6*$^{+/+}$ and *Pax6*$^{SeyNeu/+}$ mice at both 4-5M and 12-13M. The olfactory

bulb (Figure 3A,B) is slightly smaller in the *Pax6*$^{SeyNeu/+}$ compared to *Pax6*$^{+/+}$ and is larger in the 12-13M group compared to the 4-5M group. These findings are consistent with our volumetric analysis. Interestingly though, despite a reduction in size, the organization within the *Pax6*$^{SeyNeu/+}$ olfactory bulb looks remarkably similar to the *Pax6*$^{+/+}$ with all major cell layers present. Figure 3 panels C-D and accompanied magnified views found below show that there is no gross structural change in the anterior corpus callosum between genotypes or across age groups; however, the 12-13M *Pax6*$^{+/+}$ anterior corpus callosum (Figure 3D *Pax6*$^{+/+}$) does appear to be slightly thicker at midline than the other three panels. Figure 3E-F includes three of the structures examined: the middle corpus callosum, the anterior commissure, and the optic chiasm. All three structures are still present across genotype and age and only the optic chiasm shows gross differences between genotypes. The middle corpus callosum is visibly unchanged in Figure 3 panel E-F and no visible changes can be seen between genotypes at either age. The anterior commissure is also very similar across genotype and age, with the 12-13M *Pax6*$^{+/+}$ (Figure 3F *Pax6*$^{+/+}$) appearing slightly thicker than the other groups. Optic chiasms for both age groups are significantly smaller in the *Pax6*$^{SeyNeu/+}$ animals compared to *Pax6*$^{+/+}$ (Figure 3E *Pax6*$^{SeyNeu/+}$ and Figure 3F *Pax6*$^{+/+}$). The posterior corpus callosum and the dorsal hippocampal commissure are seen in Figure 3 panels G-H (PC and DHC on the figure indicate the structures: posterior commissure and dorsal hippocampal commissure, respectively). There is no discernable change in either structure as a function of age or genotype. Lastly, the posterior commissure is presented in Figure 3 panels I-J and, and like the posterior corpus callosum and the dorsal hippocampal commissure, there is no visible change across genotype or age.

Histological measurements of white matter tracts

In our recent study of white matter tracts in the brains of humans with aniridia, we noted that any differences in commissures between *PAX6*-normal individuals and individuals with aniridia were relatively small reductions of commissure diameter [21]. Therefore, to gain a deeper, quantitative understanding of the changes that could be occurring in the brains of $Pax6^{SeyNeu/+}$ animals, we measured the thickness of selected white matter tracts at the midline of the brain. The white matter tracts examined in Figure 3 were measured in 8 mice for each age group, 4 representing each genotype. Each point on the graph in Figure 4, Figure 5, and Supplementary Figure 3 represents an average for the mice in that group at that section and standard error of the mean (SEM) is represented in bars above and below each mean.

Since Pax6 is necessary for eye development and maintenance, and the histology demonstrated that the optic chiasm is significantly smaller in the $Pax6^{SeyNeu/+}$ mice, we started with this structure for measurements of thickness. Figure 4A represents the difference in $Pax6^{+/+}$ and $Pax6^{SeyNeu/+}$ optic chiasm midline thickness at the 4-5M age group. Two-way ANOVA analysis revealed a significant main effect of genotype ($F_{1,120}$=47.94, p<0.0001). Figure 4B represents the difference in $Pax6^{+/+}$ and $Pax6^{SeyNeu/+}$ optic chiasm midline thickness at the 12-13M age group. Two-way ANOVA analysis for the older age group revealed a significant main effect of genotype ($F_{1,119}$=487.1, p<0.0001). The total difference between $Pax6^{+/+}$ and $Pax6^{SeyNeu/+}$ increases as a result of age, which can be seen as the difference between means of the 4-5M group at 74 μm and the 12-13M group at 135 μm. Additionally, the SEM is reduced as a product of age. When looking at the difference in age effect of just the $Pax6^{+/+}$ or just the $Pax6^{SeyNeu/+}$, we see that only the $Pax6^{+/+}$ have a significant main effect of age (Figure 5A-B). Two-way ANOVA analysis revealed that there is a significant main effect of age ($F_{1,119}$=56.62, p<0.0001) in the $Pax6^{+/+}$ but not of section ($F_{19,119}$=0.3947, p=0.9887) (Figure 5A).

Comparisons of the *Pax6*$^{SeyNeu/+}$ optic chiasm between the 4-5M and the 12-13M age groups did not reveal a significant main effect of either age ($F_{1,120}$=0.3562, p=0.5517) or section ($F_{19,120}$=0.0482, p>0.9999) (Figure 5B).

We next systematically measured the corpus callosum at three separate points in the structure: the anterior start of the structure, the middle, and the posterior end of the structure. The corpus callosum has been shown to change in some reports on aniridia, although this has not been shown in all aniridia structural brain studies [21, 23, 26, 45]. We compared the anterior corpus callosum between genotypes at both age groups. Interestingly, at the 4-5M age, the *Pax6*$^{SeyNeu/+}$ anterior corpus callosum is thicker than the *Pax6*$^{+/+}$ (Figure 4C) while in the 12-13M group the opposite is seen with *Pax6*$^{SeyNeu/+}$ trending lower than *Pax6*$^{+/+}$ (Figure 4D). Two-way ANOVA comparing *Pax6*$^{+/+}$ to *Pax6*$^{SeyNeu/+}$ at 4-5M revealed a significant main effect of both genotype ($F_{1,120}$=58.53, p<0.0001) and section ($F_{19,120}$=11.4, p<0.0001). Two-way ANOVA comparing *Pax6*$^{+/+}$ to *Pax6*$^{SeyNeu/+}$ at the 12-13M age also revealed a significant main effect of both genotype ($F_{1,120}$=80.54, p<0.0001) and section ($F_{19,120}$=25.07, p<0.0001). The anterior corpus callosum was an interesting structure because of the change within genotype as a function of age. Figure 5C-D show the difference in the anterior corpus callosum within a genotype as a function of age. Figure 5C is *Pax6*$^{+/+}$ only separated by age, and shows a significant increase in anterior corpus callosum thickness at midline in the *Pax6*$^{+/+}$ 12-13M group compared to the 4-5M group. Two-way ANOVA analysis revealed a significant main effect of age ($F_{1,120}$=179.2, p<0.0001) and section ($F_{19,120}$=18.17, p<0.0001). The main effect of section is due to the nature of the section, with commissure thickness increasing from the most anterior section to the most posterior section in this structure. Figure 5D is *Pax6*$^{SeyNeu/+}$ only separated by age, and shows a decrease in anterior corpus callosum thickness at midline in the *Pax6*$^{+/+}$ 12-13M group compared

to the 4-5M group, opposite of the directionality of the *Pax6*$^{+/+}$ mice. Additionally, the difference in the two age groups for the *Pax6*$^{SeyNeu/+}$ only data is significantly less than in the *Pax6*$^{+/+}$ group. Two-way ANOVA analysis revealed a significant main effect of age ($F_{1,120}$=14.5, p=0.0002) and section ($F_{19,120}$=14.96, p<0.0001). All this data taken together shows that there is indeed a significant difference across genotype and age in the anterior corpus callosum and suggests that the *Pax6*$^{SeyNeu/+}$ mice change to a lesser extent as a function of age than the *Pax6*$^{+/+}$ for this structure.

The middle corpus callosum also has a significantly reduced midline thickness in *Pax6*$^{SeyNeu/+}$ mice compared to *Pax6*$^{+/+}$, however only in the 4-5M age groups. Figure 4E shows the difference in the two genotypes at the 4-5M age group, and two-way ANOVA reveals a significant main effect of genotype ($F_{1,120}$=21.77, p<0.0001) but not section ($F_{19,120}$=0.5159, p=0.9955). There is no significant effect of section in this area of the corpus callosum because the section measurements were taken in an area of the structure that had a relatively consistent thickness. The 12-13M middle corpus callosum showed no significant main effect of genotype ($F_{1,120}$=1.059, p=0.3056) or section ($F_{19,120}$=0.9566, p=0.5162) (Figure 4F). Both in *Pax6*$^{+/+}$ only and *Pax6*$^{SeyNeu/+}$ only analysis comparing just age within the genotype, the 12-13M mice had a significantly thicker middle corpus callosum than the 4-5M (Figure 5E-F). Two-way ANOVA of *Pax6*$^{+/+}$ only comparing between the 4-5M and the 12-13M age groups showed a significant main effect of age ($F_{1,120}$=7.932, p=0.0057) and section ($F_{19,120}$=1.825, p=0.0272) (Figure 5E). The same analysis conducted on the *Pax6*$^{SeyNeu/+}$ middle corpus callosum comparing 4-5M to 12-13M showed only a significant main effect of age ($F_{1,120}$=26.6, p<0.0001) but not of section ($F_{19,120}$=0.3384, p=0.9957) (Figure 5F).

Analysis of the posterior corpus callosum revealed no genotype-specific changes in commissure thickness. At the 4-5M group comparing *Pax6*$^{SeyNeu/+}$ to *Pax6*$^{+/+}$ there was no significant main effect of genotype ($F_{1,120}$=0.0775, p=0.7812), but we did find a significant main effect of section ($F_{19,120}$=5.677, p<0.0001) using a two-way ANOVA (Figure 4G). Again, this section main effect is due to the nature of how this area in the commissure was measured. We found a similar result in the posterior corpus callosum at the 12-13M age group (Figure 4H). Two-way ANOVA at this age revealed no main effect of genotype ($F_{1,120}$=0.6406, p=0.4251) but a main effect of section ($F_{19,120}$=5.097, p<0.0001). Analysis of each genotype individually revealed a significant main effect of age and section for both *Pax6*$^{+/+}$ and *Pax6*$^{SeyNeu/+}$ where both genotypes had slightly thicker commissures in the older age group (Supplementary Figure 3A-B).

We analyzed the three additional commissure that were seen in Figure 3: the anterior commissure, the posterior commissure, and the dorsal hippocampal commissure. The anterior commissure shows no difference in genotype at the 4-5M age group, but there is a significant decrease in the *Pax6*$^{SeyNeu/+}$ thickness compared to the *Pax6*$^{+/+}$ at the 12-13M age group. Figure 4I is the 4-5M age group showing the thickness at midline for the anterior commissure: the two lines representing genotypes are virtually identical and show no significant main effect of genotype ($F_{1,120}$=0.2504, p=0.6177) as analyzed by a two-way ANOVA. We do however, still see a significant main effect of section ($F_{19,120}$=12.72, p<0.0001) due to the nature of the structure. At the 12-13M age group, the anterior commissure is significantly different in the *Pax6*$^{SeyNeu/+}$ population as seen in Figure 4J where the *Pax6*$^{+/+}$ has a greater thickness than the *Pax6*$^{SeyNeu/+}$ for the majority of the commissure. Two-way ANOVA revealed a significant main effect of both genotype ($F_{1,120}$=39.39, p<0.0001) and section ($F_{19,120}$=19.25, p<0.0001).

Comparisons within genotype and between age groups revealed similar results to the anterior corpus callosum, where the *Pax6*$^{+/+}$ changed more with age than the *Pax6*$^{SeyNeu/+}$ mice did (Figure 5G-H). Two-way ANOVA of the *Pax6*$^{+/+}$ only group comparing both age groups (Figure 5G) revealed a significant main effect of both age ($F_{1,120}$=44.98, p<0.0001) and section ($F_{19,120}$=14.27, p<0.0001). The same analysis of the *Pax6*$^{SeyNeu/+}$ only group comparing both age groups (Figure 5H) revealed a significant main effect of section ($F_{19,120}$=13.41, p<0.0001) but no significant difference for age ($F_{1,120}$=2.696, p=0.1032).

Next, we quantified thickness of the posterior commissure in each group. Analysis of the posterior commissure comparing *Pax6*$^{+/+}$ to *Pax6*$^{SeyNeu/+}$ at the 4-5M age group using a two-way ANOVA revealed no significant main effect of genotype ($F_{1,70}$=0.2136, p=0.6454). Figure 4K shows the comparison, and the two genotypes look extremely similar. Interestingly, at the 12-13M age group there is a significant difference (although slight) between *Pax6*$^{+/+}$ and *Pax6*$^{SeyNeu/+}$, and two-way ANOVA analysis revealed a significant main effect of genotype ($F_{1,72}$=4.319, p=0.0413) (Figure 4L). Neither the *Pax6*$^{+/+}$ only nor the *Pax6*$^{SeyNeu/+}$ only comparisons had significant changes in posterior commissure thickness across age groups (Supplementary Figure 3C-D).

Finally, we investigated the thickness at midline of the dorsal hippocampal commissure. Because of the difficulty in identifying the difference between the dorsal fornix and the dorsal hippocampal commissure using our histological approach, they were combined for measurement analysis and referred to as the dorsal hippocampal commissure in all figures. For most of our structures analyzed, when we saw a change in the genotypes, the *Pax6*$^{SeyNeu/+}$ was generally trending below the *Pax6*$^{+/+}$; however, for the dorsal hippocampal commissure, the *Pax6*$^{SeyNeu/+}$ trends higher than the *Pax6*$^{+/+}$ in both the 4-5M and the 12-13M groups (Figure 4M-N). Figure

4M shows the difference in the two genotypes at the 4-5M age group, and two-way ANOVA analysis revealed a significant main effect of genotype ($F_{1,60}$=11.67, p=0.0011). Although the trend still shows *Pax6*$^{SeyNeu/+}$ as having a slightly thicker dorsal hippocampal commissure in the 12-13M group as well, there is only a weak significant main effect of genotype after two-way ANOVA analysis ($F_{1,60}$=3.991, p=0.05) (Figure 4N). For both Pax6+/+ and *Pax6*$^{SeyNeu/+}$, the dorsal hippocampal commissure increases significantly because of age (Supplementary Figure E-F). A summary of histological analyses can be found in Table 1.

3.4 Discussion

This study used high resolution MRI and histology to extensively investigate the structural consequences in the brain of heterozygous loss-of-function of *Pax6* at two distinct ages in the adult mouse. This is one of the only studies to employ both volumetric analyses and histological analyses to give a more global understanding of the consequences of having presumably half of the normal amount of Pax6 during both development and adulthood. Further, leveraging both techniques allows for more parallel comparisons to human studies (MRI) while affording the resolution to detect subtle changes in the tissue not detectable by non-invasive methodologies (histology). Our results indicate volumetric changes in the olfactory bulbs and the cerebellum, and in the thickness of specific commissures throughout the brain. Interestingly, it appears the changes to commissures are more severe in the most anterior structures, while the more posteriorly located commissures are not changed to the same extent. Furthermore, this study showed that while genotype played a role in structural differences, there were also significant changes in our *Pax6*$^{+/+}$ and *Pax6*$^{SeyNeu/+}$ mice as a result of age. The most interesting of these changes found was the difference in how *Pax6*$^{+/+}$ and *Pax6*$^{SeyNeu/+}$ structures changed during ageing. *Pax6*$^{SeyNeu/+}$ volume and commissure measurements stayed more consistent from

the younger age group to the older age group than the same age comparisons within *Pax6*$^{+/+}$. Collectively, these findings suggest a role for Pax6 in the plasticity of the adult brain.

There were no gross anatomical changes between the two genotypes or across age groups, as seen in Figure 1A. Our whole-brain analysis using total brain weight and whole brain volume revealed that genotype did not play a role in brain weight or volume; however, brain weight decreased with age but brain volume did not. Because we see a reduction in weight as a function of age but not volume, the density of the brain is likely changing with age. This age-related decrease in density could be attributed to increased cell death, reductions in re-myelination capacities, or a reduction of plastic cellular processes connecting neurons (i.e., axons, dendrites, dendritic spines) [46–49]. Alternatively, it is possible that this discrepancy between brain weight and volume could be a product of a lack of sensitivity to whole-brain volume in MRI analyses.

Next, MRI region of interest analysis was used to investigate volumes of the eyes and specific regions of the brain. Eye morphology has been analyzed in many studies using homozygous and heterozygous *Pax6* mutants; however, to our knowledge MRI-based volumes have yet to be measured on the *Pax6*$^{SeyNeu/+}$ mice, or any other mouse model of aniridia. We know from previous studies that eye size and morphology is changed in the *Pax6*$^{SeyNeu/+}$ mice, however here, we show for the first time that volume is significantly decreased in the *Pax6*$^{SeyNeu/+}$ eye.

The olfactory bulb volume decreased as a function of genotype, with *Pax6*$^{SeyNeu/+}$ mice having significantly smaller olfactory bulbs than *Pax6*$^{+/+}$. The olfactory bulb is also an example of differential changes during ageing in the *Pax6*$^{+/+}$ and *Pax6*$^{SeyNeu/+}$ mice. We found a significant main effect of age within the *Pax6*$^{+/+}$ olfactory bulb volumes, where the 12-13M

Pax6$^{+/+}$ olfactory bulb volume was significantly greater than the 4-5M *Pax6*$^{+/+}$ olfactory bulb volume. This change, however, was not seen in the *Pax6*$^{SeyNeu/+}$ mice, where there was virtually no difference in volume between the two age groups. Previous work has shown that with another mutant allele of Pax6 (*Sey*), that olfactory bulb morphology is changed during development [50]. Additionally, Pax6 is known to be highly expressed in the olfactory bulb during development and adulthood, and that the olfactory bulb increases with age in the *Pax6*$^{+/+}$ mouse [31, 51, 52]. What is surprising is the lack of change in the *Pax6*$^{SeyNeu/+}$ mouse olfactory bulb during ageing compared to *Pax6*$^{+/+}$. We see a very significant increase in volume in the *Pax6*$^{+/+}$ olfactory bulb from the younger to the older group that is entirely absent in the *Pax6*$^{SeyNeu/+}$ mouse. This lack of change within the olfactory bulb could be related to the role of Pax6 as a necessary transcription factor for maintaining progenitor cell populations [53]. We know from multiple studies on developmental consequences of loss of Pax6 that without it, neurons prematurely differentiate and lose their progenitor cell state [34, 53–55]. Additionally, within the adult brain, there are discreet regions of neurogenesis, one of these regions being the subventricular zone (SVZ). The SVZ is the site within the adult brain where neural stem cells produce neuroblasts that migrate through the rostral migratory stream (RMS) traveling to the olfactory bulb, where they become neurons which are important for the sense of smell [56]. We hypothesize that the haploinsufficiency of Pax6 within the *Pax6*$^{SeyNeu/+}$ adult brain either reduces the total number of adult neural progenitor cells, or reduces the progenitor cells' ability to produce neuroblasts. This reduction in number or activity of the neural progenitor cell population within the SVZ would result in fewer new neurons within the olfactory bulb in adulthood, and would explain the absence of olfactory bulb growth in our *Pax6*$^{SeyNeu/+}$ mice during the ageing process.

In addition to the olfactory bulb, Pax6 is also highly expressed by cells in the granular layer of the cerebellum. When we examine the volume of the cerebellum, we found age-related differences between the genotypes. In *Pax6*$^{+/+}$ mice, cerebellum volume decreases with age; *Pax6*$^{+/+}$ mice in the 12-13M age group have significantly smaller cerebellum volumes than *Pax6*$^{+/+}$ does in the 4-5M group. Similar to findings in the olfactory bulb, this change does not happen in the *Pax6*$^{SeyNeu/+}$ groups: both age groups have almost identical means of cerebellum volume. Cerebellum volume decreases in *Pax6*$^{+/+}$ mice during the normal ageing process, and this reduction has also been seen in humans [44, 51, 57]. In humans, it was found that Purkinje cell volume decreased as a function of age, but total number of purkinje cells did not change [57]. In the mouse, total number of purkinje cells and total number of neurons decreased during the ageing process in the cerebellum [44, 51]. It is possible that the volumetric changes we see in the *Pax6*$^{SeyNeu/+}$ mice compared to *Pax6*$^{+/+}$ in the 4-5M group, although not significant, could be due to a reduction in purkinje cell density. We were unable to assess Purkinje cell density with our current study analyses; however, future work should aim at quantifying the differences in Purkinje cells between the *Pax6*$^{+/+}$ and *Pax6*$^{SeyNeu/+}$ cerebellum at both ages. Within aniridia research, it has been hypothesized that the eye-related phenotypes might be a result of premature ageing of the structures, or an overall reduction in the numbers or ability of progenitor cell populations within the eye. It is possible that we see a similar phenomenon in the cerebellum wherein the *Pax6*$^{+/+}$ mouse at the younger age group has more neurons within the cerebellum and as ageing occurs, it loses these neurons normally and ultimately has a smaller cerebellum volume at the older time point. Following this hypothesis, the *Pax6*$^{SeyNeu/+}$ brain is more of an "aged" brain beginning at the younger time point, and because it is already in an aged state, there are fewer neurons to lose as ageing progresses. This explains the similarities in volumes seen in

the 4-5M *Pax6*$^{SeyNeu/+}$ and the older 12-13M *Pax6*$^{+/+}$, and the overall lack of change between age groups for the *Pax6*$^{SeyNeu/+}$ mice. The *Pax6*$^{SeyNeu/+}$ is already in a progenitor cell deficit at the younger time point, so there are fewer cells to lose and ultimately less volume available for age-related reduction.

We found no change in cortex volume as a result of genotype or age. This could be a true anatomical finding of the heterozygous mutant, or it could be an artifact of our resolution using 3D MRI, which does not allow for the separation and analysis of specific regions of the cortex. Within a cortex-specific *Pax6* knockout, there are significant changes to the layering and cell identity, specifically due to early cell cycle exit of progenitor cells and early cell differentiation [34]. As previously mentioned, this is not the same as the human disorder, aniridia, because *Pax6* is knocked out in just the cortex, and both alleles are affected. While this work identifies PAX6 as critical for proper cortical development, our data suggest that haploinsufficient levels of the protein are sufficient to regulate seemingly normal corticogenesis. Our *Pax6*$^{SeyNeu/+}$ mice still have one functional copy of *Pax6* which could be sufficient for normal cortex development and adult maintenance. Alternatively, the cortex may not be an area of neurogenesis in the adult, and if the progenitor cell hypothesis we proposed is correct, this would result in no real changes in the cortex as shown volumetrically.

Histological examination of both genotypes in both age groups revealed that most genotype-specific changes occurred to commissures found in the most anterior half of the brain. At both the 4-5M age group and the 12-13M age group the optic chiasm was significantly less thick in the *Pax6*$^{SeyNeu/+}$ mice compared to *Pax6*$^{+/+}$; however, the reduction was more pronounced in the older group. The reduction to optic chiasm thickness was also seen in our patient population of aniridia [21, 58]. The larger mean difference in the 12-13M age group

compared to the 4-5M age group can be explained by looking at the within genotype comparisons in Figure 5A-B. Comparing within only the *Pax6*$^{+/+}$ groups, the optic chiasm was significantly thicker at the 12-13M age than at the 4-5M age. This significant increase in optic chiasm thickness was not seen, however, in the *Pax6*$^{SeyNeu/+}$ mice, again similar to the lack of change seen in the olfactory bulb and cerebellum volume measurements. Because of the necessity of Pax6 during development of the eye, these changes could be a result of reduced input from a smaller number of retinal ganglion cells within the retina. It is generally known that the eyes of the *Pax6*$^{SeyNeu/+}$ mice are significantly smaller than the *Pax6*$^{+/+}$, partially due to a reduction in cells of the retina and therefore fewer inputs to the optic chiasm. Additionally, as the eye phenotypes get increasingly worse with age, vision becomes more difficult for the mice, and reductions to optic chiasm inputs would be likely. Collectively, this would lead to a reduction of optic chiasm thickness in the *Pax6*$^{SeyNeu/+}$ mice. The reductions we see in the optic chiasm between our genotypes are likely due to both developmental consequences of Pax6 and maintenance-related roles of Pax6 within the adult.

Measurements of the thickness of the corpus callosum revealed genotype-specific changes in the anterior and middle corpus callosum, but not in the posterior corpus callosum. The most anterior portion of the corpus callosum was significantly different between *Pax6*$^{+/+}$ and *Pax6*$^{SeyNeu/+}$ in both the 4-5M age group and the 12-13M age group. Surprisingly, in the 4-5M age group, *Pax6*$^{SeyNeu/+}$ mice had a significantly thicker anterior corpus callosum than the *Pax6*$^{+/+}$ mice, while the opposite was true at the 12-13M age group. A difference is also seen when comparing the two ages within one genotype. The *Pax6*$^{+/+}$ anterior corpus callosum is significantly thicker at midline in the 12-13M age group compared to the 4-5M group. The *Pax6*$^{SeyNeu/+}$ mice have almost an opposite result, where the 4-5M age anterior corpus callosum is

significantly thicker than the 12-13M group. The anterior corpus callosum, or the rostrum and genu, are interhemispheric crossing points for inputs from the prefrontal and premotor cortices, and this anterior area of the corpus callosum is involved with gustatory and olfactory responses [59]. Reductions in olfactory input due to reduced olfactory bulb volume in the *Pax6*$^{SeyNeu/+}$ mouse during ageing could explain the reduced thickness of the *Pax6*$^{SeyNeu/+}$ anterior corpus callosum in the 12-13M group, both comparing within genotype and between genotype. Pax6 is necessary for appropriate crossing of neurons at the midline of the brain [5, 60, 61]. As such, the increased thickness of the anterior corpus callosum in the *Pax6*$^{SeyNeu/+}$ compared to *Pax6*$^{+/+}$ at the 4-5M group could be a result of inappropriate midline crossing of fibers within the *Pax6*$^{SeyNeu/+}$ mouse. Finally, in the aniridia population, children with the disorder have difficulty deciphering what information should be paid attention to when in a loud environment such as a classroom, leading to difficulties with learning. As previously stated, the anterior corpus callosum is the interhemispheric connection for the prefrontal cortex, which is involved with sensory gating or the ability to filter irrelevant stimuli [62, 63]. The changes we see in the *Pax6*$^{SeyNeu/+}$ mice within the anterior corpus callosum, could in part explain the symptoms our patient population reports, but the resolution we can obtain with MRI analysis in patients is not of high enough to detect these subtle changes that are detectable in our mouse model.

At the middle corpus callosum in the 4-5M age group, *Pax6*$^{SeyNeu/+}$ have a significantly less thick structure than *Pax6*$^{+/+}$ but by 12-13M that difference is no longer seen, and both thicknesses is nearly the same. Although the change in the middle corpus callosum was significant in our analysis, it is important to note that the differences in the mean between *Pax6*$^{+/+}$ and *Pax6*$^{SeyNeu/+}$ is only 10 μm. This is the distance of one cell diameter, so although there is statistical significance, it is still an extremely small change in this structure. Both

Pax6$^{+/+}$ only and *Pax6*$^{SeyNeu/+}$ only comparisons of age groups revealed the 12-13M group has a thicker middle corpus callosum than the 4-5M age group. Again, for these age-related increases in thickness, it is between 10-30 μm, which is a small change. With the posterior corpus callosum, there is no change between genotypes at either the 4-5M or at 12-13M ages; however, both *Pax6*$^{+/+}$ and *Pax6*$^{SeyNeu/+}$ posterior commissures are slightly thicker as a result of age.

The anterior commissure is another structure in which age seems to play a role in the changes seen between genotypes. At the 4-5M age group, the *Pax6*$^{+/+}$ and *Pax6*$^{SeyNeu/+}$ anterior commissures are of identical thickness, but by 12-13M the *Pax6*$^{+/+}$ anterior commissure is thicker than the *Pax6*$^{SeyNeu/+}$. The anterior commissure also changes as a function of age, but only in the *Pax6*$^{+/+}$ mice. In the *Pax6*$^{+/+}$ only analysis, we showed that the 12-13M anterior commissure is significantly thicker than the 4-5M anterior commissure. In the *Pax6*$^{SeyNeu/+}$ comparison there is no significant difference between the two age groups. The anterior limb of the anterior commissure is the major interhemispheric transfer location for inputs from the olfactory bulb for regulation of the contralateral bulb [64]. The anterior commissure thickness differences are likely due to reduced inputs from the olfactory bulbs in the *Pax6*$^{SeyNeu/+}$ mouse. Similar to the olfactory bulb volume, we see no change in the *Pax6*$^{SeyNeu/+}$ anterior commissure thickness from the 4-5M group to the 12-13M group, although there is a significant change with age in the *Pax6*$^{+/+}$. This structure, like the olfactory bulb and cerebellum volume, does not seem to have the *Pax6*$^{+/+}$ level plasticity in the *Pax6*$^{SeyNeu/+}$ mouse.

The only comparison in which the posterior commissure is changed is in the 12-13M comparison where the *Pax6*$^{SeyNeu/+}$ posterior commissure (mean of 84 μm) is slightly less thick than the *Pax6*$^{+/+}$ (mean of 96 μm) at that age, but less than a 40 μm change at the greatest point of difference. All other comparisons show no change to the posterior commissure. Lastly, within

both the 4-5M and the 12-13M groups the *Pax6*$^{SeyNeu/+}$ dorsal hippocampal commissure trended thicker than the *Pax6*$^{+/+}$, though this was only statistically significant in the 4-5M group. Analysis of the dorsal hippocampal commissure within genotype revealed that in both genotypes, the 12-13M had thicker dorsal hippocampal commissures.

During development Pax6, is expressed in a rostral (anterior) to caudal (posterior) gradient within the brain where the highest level of Pax6 expression is in the rostral brain with decreasing amount of Pax6 expressed as you move caudally [65, 66]. This results in structures in the most anterior part of the brain see the highest levels of Pax6 during development, structures in the mid part of the brain see moderate levels of Pax6 during development, and the most posteriorly located structures see the lowest levels of Pax6 during development. Because of this, it can be hypothesized that if you were to lose half of your functional Pax6, structures that require the highest levels of Pax6 during development might be changed to the greatest degree when those levels shift, and structures that required the least amount of Pax6 may not be affected quite as heavily. This shift in expression and gradient could lead to the most anterior structures being the most developmentally affected as a result of Pax6-deficiency, which is indeed what we saw with our histological data: the anterior corpus callosum, anterior commissure, and optic chiasm were the most severely affected, and the posterior structures had fewer changes between genotype.

One of the most interesting findings in this study is the level of relative normalcy in the *Pax6*$^{SeyNeu/+}$ mouse brains, especially in the context of how the eye is altered in the *Pax6*$^{SeyNeu/+}$ mouse. Our study found structures that are altered, but no structure is missing or severely malformed. In the aniridia population that our lab has studied using structural MRI, we found that the structures were changed in a much less severe manner than previously reported. The

results we saw in our mouse model, *Pax6*$^{SeyNeu/+}$, echo these patient findings in that most structures were nearly normal with only slight changes in thickness in specific structures. This study also found that using MRI can detect global changes in volume for large regions of the brain, but for smaller structures we could not detect any changes in our mice. This suggests that within the human population there may be more subtle changes present that we are unable to detect with the current tools available. This enforces the utility of having a study paradigm where we can leverage similar tools in our animal model that are available for human measurement, but additionally use higher resolution techniques for a more thorough investigation that leads to new discoveries and a better understanding of the consequences of the disorder. Although future work in this area of inquiry is necessary, the present study suggests that the structural changes we see in the mouse brain could be due to a reduction in capacity or number of adult neurogenic progenitor cell populations within the adult brain rather than a mostly developmentally driven change. Historically, Pax6 has been viewed as a developmentally required gene, however our study suggests that its role in adulthood could be more important than previously thought.

3.5 References

1. Grindley JC, Davidson DR, Hill RE (1995) The role of Pax-6 in eye and nasal development. Development 121:1433–42
2. Walther C, Gruss P (1991) Pax-6, a murine paired box gene, is expressed in the developing CNS. Development 113:
3. Sander M, Neubuser A, Kalamaras J, et al (1997) Genetic analysis reveals that PAX6 is required for normal transcription of pancreatic hormone genes and islet development. Genes Dev 11:1662–1673
4. Stoykova A, Gruss P (1994) Roles of Pax-genes in developing and adult brain as suggested by expression patterns. J Neurosci 14:1395–1412
5. Mastick GS, Davis NM, Andrew GL, Easter Jr. SS (1997) Pax-6 functions in boundary formation and axon guidance in the embryonic mouse forebrain. Development 124:1985–1997
6. Manuel M, Price DJ (2005) Role of Pax6 in forebrain regionalization. Brain Res Bull 66:387–393. https://doi.org/10.1016/j.brainresbull.2005.02.006
7. Simpson TI, Price DJ (2002) Pax6; a pleiotropic player in development. Bioessays 24:1041–1051. https://doi.org/10.1002/bies.10174
8. Osumi N (2001) The role of Pax6 in brain patterning. Tohoku J Exp Med 193:163–174
9. Stoykova A, Fritsch R, Walther C, Gruss P (1996) Forebrain patterning defects in Small eye mutant mice. Development 122:3453–65
10. Bishop KM, Goudreau G, O'Leary DD (2000) Regulation of area identity in the mammalian neocortex by Emx2 and Pax6. Science (80-) 288:344–9.
11. Stoykova A, Gotz M, Gruss P, Price J (1997) Pax6-dependent regulation of adhesive

patterning, R-cadherin expression and boundary formation in developing forebrain. Development 124:3765–3777

12. Fujiwara M, Uchida T, Osumi-Yamashita N, Eto K (1994) Uchida rat (rSey): a new mutant rat with craniofacial abnormalities resembling those of the mouse Sey mutant. Differentiation 57:31–8.

13. Hill RE, Favor J, Hogan BL, et al (1992) Mouse Small eye results from mutations in a paired-like homeobox-containing gene. Nature 355:750

14. Numayama-Tsuruta K, Arai Y, Osumi N (2007) The rat Small eye homozygote (rSey2/rSey2) can be regarded as a Pax6 null mutant. In: Esashi M, Ishii K, Ohuchi N, et al (eds) Future Medical Engineering Based on Bionanotechnology: Proceedings of the Final Symposium of the Tohoku University 21st Century Center for Excellence Program. Imperial College Press, pp 151–161

15. Glaser T, Lane J, Housman D (1990) A mouse model of the aniridia-Wilms tumor deletion syndrome. Science (80-) 250:823–827

16. Ton CC, Miwa H, Saunders GF (1992) Small eye (Sey): cloning and characterization of the murine homolog of the human aniridia gene. Genomics 13:251–256

17. Glaser T, Walton DS, Maas RL (1992) Genomic structure, evolutionary conservation and aniridia mutations in the human PAX6 gene. Nat Genet 2:232–239. https://doi.org/10.1038/ng1192-232

18. Glaser T, Jepeal L, Edwards JG, et al (1994) PAX6 gene dosage effect in a family with congenital cataracts, aniridia, anophthalmia and central nervous system defects [published erratum appears in Nat Genet 1994 Oct;8(2):203]. Nat Genet 7:463–471

19. Bobilev AM, McDougal ME, Taylor WL, et al (2015) Assessment of PAX6 alleles in 66

families with aniridia. Clin Genet. https://doi.org/10.1111/cge.12708

20. Prosser J, van Heyningen V (1998) PAX6 mutations reviewed. Hum Mutat 11:93–108. https://doi.org/10.1002/(SICI)1098-1004(1998)11:2<93::AID-HUMU1>3.0.CO;2-M

21. Grant MK, Bobilev AM, Pierce JE, et al (2017) Structural brain abnormalities in 12 persons with aniridia. F1000Research 6:255. https://doi.org/10.12688/f1000research.11063.2

22. Mitchell TN, Stevens JM, Free SL, et al (2002) Anterior commissure absence without callosal agenesis: a new brain malformation. Neurology 58:1297–9

23. Bamiou DE, Musiek FE, Sisodiya SM, et al (2004) Deficient auditory interhemispheric transfer in patients with PAX6 mutations. Ann Neurol 56:503–509. https://doi.org/10.1002/ana.20227

24. Bamiou DE, Free SL, Sisodiya SM, et al (2007) Auditory interhemispheric transfer deficits, hearing difficulties, and brain magnetic resonance imaging abnormalities in children with congenital aniridia due to PAX6 mutations. Arch Pediatr Adolesc Med 161:463–469. https://doi.org/10.1001/archpedi.161.5.463

25. Sisodiya SM, Free SL, Williamson KA, et al (2001) PAX6 haploinsufficiency causes cerebral malformation and olfactory dysfunction in humans. Nat Genet 28:214–216. https://doi.org/10.1038/90042

26. Abouzeid H, Youssef MA, ElShakankiri N, et al (2009) PAX6 aniridia and interhemispheric brain anomalies. Mol Vis 15:2074–83

27. Mitchell TN, Free SL, Williamson KA, et al (2003) Polymicrogyria and absence of pineal gland due to PAX6 mutation. Ann Neurol 53:658–663. https://doi.org/10.1002/ana.10576

28. Hanish AE, Butman JA, Thomas F, et al (2015) Pineal hypoplasia, reduced melatonin and

sleep disturbance in patients with PAX6 haploinsufficiency. J Sleep Res. https://doi.org/10.1111/jsr.12345

29. Shimo N, Yasuda T, Kitamura T, et al (2014) Aniridia with a heterozygous PAX6 mutation in which the pituitary function was partially impaired. Intern Med 53:39–42

30. Pierce JE, Krafft CE, Rodrigue AL, et al (2014) Increased functional connectivity in intrinsic neural networks in individuals with aniridia. Front Hum Neurosci 8:1013. https://doi.org/10.3389/fnhum.2014.01013

31. Duan D, Fu Y, Paxinos G, Watson C (2013) Spatiotemporal expression patterns of Pax6 in the brain of embryonic, newborn, and adult mice. Brain Struct Funct 218:353–372. https://doi.org/10.1007/s00429-012-0397-2

32. Boretius S, Michaelis T, Tammer R, et al (2009) In vivo MRI of altered brain anatomy and fiber connectivity in adult pax6 deficient mice. Cereb Cortex 19:2838–2847. https://doi.org/10.1093/cercor/bhp057

33. Piñon MC, Tuoc TC, Ashery-Padan R, et al (2008) Altered molecular regionalization and normal thalamocortical connections in cortex-specific Pax6 knock-out mice. J Neurosci 28:8724–34. https://doi.org/10.1523/JNEUROSCI.2565-08.2008

34. Tuoc TC, Radyushkin K, Tonchev AB, et al (2009) Selective cortical layering abnormalities and behavioral deficits in cortex-specific Pax6 knock-out mice. J Neurosci 29:8335–49. https://doi.org/10.1523/JNEUROSCI.5669-08.2009

35. Hill RE, Favor J, Hogan BL, et al (1991) Mouse small eye results from mutations in a paired-like homeobox-containing gene. Nature 354:522–525. https://doi.org/10.1038/354522a0

36. Vincent M-C, Pujo A-L, Olivier D, Calvas P (2003) Screening for PAX6 gene mutations

is consistent with haploinsufficiency as the main mechanism leading to various ocular defects. Eur J Hum Genet 11:163–9. https://doi.org/10.1038/sj.ejhg.5200940

37. Yogarajah M, Matarin M, Vollmar C, et al (2016) PAX6 , brain structure and function in human adults: advanced MRI in aniridia. Ann Clin Transl Neurol. https://doi.org/10.1002/acn3.297

38. Kim J, Lauderdale JD (2006) Analysis of Pax6 expression using a BAC transgene reveals the presence of a paired-less isoform of Pax6 in the eye and olfactory bulb. Dev Biol 292:486–505

39. Free SL, Mitchell TN, Williamson KA, et al (2003) Quantitative MR image analysis in subjects with defects in the PAX6 gene. Neuroimage 20:2281–2290

40. Ellison-Wright Z, Heyman I, Frampton I, et al (2004) Heterozygous PAX6 mutation, adult brain structure and fronto-striato-thalamic function in a human family. Eur J Neurosci 19:1505–12. https://doi.org/10.1111/j.1460-9568.2004.03236.x

41. Georgala PA, Manuel M, Price DJ (2011) The generation of superficial cortical layers is regulated by levels of the transcription factor Pax6. Cereb Cortex 21:81–94. https://doi.org/10.1093/cercor/bhq061

42. Engelkamp D, Rashbass P, Seawright A, van Heyningen V (1999) Role of Pax6 in development of the cerebellar system. Development 126:3585–96.

43. Kayam G, Kohl A, Magen Z, et al (2013) A novel role for Pax6 in the segmental organization of the hindbrain. Development 140:2190–202. https://doi.org/10.1242/dev.089136

44. Woodruff-Pak DS, Foy MR, Akopian GG, et al (2010) Differential effects and rates of normal aging in cerebellum and hippocampus. Proc Natl Acad Sci U S A 107:1624–9.

https://doi.org/10.1073/pnas.0914207107

45. Bamiou D-E, Campbell NG, Musiek FE, et al (2007) Auditory and verbal working memory deficits in a child with congenital aniridia due to a PAX6 mutation. Int J Audiol 46:196–202. https://doi.org/10.1080/14992020601175952

46. Raz N (2004) The aging brain: Structural changes and their implications for cognitive aging. In: New Frontiers in Cognitive Aging. Oxford University Press, pp 115–134

47. Peters R (2006) Ageing and the brain. Postgrad Med J 82:84. https://doi.org/10.1136/PGMJ.2005.036665

48. Shields SA, Gilson JM, Blakemore WF, Franklin RJ (1999) Remyelination occurs as extensively but more slowly in old rats compared to young rats following gliotoxin-induced CNS demyelination. Glia 28:77–83

49. Svennerholm L, Boström K, Jungbjer B (1997) Changes in weight and compositions of major membrane components of human brain during the span of adult human life of Swedes. Acta Neuropathol 94:345–52

50. Dellovade TL, Pfaff DW, Schwanzel-Fukuda M (1998) Olfactory bulb development is altered in small-eye (Sey) mice. J Comp Neurol 402:402–18

51. Fu Y, Yu Y, Paxinos G, et al (2015) Aging-dependent changes in the cellular composition of the mouse brain and spinal cord. Neuroscience 290:406–420. https://doi.org/10.1016/J.NEUROSCIENCE.2015.01.039

52. Mirich JM, Williams NC, Berlau DJ, Brunjes PC (2002) Comparative Study of Aging in the Mouse Olfactory Bulb. J Comp Neurol 454:361–372. https://doi.org/10.1002/cne.10426

53. Curto GG, Nieto-Estévez V, Hurtado-Chong A, et al (2014) Pax6 is essential for the

maintenance and multi-lineage differentiation of neural stem cells, and for neuronal incorporation into the adult olfactory bulb. Stem Cells Dev 23:2813–30. https://doi.org/10.1089/scd.2014.0058

54. Asami M, Pilz GA, Ninkovic J, et al (2011) The role of Pax6 in regulating the orientation and mode of cell division of progenitors in the mouse cerebral cortex. Development 138:5067–5078. https://doi.org/10.1242/dev.074591

55. Maekawa M, Takashima N, Arai Y, et al (2005) Pax6 is required for production and maintenance of progenitor cells in postnatal hippocampal neurogenesis. Genes to Cells 10:1001–1014. https://doi.org/10.1111/j.1365-2443.2005.00893.x

56. Lennington JB, Yang Z, Conover JC (2003) Neural stem cells and the regulation of adult neurogenesis. Reprod Biol Endocrinol 1:99. https://doi.org/10.1186/1477-7827-1-99

57. Andersen BB, Gundersen HJG, Pakkenberg B (2003) Aging of the human cerebellum: A stereological study. J Comp Neurol 466:356–365. https://doi.org/10.1002/cne.10884

58. Burton CR, Schaeffer DJ, Bobilev AM, et al (2018) Microstructural differences in visual white matter tracts in people with aniridia. Neuroreport 1. https://doi.org/10.1097/WNR.0000000000001135

59. Fabri M, Polonara G, Mascioli G, et al (2011) Topographical organization of human corpus callosum: An fMRI mapping study. Brain Res 1370:99–111. https://doi.org/10.1016/J.BRAINRES.2010.11.039

60. Hevner RF, Miyashita-Lin E, Rubenstein JLR (2002) Cortical and thalamic axon pathfinding defects in Tbr1, Gbx2, and Pax6 mutant mice: evidence that cortical and thalamic axons interact and guide each other. J Comp Neurol 447:8–17. https://doi.org/10.1002/cne.10219

61. Jones L, Lopez-Bendito G, Gruss P, et al (2002) Pax6 is required for the normal development of the forebrain axonal connections. Development 129:5041–5052

62. Boutros NN, Belger A (1999) Midlatency evoked potentials attenuation and augmentation reflect different aspects of sensory gating. Biol Psychiatry 45:917–922. https://doi.org/10.1016/S0006-3223(98)00253-4

63. Knight RT, Staines WR, Swick D, Chao LL (1999) Prefrontal cortex regulates inhibition and excitation in distributed neural networks. Acta Psychol (Amst) 101:159–78

64. Brunjes PC (2012) The mouse olfactory peduncle. 2.The anterior limb of the anterior commissure. Front Neuroanat 6:51. https://doi.org/10.3389/fnana.2012.00051

65. Stoykova A, Gruss P, Rubenstein JLR, Alvarez-Buylla A (1994) Roles of Pax-genes in developing and adult brain as suggested by expression patterns. J Neurosci 14:1395–412. https://doi.org/20026588

66. Grindley JC, Hargett LK, Hill RE, et al (1997) Disruption of PAX6 function in mice homozygous for the Pax6Sey-1Neu mutation produces abnormalities in the early development and regionalization of the diencephalon. Mech Dev 64:111–26

Table 3.1: Results from histological measurements of all structures examined.

	4-5M Genotype Comparison	**12-13M Genotype Comparison**	***Pax6*$^{+/+}$ Age Comparison**	***Pax6*$^{SeyNeu/+}$ Age Comparison**
Optic Chiasm	*Pax6*$^{+/+}$ > *Pax6*$^{SeyNeu/+}$	*Pax6*$^{+/+}$ > *Pax6*$^{SeyNeu/+}$	12M > 4M	No Change
Anterior Corpus Callosum	*Pax6*$^{SeyNeu/+}$ > *Pax6*$^{+/+}$	*Pax6*$^{+/+}$ > *Pax6*$^{SeyNeu/+}$	12M > 4M	4M > 12M
Middle Corpus Callosum	*Pax6*$^{+/+}$ > *Pax6*$^{SeyNeu/+}$	No Change	12M > 4M	12M > 4M
Posterior Corpus Callosum	No Change	No Change	12M > 4M	12M > 4M
Anterior Commissure	No Change	*Pax6*$^{+/+}$ > *Pax6*$^{SeyNeu/+}$	12M > 4M	No Change
Posterior Commissure	No Change	*Pax6*$^{+/+}$ > *Pax6*$^{SeyNeu/+}$ †	No Change	No Change
Dorsal Hippocampal Commissure	*Pax6*$^{SeyNeu/+}$ > *Pax6*$^{+/+}$	No Change	12M > 4M	12M > 4M

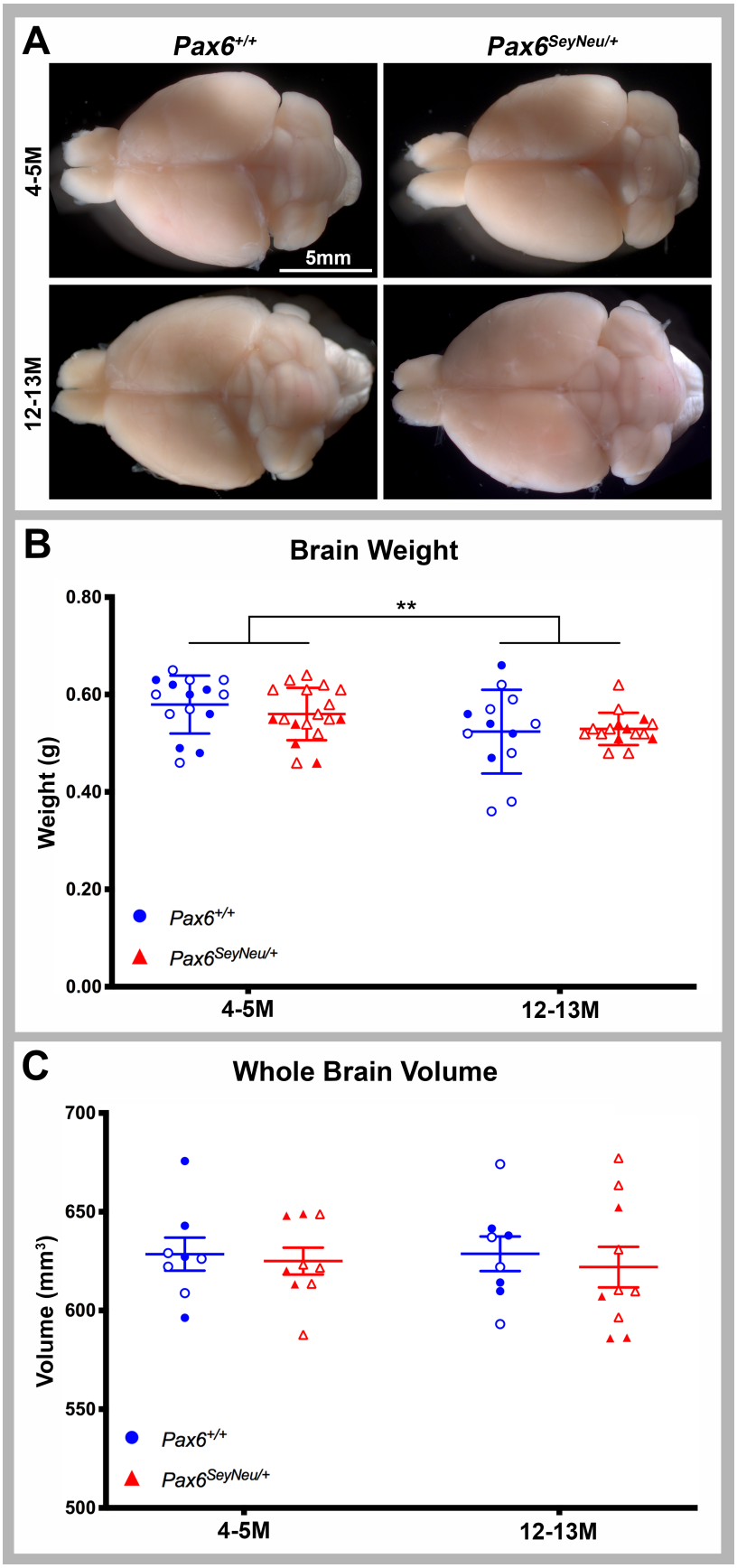
A
Pax6+/+
Pax6SeyNeu/+
4-5M
12-13M
5mm
B
Brain Weight
**
Weight (g)
0.80
0.60
0.40
0.20
0.00
Pax6+/+
Pax6SeyNeu/+
4-5M
12-13M
C
Whole Brain Volume
Volume (mm3)
700
650
600
550
500
Pax6+/+
Pax6SeyNeu/+
4-5M
12-13M

Figure 3.1: Whole brain analyses revealed no change between *Pax6*$^{+/+}$ and *Pax6*$^{SeyNeu/+}$ in gross anatomy, brain weight, or brain volume. A Dissected whole brains of both genotypes and both ages showed no gross anatomical changes. **B-C** Blue circles represent *Pax6*$^{+/+}$ and red triangles represent *Pax6*$^{SeyNeu/+}$. Closed shapes represent males and open shapes represent females. Age groups are on the x-axis. Stars represent degrees of significance as assessed by two-way ANOVA. **B** Total brain weight did not reveal any genotype effects, but did reveal a significant main effect of age ($F_{1,58}$=8.07, p=0.0062). **C** There were no significant differences in whole brain volume assessed by MRI for genotype or age

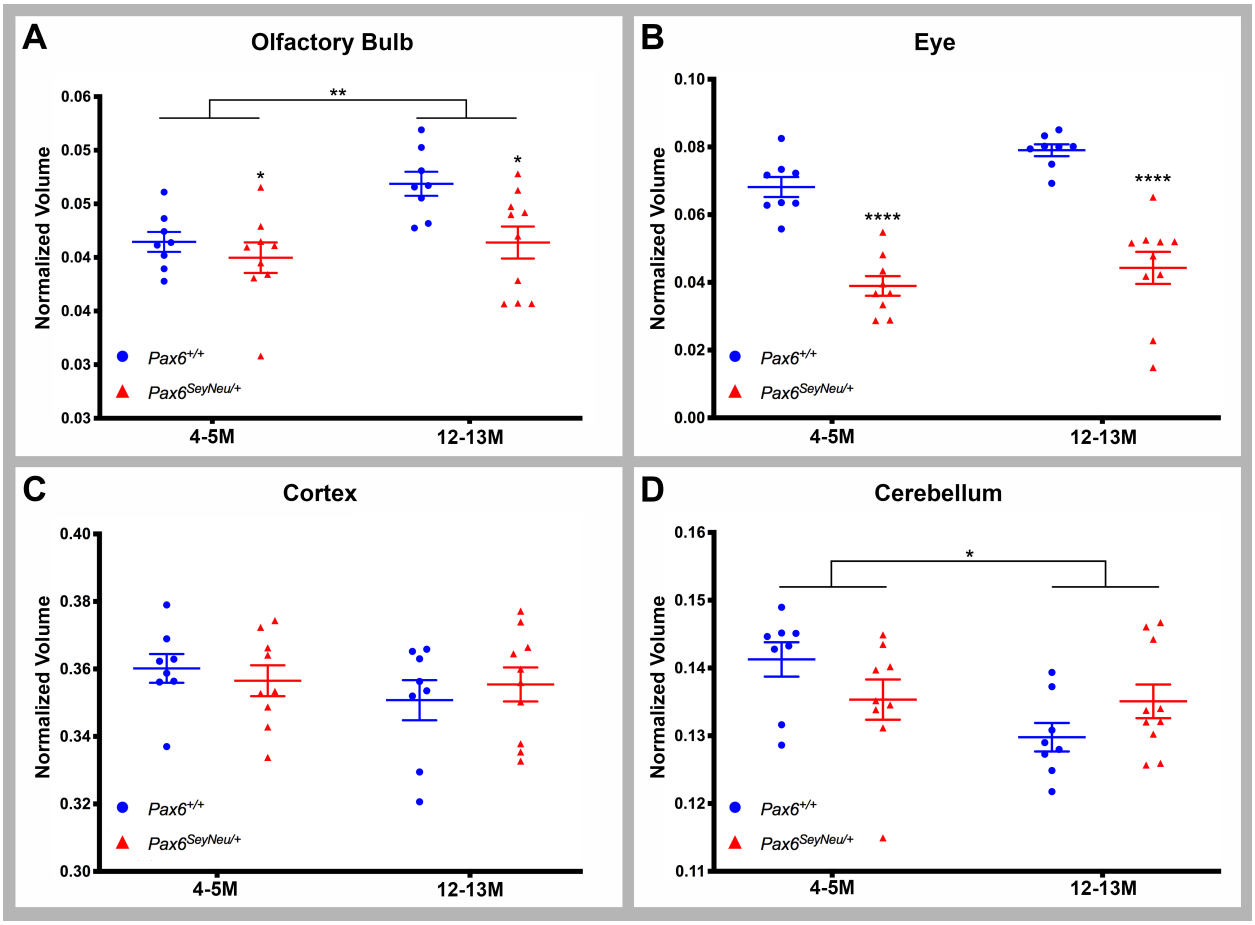

Figure 3.2: Volume of the olfactory bulbs and eyes are significantly different from *Pax6*$^{+/+}$ in the *Pax6*$^{SeyNeu/+}$ mice. A-D Blue circles represent *Pax6*$^{+/+}$ and red triangles represent *Pax6*$^{SeyNeu/+}$. For each panel, age groups are on the x-axis and normalized volume (structure volume/whole brain volume) is on the y-axis. Mean is represented as middle line in each group and standard error of the mean (SEM) is represented in bars above and below each mean. Stars represent degrees of significance as assessed by two-way ANOVA. **A** Olfactory bulb volume in *Pax6*$^{SeyNeu/+}$ mice changed as a result of age and genotype. Two-way ANOVA analysis revealed a significant main effect of both age ($F_{1,31}$=6.7, p=0.0144) and genotype ($F_{1,31}$=6.9, p=0.0129). **B** Eye volume is significantly less in *Pax6*$^{SeyNeu/+}$ compared to *Pax6*$^{+/+}$ ($F_{1,31}$=83.59, p<0.0001). **C** Cortex volume showed no differences as a result of age or genotype. **D** Cerebellum volume was

not significantly different comparing genotypes but did show a main effect of age ($F_{1,31}$=5.143, p=0.0305) and an interaction ($F_{1,31}$=5.143, p=0.0305)

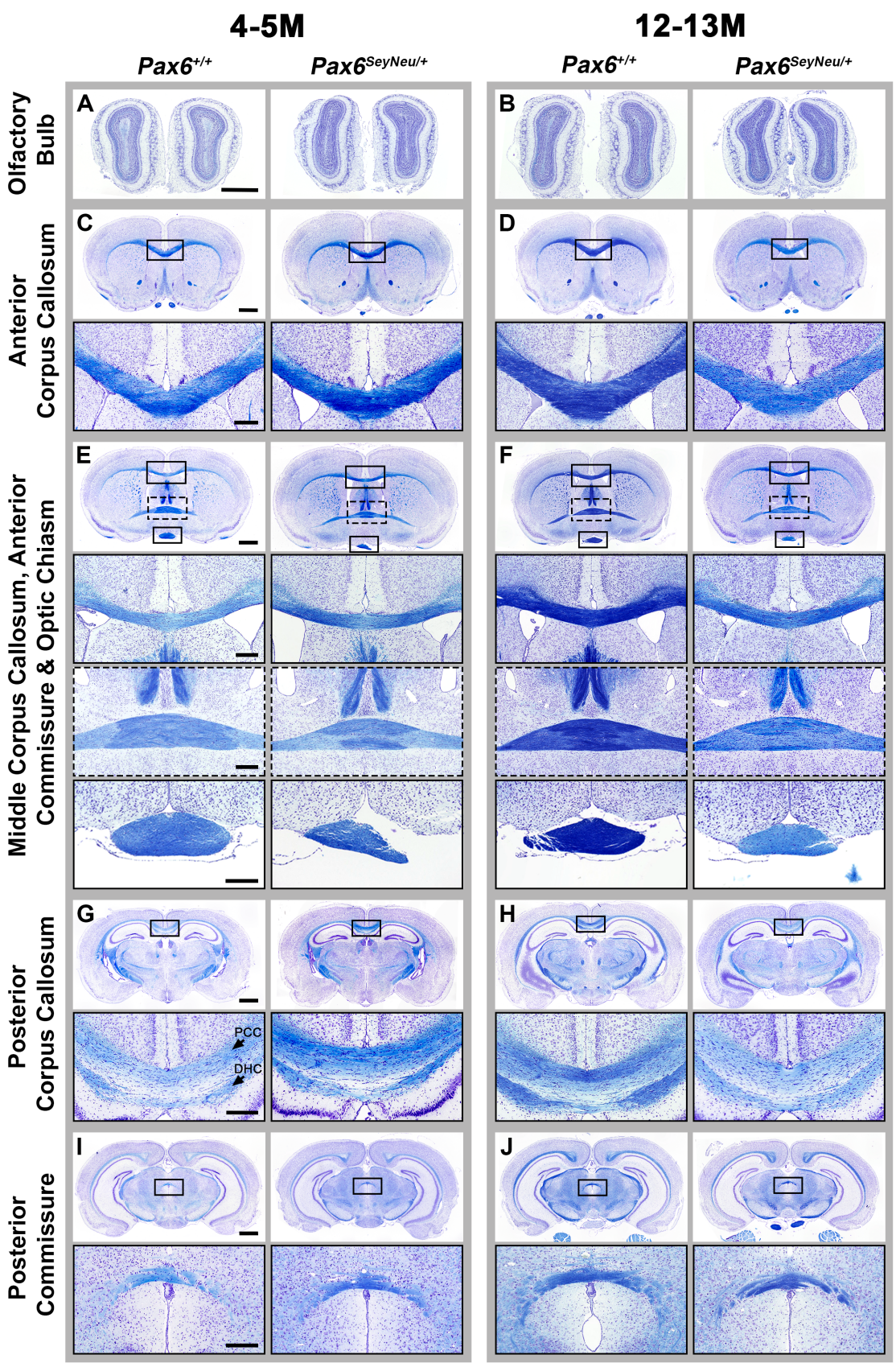
4-5M
12-13M
Pax6+/+
Pax6SeyNeu/+
Pax6+/+
Pax6SeyNeu/+
Olfactory Bulb
Anterior Corpus Callosum
Middle Corpus Callosum, Anterior Commissure & Optic Chiasm
Posterior Corpus Callosum
Posterior Commissure
A
B
C
D
E
F
G
H
I
J
PCC
DHC

Figure 3.3: Histological analysis revealed subtle changes to the olfactory bulbs, anterior corpus callosum, and optic chiasm. A-J Luxol blue (myelinated structures) and cresyl violet (cell bodies) stained 10 μm coronal sections. Age groups and genotype are along the top of the figure. Structure is along the left side of the figure. Scale bars are 1mm for zoomed-out images (A-J) and 250 μm for magnified views of each structure. Scale bars in left-most column are representative for all figures in respective row. **A-B** Olfactory bulb. **C-D** Anterior corpus callosum. **E-F** Middle corpus callosum, anterior commissure, and optic chiasm. **G-H** Posterior corpus callosum and dorsal hippocampal commissure (marked as PCC and DHC in magnified inlays). **I-J** Posterior commissure

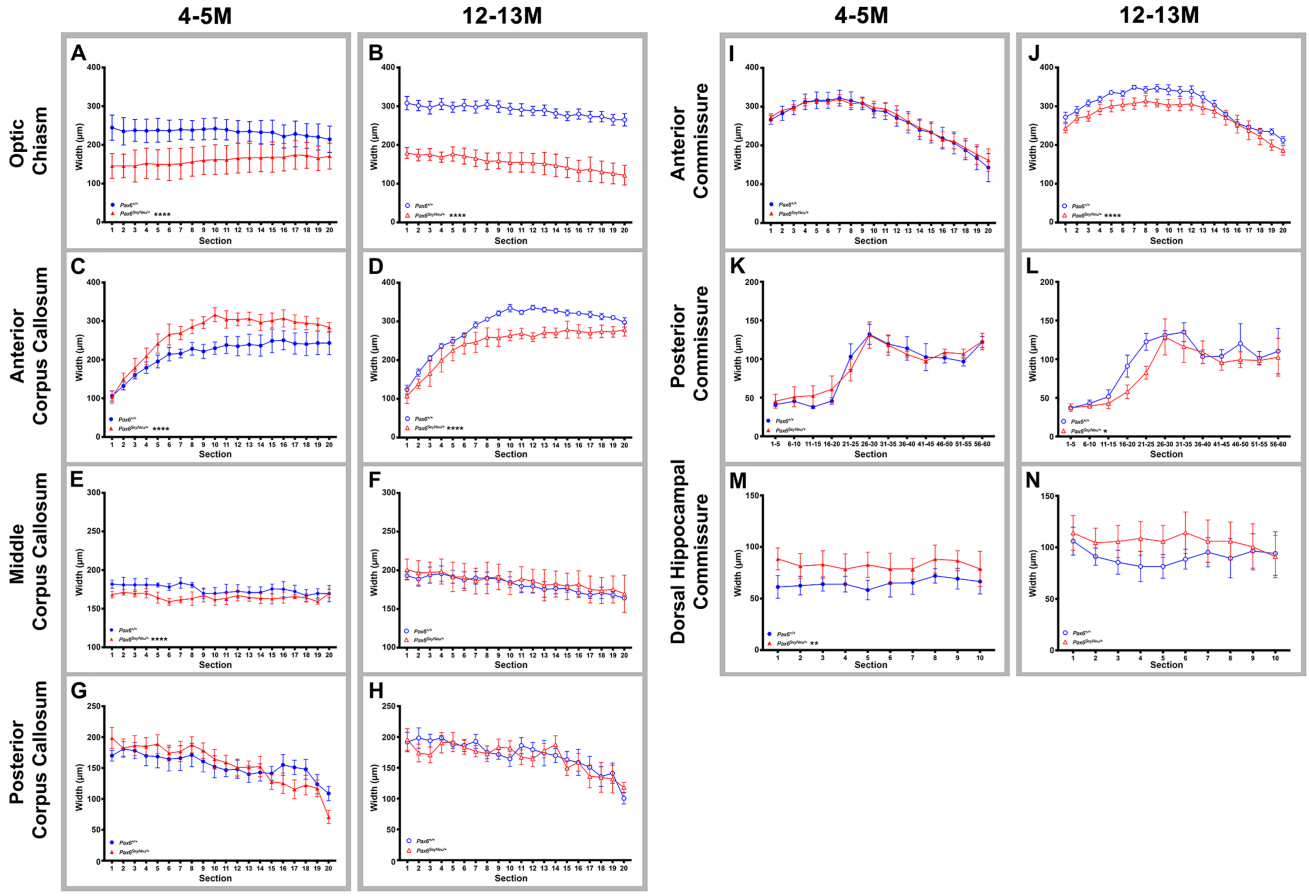

Figure 3.4: Histology measurements reveal genotype-specific changes in the optic chiasm, anterior corpus callosum, middle corpus callosum and anterior commissure. Blue circles represent *Pax6*$^{+/+}$ and red triangles represent *Pax6*$^{SeyNeu/+}$. Closed circles and triangles represent the 4-5M group, and open circles and triangles represent the 12-13M group. Mean is represented as the point and standard error of the mean (SEM) is represented in bars above and below each mean. The y-axis is width of the structure at midline measured in millimeters. The x-axis is section number starting anteriorly (ex. 1) and moving posteriorly (ex. 20). Significance is represented in figure legend with stars representing level of significance. **A, C, E, G, I, K, M** Comparisons between genotypes for the 4-5M age group. **B, D, F, H, J, L, N** Comparisons between genotypes for the 12-13M age group. **A,B** Optic chiasm is significantly less thick in the *Pax6*$^{SeyNeu/+}$ mice compared to *Pax6*$^{+/+}$ mice at both the 4-5M ($F_{1,120}$=47.94, p<0.0001) and 12-

13M ($F_{1,119}$=487.1, p<0.0001) age groups. **C,D** At the 4-5M age the anterior corpus callosum is significantly thicker in the *Pax6*$^{SeyNeu/+}$ mice ($F_{1,120}$=58.53, p<0.0001); at the 12-13M group, the anterior corpus callosum is significantly thicker in the *Pax6*$^{+/+}$ mice ($F_{1,120}$=80.54, p<0.0001). **E,F** The middle corpus callosum is slightly thicker in the *Pax6*$^{+/+}$ mice at 4-5M ($F_{1,120}$=21.77, p<0.0001), but there is no change at 12-13M. **G,H** There was no difference between genotypes for the posterior corpus callosum at either age group. **I,J** The anterior commissure was the same for both genotypes at the 4-5M group, but the *Pax6*$^{+/+}$ commissure was significantly thicker at the 12-13M group $F_{1,120}$=39.39, p<0.0001). **K,L** The posterior commissure was very similar for both genotypes at both age groups, with only a slightly thicker commissure in the 12-13M *Pax6*$^{+/+}$ ($F_{1,72}$=4.319, p=0.0413). **M,N** Dorsal hippocampal commissure is thicker in *Pax6*$^{SeyNeu/+}$ at the 4-5M age group ($F_{1,60}$=11.67, p=0.0011)

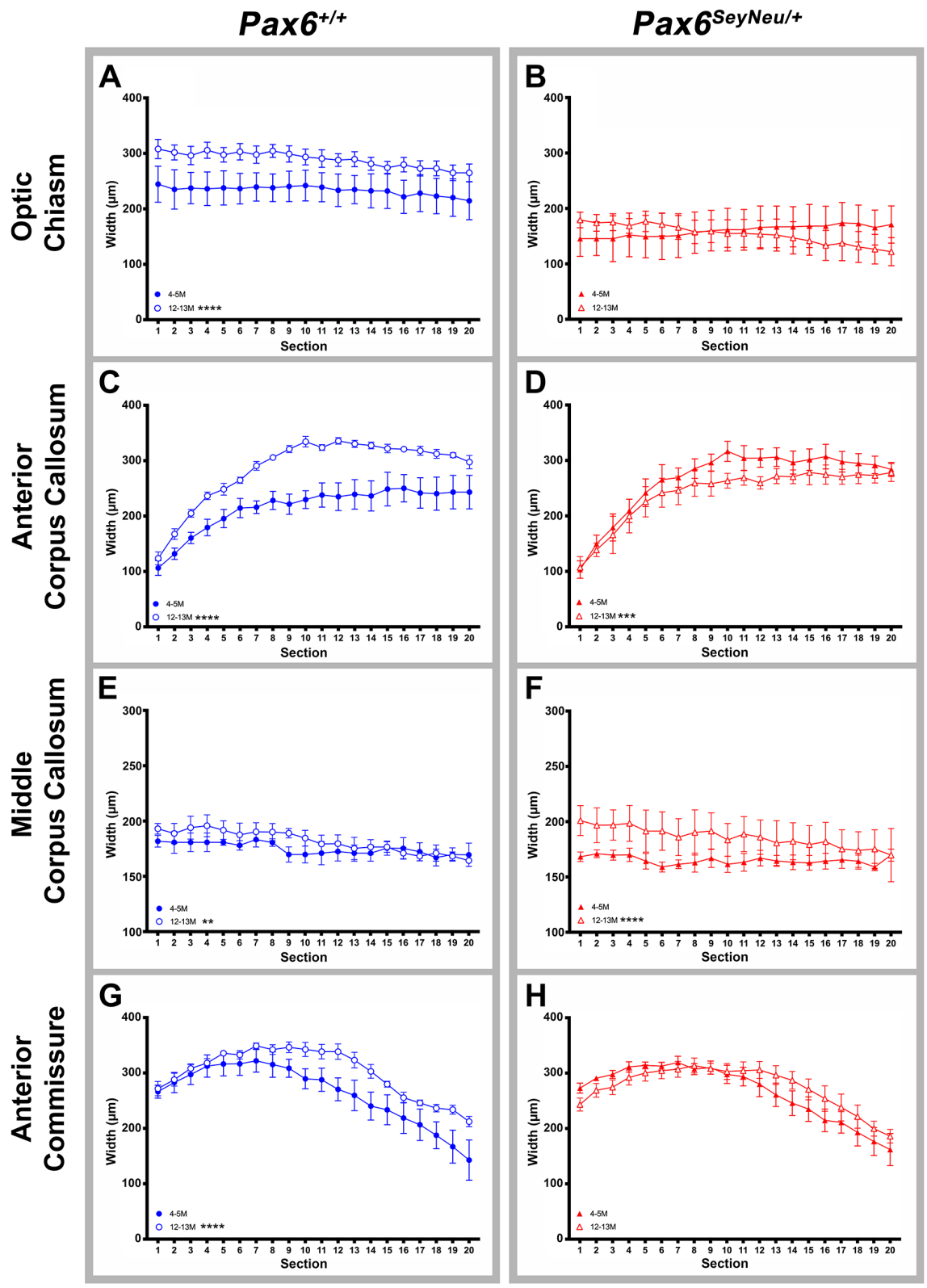
Pax6+/+
Pax6SeyNeu/+
Optic Chiasm
Anterior Corpus Callosum
Middle Corpus Callosum
Anterior Commissure
A
B
C
D
E
F
G
H
Width (µm)
Section
4-5M
12-13M ****
12-13M ***
12-13M **
12-13M

Figure 3.5: Age-related changes are seen in the optic chiasm, anterior corpus callosum, middle corpus callosum, and anterior commissure. Blue circles represent *Pax6*$^{+/+}$ and red triangles represent *Pax6*$^{SeyNeu/+}$. Closed circles and triangles represent the 4-5M group, and open circles and triangles represent the 12-13M group. Mean is represented as the point and standard error of the mean (SEM) is represented in bars above and below each mean. The y-axis is width of the structure at midline measured in millimeters. The x-axis is section number starting anteriorly (ex. 1) and moving posteriorly (ex. 20). Significance is represented in figure legend with stars representing level of significance. **A, C, E, G** *Pax6*$^{+/+}$ only comparisons with both age groups. **B, D, F, H** *Pax6*$^{SeyNeu/+}$ only comparisons with both age groups. **A, B** The optic chiasm is only significantly different between age groups for the *Pax6*$^{+/+}$ only group ($F_{1,119}$=56.62, p<0.0001). **C,D** Both *Pax6*$^{+/+}$ ($F_{1,120}$=179.2, p<0.0001) only and *Pax6*$^{SeyNeu/+}$ ($F_{1,120}$=14.5, p=0.0002) only shows a significant difference between ages. **E,F** In the middle corpus callosum, both the *Pax6*$^{+/+}$ only ($F_{1,120}$=7.932, p=0.0057) and the *Pax6*$^{SeyNeu/+}$ only ($F_{1,120}$=26.6, p<0.0001) 12-13M groups are thicker than the 4-5M groups. **G,H** Age comparisons of the anterior commissure show significant differences in the *Pax6*$^{+/+}$ only ($F_{1,120}$=44.98, p<0.0001) group but not the *Pax6*$^{SeyNeu/+}$ only group

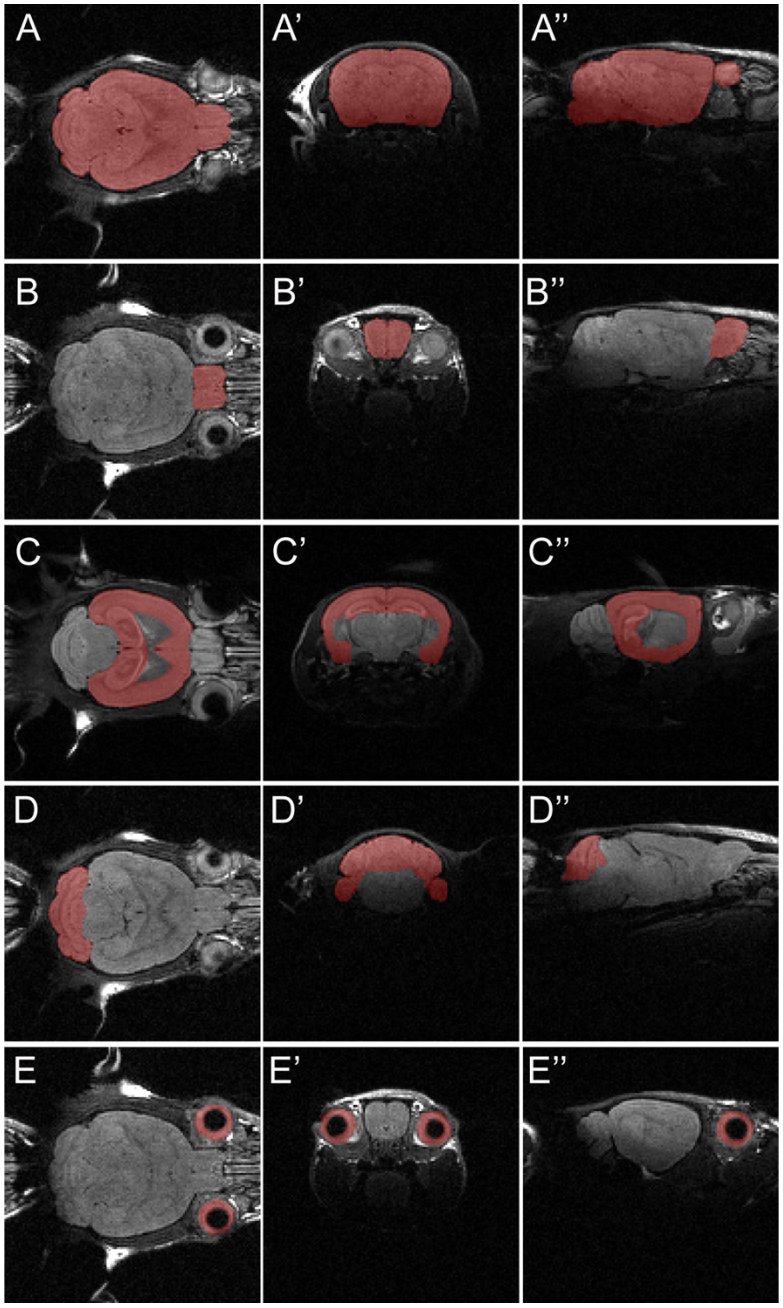

Figure 3.S.1: Representation of MRI masking. **A-E** Examples of how masking was conducted for MRI data for each structure we examined. All three axes are represented for each structure. **A** Whole brain. **B** Olfactory bulbs. **C** Cortex. **D** Cerebellum. **E** Eyes

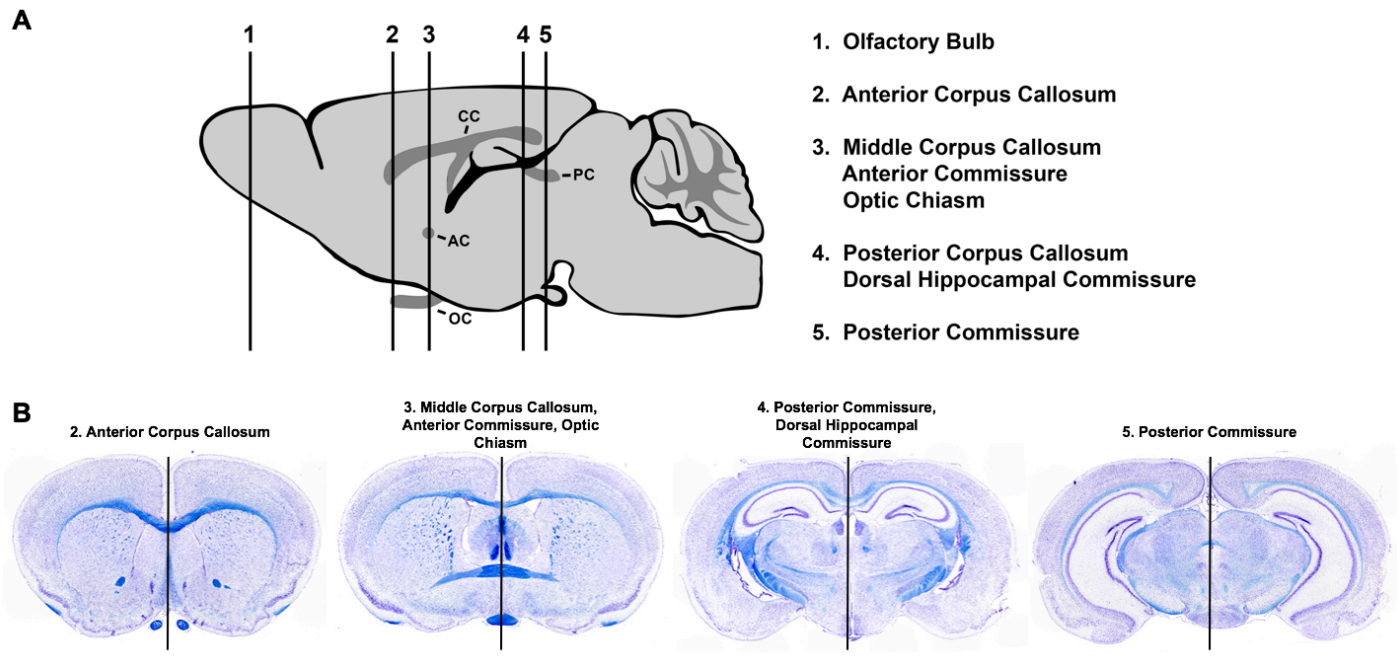

Figure 3.S.2: Histological section plane and location. A Mouse brain representing the plane of section for all histological sections and location in the brain each structure was measured. Structure location is noted with a number above the line on the mouse brain which correlates to the key at the right. **B** Representative histology sections for each of the areas measurements were taken. Black line shows where at midline each commissure measurement was taken

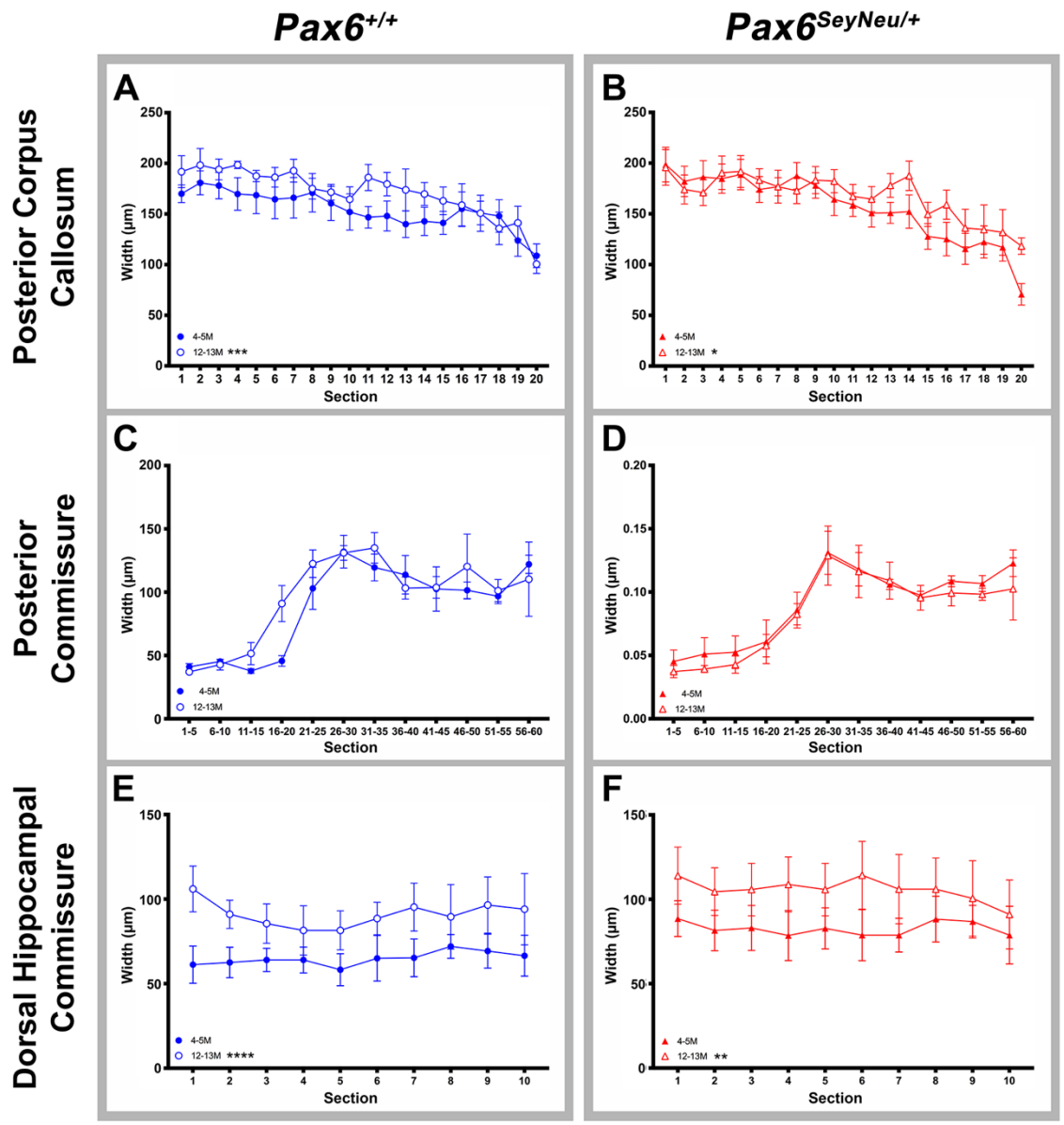

Figure 3.S.3: **Age-related changes to remaining structures not included in Figure 5**. Blue circles represent *Pax6*$^{+/+}$ and red triangles represent *Pax6*$^{SeyNeu/+}$. Closed circles and triangles represent the 4-5M group, and open circles and triangles represent the 12-13M group. Mean is represented as the point and standard error of the mean (SEM) is represented in bars above and below each mean. The y-axis is width of the structure at midline measured in millimeters. The x-axis is section number starting anteriorly (ex. 1) and moving posteriorly (ex. 20). Significance is

represented in figure legend with stars representing level of significance. **A, C, E,** *Pax6*$^{+/+}$ only comparisons with both age groups. **B, D, F,** *Pax6*$^{SeyNeu/+}$ only comparisons with both age groups. **A,B** Posterior corpus callosum is slightly thicker at the 12-13M age group in both *Pax6*$^{+/+}$ only and *Pax6*$^{SeyNeu/+}$ only comparisons. **C,D** No change was seen for either genotype in the posterior commissure as a function of age. **E,F** Both *Pax6*$^{+/+}$ only and *Pax6*$^{SeyNeu/+}$ only comparisons of the dorsal hippocampal commissure showed the 12-13M group as significantly thicker at midline

CHAPTER 4:

DISCUSSION AND CONCLUSION

4.1 PAX6 as a regulator of brain development and maintenance

Development and maintenance of the central nervous system is a highly important area of research. Developmentally, timing of cell specification and structural organization is imperative to the correct functioning of the brain. Maintenance of structures in adulthood is vital for the continued functioning of the brain, and breakdown of this leads to neurodegeneration in a variety of forms. Understanding the mechanisms surrounding neurogenesis in adulthood has the potential to lead to breakthroughs in central nervous system regeneration research. The coordination of normal development, organization and specification, and adult brain maintenance is highly dependent on transcription factors, such as PAX6. The *PAX6* gene is a necessary transcription factor for the development of the eyes and central nervous system. PAX6 is a complex gene with multiple promoters, at least three isoforms, and a complex regulation scheme. Because of the necessity of PAX6 during development, there has been a tremendous amount of research on the developmental consequences of loss of PAX6. We know from a multitude of research that absence of the gene in development leads to gross anatomical changes in the eye and the brain. Conditional knockout of Pax6 in the developing cortex of the mouse leads to both organizational and cell specification dysfunction. In addition to the roles it plays during development, we know that Pax6 is expressed in the central nervous system throughout adulthood, and its function in that capacity has been largely ignored [1].

Heterozygous loss-of-function of PAX6 is causal for the disorder aniridia in humans and *Small Eye* in the mouse. Aniridia is predominately known for its eye-related phenotypes such as iris absence or hypoplasia, cataracts, keratopathy, and glaucoma; however, recent evidence, both functional and structural, has pointed to central nervous system phenotypes. These include patient reports of issues such as sleep-wake cycle difficulties, hyposmia (or reduced sense of smell), sensitivity to pain, and difficulty paying attention in loud environments. These patient complaints led to the hypothesis that there may be structural changes within the brain of these patients that lead to the phenotypes. The studies conducted in this body of work aimed to understand the structural consequences in the brain of heterozygous loss-of-function of Pax6 in aniridia and our mouse model, *Small eye*. Here we showed that loss of one functional copy of *PAX6* does lead to structural changes in the brain of both aniridia patients and the mouse model of the disorder. We also show that these structural changes are relatively conserved in the mouse and are less severe than previously reported. Additionally, we show evidence for PAX6's role as a regulator of adult neurogenesis and plasticity within the central nervous system.

4.2 Structural changes in the brain of PAX6-mediated aniridia patients

Within the field of aniridia research, there has long been disagreement with the idea of a genotype-phenotype correlation where mutation can determine the phenotypes present. If the field can determine a genotype-phenotype correlation there is potential for much better patient care and symptom management in aniridia. Additionally, we know that there are functional abnormalities in the patient population, which include auditory processing deficits and sensory system problems; however, there has been little research aimed at understanding the underlying cause of these neurological changes seen. This study was motivated by two main things: (1) the benefit of adding a cohort of patients to the published literature to try to further investigate this

idea of genotype-phenotype correlations, which could lead to better patient care, and (2) better understanding of what structural changes are causing the functional outcomes in patients.

With regards to the genotype-phenotype correlation, studies focusing on eye phenotypes in patients have rarely been able to identify any correlation between type or severity of abnormalities with specific PAX6 mutations. It is assumed that for many PAX6 mutations (any that result in a premature termination codon), mutant transcripts are degraded through nonsense-mediated decay and the individual is rendered haploinsufficient for PAX6 [2]. Although this idea of nonsense-mediated decay is accepted as the mechanism happening in many aniridia cases, it has not been proven. This led to the hypothesis that there would be no discernable genotype-phenotype associations because most mutations would result in haploinsufficiency. If, however, nonsense-mediated decay was not occurring one would expect to see some mutations to lead to a much more severe phenotype in patients, especially if mutated protein was made that still retained its DNA binding abilities and could lead to dominant-negative effects. Our study was motivated by the need to understand if there is a genotype-phenotype correlation which could add to or reduce evidence for nonsense-mediated decay, and potentially help doctors in patient-specific treatment options for aniridia.

In the small number of studies conducted on structural changes in the brain of aniridia patients, there has been much variation with the findings. Some studies found severe phenotypes, such as absence of structures, while others reported more mild phenotypes such as small reductions to structures [3–7]. Group-wise analyses of volumetric changes in the brain have also discovered a variety of changes, but little consistency in those changes across studies. White matter and grey matter have been shown to both increase and decrease in certain areas of the brain in aniridia patients compared to PAX6-normal individuals [8, 9]. What does seem to be

consistent are the types of structural of changes seen within the brain of aniridia patients. These mostly include reductions in major interhemispheric white matter tracts such as the corpus callosum, anterior commissure, and posterior commissure. The studies that have focused on brain abnormalities in aniridia have mostly picked only a few structures on which to focus, leaving a gap in the full understanding of the disorder within the brain. The aim of this study was to gain a deeper understanding of the consequences of heterozygous loss-of-function of PAX6 in the adult brain using 3T structural MRI. We surveyed multiple structures that had previously been reported to be altered in aniridia. Furthermore, we analyzed a new population of aniridia patients with a variety of mutations in multiple gene loci that adds to the diversity of mutation analysis within the literature. Understanding the abnormalities in the aniridia brain will help us understand the functional consequences patients report with, and will assist in determining if and where early clinical intervention can be used.

In this study, we analyzed structural changes in the brain of 12 patients with aniridia and 12 PAX6-normal age and gender matched individuals. We found structural changes in five major structures: the anterior commissure, the posterior commissure, the corpus callosum, the optic chiasm, and the pineal gland. The most commonly altered structure in our population of aniridia patients was the anterior commissure, with every aniridia patient in our cohort having reductions to this structure. Previous studies looking at the anterior commissure found both reductions and the absence all together of the structure; however, we did not find any patients who were completely missing the structure [3–5, 8]. Our analysis of the posterior commissure revealed mild changes in aniridia patients compared to PAX6-normal individuals. Fewer than half of the patients we examined had reductions to the structure and in no patient was it missing. We did have one patient who appeared to have a reduction to the posterior commissure at midline with a

bulbous appearance on either hemisphere of the brain, suggesting a potential for incomplete commissure crossing at midline. This is particularly interesting because PAX6 is necessary for normal axonal midline crossing and necessary for normal formation of the posterior commissure [10]. This finding could be a direct consequence of loss of one functional copy of PAX6. Again, these findings in the posterior commissure in our patient cohort are relatively mild compared to those structural changes seen in previous studies [3, 8].

The pineal gland is reduced or absent in many our patients, which both agrees with previous reports and can explain some of the patient complaints of sleep cycle regulation. The corpus callosum was also analyzed in our patient population due to previous reports of major deficits in the structure [3, 4, 7]. We found very few patients with visible alterations to the corpus callosum, and the slight changes we do see fall within the expected population variation. Additionally, we conducted volumetric analysis of the corpus callosum and no change was seen in the aniridia patients compared to their PAX6-normal comparators. We found major reductions to the optic chiasm in greater than half of our patients. Reductions to this structure could be due to developmental deficits of PAX6 because of the major changes seen in the eye or could be due to a reduction of inputs from the eye as the disorder progresses and eyesight is increasingly compromised.

Our study revealed changes to similar structures as previously reported, however, at a lower degree of severity and number of affected individuals. One explanation of this could be the difference in structural MRI magnet strength used. A majority of the studies mentioned above used a 1.5T magnet, commonly found in hospitals. Our study used a 3T magnet which has almost double magnet strength and resolution as the 1.5T. Because of the relative size of the structures being analyzed it is possible that other studies called a structure “absent” where we

called it “reduced” due to this difference in resolution in our MRI data. Because of how small structures like the anterior and posterior commissure are, it is very likely that a major reduction to them could be seen as absence on a 1.5T MRI scan. It is also possible that the collective age of our group of patients, which ranged from 18 years old into the 60s, could have been a factor in the different structural findings. Accelerated age-related cortical thinning in aniridia patients has been shown in the Yogarajah 2016 paper, which suggests that the age of a patient group might affect the structural results [9]. The mean age of a patient population being studied might play a role in the findings from that study, especially since it has been shown that even in a healthy population, there are age-related reductions in commissures.

Group-wise comparisons of grey and white matter volume in studies have shown both reductions and increases in different regions of the brain, which has been explained as a global re-organization [8, 11]. Surprisingly, in these group-wise studies conducted with mostly voxel-based morphometry, structures such as the pineal, anterior commissure, and posterior commissure did not get picked up as statistically different in the aniridia population. Again, these studies used entirely different groups of patients with different mean ages and different mutations than our study. Even with the different patient population, this suggests that either the structural variation we see in our population is not as common as thought, or that there is a large variation in abnormalities in the global aniridia population.

This study found similar structural changes in aniridia patient brains as previously reported in the literature; however, our study revealed these changes were fewer and less severe. Our patient population included unique mutations that give more insight into the potential genotype-phenotype correlation in aniridia and a deeper understanding of mechanisms governing the functional changes seen. We did not see any structural changes that could be attributed to a

specific mutation, and this is specifically shown by the fact that we had three members from the same family that did not have the same structural changes. This study showed that structural changes within the aniridia population have a high level of variability, which could in part be due to modifier effects in humans that might contribute to the wide diversity of phenotypes that have been reported in aniridia. Our findings also indicate that there is likely both a developmental consequence of heterozygous loss-of function to PAX6 and an adult/maintenance role of the protein within the central nervous system. To be able to further investigate the role of Pax6 in the nervous system, we turned to the mouse model of the disorder, *Small Eye*. This model allows for a deeper investigation into the role of PAX6 for structural alterations in the brain while controlling for modifier effects and mutation type.

4.3 Structural findings from our mouse model of aniridia

Following our human study, we decided to turn to our mouse model of aniridia, *Small eye*. This model allows for a higher resolution examination of the consequences in the brain of heterozygous loss-of-function of Pax6. We were able to use similar techniques that we used on our human population, specifically structural MRI, while also utilizing a higher resolution sectioned histology approach to understand subtle differences in the brain that may not be detectable by MRI analysis. By combining the volumetric approach with a high-resolution approach, we found that our mouse model does indeed show similar structural changes as our human aniridia population, and moreover, the changes in the mouse are equally as subtle as the changes we see in our patients.

Like our aniridia study, we began the mouse study by conducting high-resolution structural MRI using a 7T magnet on $Pax6^{+/+}$ and $Pax6^{SeyNeu/+}$ mice in two different age groups, a 4-5M and a 12-13M group. Whole brain analyses assessed gross anatomical organization,

brain weight, and brain volume between genotypes and age groups. No gross anatomical changes existed between the *Pax6*$^{+/+}$ and *Pax6*$^{SeyNeu/+}$ mice in either age group. Brain weight was changed as a function of age but not genotype, with the older age group having lower brain weights. Brain volume was not changed across genotype or age, suggesting that density of the brain is changing. This could be due to many different things such as cell death, inability of adult neurogenesis, or reductions to connections within the brain.

After conducting whole-brain analyses we decided to move to a brain region-specific analysis of the major parts of the mouse brain still using our MRI data. We assessed volume of the olfactory bulbs, cortex, cerebellum, and eyes of all of our groups. Not surprisingly, eye volume was significantly reduced in the *Pax6*$^{SeyNeu/+}$ mice compared to *Pax6*$^{+/+}$ in both age groups. The olfactory bulbs, which we know express Pax6 in development and adulthood, were also reduced in the *Pax6*$^{SeyNeu/+}$ mice. This reduction in volume is expected, but what was interesting in the case of the olfactory bulb is the way the *Pax6*$^{SeyNeu/+}$ mice change during ageing compared to *Pax6*$^{+/+}$. In our volumetric analysis, we see that the *Pax6*$^{+/+}$ olfactory bulbs increase significantly in volume from the 4-5M age group to the 12-13M age group. The *Pax6*$^{SeyNeu/+}$ olfactory bulbs do not though, and stay at a very similar volume from the younger age to the older age group. This suggests a few things: first, that there is not the same neural plasticity in the *Pax6*$^{SeyNeu/+}$ brains as there is in the *Pax6*$^{+/+}$; second, *Pax6*$^{SeyNeu/+}$ mice might be starting out at a deficit like an aged *Pax6*$^{+/+}$ brain; and third, there is likely a reduction or inactivation of adult neural progenitor cells in the *Pax6*$^{SeyNeu/+}$ brain. The lack of volume increase seen in the *Pax6*$^{SeyNeu/+}$ mice are likely at least in part due to a reduction in the number or activity of neural progenitor cells within the subventricular zone of the brain. Neural progenitors that reside in the SVZ produce neuroblasts that migrate through the rostral migratory stream and end up in the

olfactory bulb. Therefore, there is an increase in volume as a function of age within the *Pax6*$^{+/+}$. The *Pax6*$^{SeyNeu/+}$ mice do not have that, suggesting a deficit in adult neurogenesis. Alternatively, this could also be a problem post progenitor cell stage where the newly born neurons do not accurately differentiate or find their final location. Either of these possibilities results in an absence of olfactory bulb increase in *Pax6*$^{SeyNeu/+}$ mice.

When we assessed cerebellum volume we found similar findings as in the olfactory bulb. There was not a tremendous change between genotypes within a specific age; however, if you look across ages, the *Pax6*$^{+/+}$ change and the *Pax6*$^{SeyNeu/+}$ do not. *Pax6*$^{+/+}$ cerebellum volume decreases as a function of age. This has been shown in a few studies to be caused in part by a reduction in the number of purkinje cells in the cerebellum [12]. The *Pax6*$^{SeyNeu/+}$ cerebellum though, does not change at all from the 4-5M group to the 12-13M group. Again, this lack of change suggests a reduction in neural plasticity within the brain of *Pax6*$^{SeyNeu/+}$ mice. It also suggests that the *Pax6*$^{SeyNeu/+}$ brains are more aged at the 4-5M group than we would expect for a normal brain. Cortex volume does not change across genotypes or age groups in our study; however, it is important to note that we do not have the resolution to parse apart cortex regional differences. There are significant organizational and cell specification problems in cortex-specific Pax6 knockout mice, so we could potentially be missing some subtle changes in the cortex with our MRI data [13, 14].

Histological analysis comparing the two genotypes in the two age groups revealed that across ages, the *Pax6*$^{SeyNeu/+}$ mice were not missing any structures that were present in *Pax6*$^{+/+}$, and any changes that were present were extremely subtle. To try to detect smaller changes we measured major commissures in the brains including the optic chiasm, corpus callosum, anterior commissure, posterior commissure, and dorsal hippocampal commissure. We found genotype-

specific changes to the optic chiasm, anterior corpus callosum, middle corpus callosum, and anterior commissure, where in most cases, but not all, the *Pax6*$^{SeyNeu/+}$ mice had reductions compared to *Pax6*$^{+/+}$. With genotype comparisons, it is interesting that the structures in the anterior portion of the brain were more heavily affected than posteriors structures. This is especially interesting when put into context of Pax6 expression during development, in which there is a high-rostral low-caudal gradient of Pax6 in the developing forebrain. Developmentally the most anterior structures likely require higher levels of Pax6 to develop normally, because in a *Pax6*$^{+/+}$ brain these anterior cells and tissues see this high level of Pax6. In contrast, as you move posteriorly in the *Pax6*$^{+/+}$ brain, the cells and tissues normally have less Pax6 during normal development. In the *Pax6*$^{SeyNeu/+}$ brain, which has half as much Pax6 as the *Pax6*$^{+/+}$, this gradient is likely shifted anteriorly with a global reduction to Pax6. Another way of looking at this is to divide the developing forebrain into three sections: the most anterior, the middle, and the most posterior. In *Pax6*$^{+/+}$ brains, the most anterior has the most Pax6 followed by the middle and then the most posterior, which has the lowest level of Pax6. In the *Pax6*$^{SeyNeu/+}$ brain, now instead of this normal Pax6 gradient, the most anterior third of the brain is seeing something likely more similar to the *Pax6*$^{+/+}$ brain middle portion, and then the *Pax6*$^{SeyNeu/+}$ brain middle portion is seeing something more like the *Pax6*$^{+/+}$ brain most posterior section. Because the normal developmental requirement is highest in the anterior third, this shift described would likely affect the anterior structures the most while leaving posterior structures less affected because they do not require high levels of Pax6 to begin with. This "gradient shift" hypothesis is likely explained by regional differences in Pax6 binding affinity and concentration requirements of all three isoforms of the protein for specification of tissues. There is a lot that still needs to be investigated in this area, and future research should aim at gaining a deeper understanding of this idea.

The anterior bias of the changes seen in major commissures can be explained by developmental consequences of Pax6. But we also must consider the age-related changes seen in the *Pax6*$^{SeyNeu/+}$ brains. As mentioned in the volumetric analysis, in the *Pax6*$^{SeyNeu/+}$ structures there seems to be lack of change as a result of ageing compared to *Pax6*$^{+/+}$. This effect is also seen in the histology measurements. The optic chiasm, anterior corpus callosum, and anterior commissure are changed differently in the *Pax6*$^{SeyNeu/+}$ brain compared to *Pax6*$^{+/+}$ during ageing. The *Pax6*$^{+/+}$ optic chiasm increases significantly with age while the *Pax6*$^{SeyNeu/+}$ stays almost the same in both age groups. Within the anterior corpus callosum we see an increase in *Pax6*$^{+/+}$ width as a function of age; however, in the *Pax6*$^{SeyNeu/+}$ mice there is a decrease in anterior corpus callosum thickness as a function of age. And like the optic chiasm, the anterior commissure in the *Pax6*$^{+/+}$ mice increases with age, but there is no change between age groups in the *Pax6*$^{SeyNeu/+}$ anterior commissure.

The genotype comparisons taken with the age-related differences in the *Pax6*$^{SeyNeu/+}$ brain collectively suggests that Pax6 plays a role both in development, but maybe much more prominently that previously thought, in adult brain maintenance. Changes in volume in the *Pax6*$^{SeyNeu/+}$ mice suggest overall reductions to plasticity in the *Pax6*$^{SeyNeu/+}$ brain and a reduction to either numbers or activity of progenitor cells in neurogenic niches within the adult brain. Histological analyses show a likely developmental result of heterozygous loss-of-function in Pax6, but at very subtle levels. There were no structures severely affected, and most structures were normal with only slight reductions to thickness. The more interesting part of this study has been the age-related differences in *Pax6*$^{SeyNeu/+}$ brains compared to *Pax6*$^{+/+}$, which suggests that the role of Pax6 in the brain continues into adulthood plays a significant role in adult neural plasticity.

4.4 Conclusions

It is evident from both studies in this body of work that structural changes within PAX6 heterozygous loss-of-function mammals are far less severe than originally thought. Our studies on patients and the mouse model of the disorder found changes to major fiber tracts in the brain, but found that these changes were not severe; most structures were formed normally and only had slight reductions in thickness. The relative normalcy of the PAX6-deficient brain is shocking. PAX6 is necessary for development of the mammalian brain and eyes, and in homozygous mutants there are severe malformations. This study shows that in the heterozygous state, the brain forms relatively normally with no major issues to gross anatomy or organization. We show that when we look at a more magnified level within the mouse there are small changes in the brain mostly to interhemispheric commissures. This suggest that we could potentially be missing the subtle changes present in aniridia patients because of the resolution of current imaging paradigms. This body of work has shown the utility of using an animal model to help with hypothesis generation for the human population. We see similar results in our mouse model and our aniridia population which proves that at least within the brain, the *Small eye* mouse is a useful tool for understanding the intricacies of aniridia. These studies also hint at a general lack of genotype-phenotype correlation as our patients (who had a variety of mutations) and our mouse model (which all had the same mutation) showed similar structural results. Additionally, the mouse model has further shown the utility of separating age groups for analysis, which is useful knowledge for future patient work.

Using our mouse model of aniridia, we showed not only genotype-specific changes in the adult brain but also age-related changes between $Pax6^{+/+}$ and $Pax6^{Pax6SeyNeu/+}$ mice. Interestingly, it seems that plasticity is altered in the $Pax6^{Pax6SeyNeu/+}$ brain compared to $Pax6^{+/+}$. This was

evidenced by the lack of change during the ageing process in the *Pax6*$^{Pax6SeyNeu/+}$ brain. This could be explained by a few different mechanisms. First, we know Pax6 is necessary for progenitor cell maintenance within the developing mouse brain. The apparent lack of olfactory bulb volume increase as a function of age that we see in our *Pax6*$^{Pax6SeyNeu/+}$ mice could be due to a reduction in number or activity of the progenitor cell population within the subventricular zone of the adult mouse. Second, and alternatively, this change could be a result of the necessity of Pax6 during differentiation of neurons within the brain. It can be hypothesized that if Pax6 is necessary for proper neural fates during development, then a reduction in Pax6 would lead to a reduction in normal differentiation. So potentially the lack of changes in the mouse brain could be a result of improper differentiation of neurons. Third, it is possible that our age-related differences in the genotypes could be an accelerated ageing phenotype. In the human population it was shown that there is an age-related acceleration in cortical thinning [9]. This could be happening in our mouse model as well, where the younger *Pax6*$^{Pax6SeyNeu/+}$ mice have a brain more similar to the older *Pax6*$^{+/+}$ group resulting in less plasticity from the beginning. These ideas could be tested in our aniridia mouse model. For testing the hypothesis of progenitor cell maintenance, we could use markers of progenitor cells in the *Pax6*$^{Pax6SeyNeu/+}$ brain compared to *Pax6*$^{+/+}$ to investigate total numbers of progenitors. Additionally, cell proliferation markers could be used to assess the total capacity for self-renewal and/or daughter cell generation in the *Pax6*$^{Pax6SeyNeu/+}$ brain compared to *Pax6*$^{+/+}$ brain. Proper differentiation and migration could also be assessed in our mouse model. All of these potential mechanisms of change could help us to discover new ways of looking at treatment for aniridia patients not only for the central nervous system, but also for the eyes.

PAX6 has traditionally been thought of as a developmental gene, which it is, but the results from these studies suggest that it also plays a role in maintenance and plasticity within the adult brain. In addition, researchers have collectively thought of aniridia as a developmental disorder with progressive phenotypes; however, I believe that our studies have shown that perhaps we should start thinking about aniridia as having maintenance and accelerated ageing phenotypes more than just developmental. Even within the eyes of aniridia patients, many of the phenotypes we see are also age-related phenotypes (glaucoma, cataracts, lens opacification). These things could represent increased ageing and decreased progenitor cell activity. Furthermore, most of the structural components of both the eye and brain do actually form normally with half as much PAX6 as one should have. This suggests that development progresses in a relatively normal fashion for aniridia patients and *Small eye* mice. Clearly neither the humans nor the mice need wild-type levels of PAX6 to make most of the structures of the brain that we assessed; however, there is a need for normal levels for progenitor cell maintenance and neural plasticity. It is possible that the brain of PAX6-deficient mammals is more sensitive to ageing: potentially through progenitor cell maintenance issues or normal differentiation and migration issues. The level of PAX6 might be more important for these roles compared to developmental roles, which leads to a sharp decrease in adult neurogenesis.

In addition to everything mentioned above, we as a field, largely ignore the fact that there are at least three isoforms of Pax6: canonical Pax6, Pax6-5a, and Pax6(ΔPD). It has been shown that these isoforms have different DNA binding abilities, and likely regulate different genes during development. As such, all three isoforms potentially have different protein level requirements, localization, and roles during both development and maintenance of the central nervous system and eye. One of these isoforms could potentially be more necessary for

progenitor cell maintenance, and one isoform more important for neural differentiation. Additionally, each isoform may have different cell requirements of levels for its action, so reduction by half may not be as detrimental for one isoform as it is for the other. Finally, within the human population there are many different types of mutations, and the location of the mutation might affect which isoforms are haploinsufficient. There is a potential for Pax6(ΔPD) to be made even if the other two isoforms are not. Depending on the specific role that this isoform plays, it might mitigate or increase severity of symptoms.

If we stop viewing aniridia as mostly developmental, and start looking at it from a different view point, we can start to investigate many new possibilities for early intervention, drug targets, and gene therapy. I think the biggest gain from these studies is now we can start to look at the aniridia in a new way. We can start to be creative with treatments that might change the way the disorder is seen in the medical field. Not only did we uncover a new set of hypotheses for the role of PAX6 in the adult brain, but we also shed some light on the potential for neurogenesis in the fully formed adult brain. Researchers have for some time been trying to identify ways in which the mammalian brain can regenerate neurons that have been lost in a myriad of ways such as TBI, degeneration, or stroke. PAX6 might play a pivotal role in adult neurogenesis and neural plasticity, and understanding its unique roles in the central nervous system is vital to understanding how the brain works.

4.5 References

1. Duan D, Fu Y, Paxinos G, Watson C (2013) Spatiotemporal expression patterns of Pax6 in the brain of embryonic, newborn, and adult mice. Brain Struct Funct 218:353–372. doi: 10.1007/s00429-012-0397-2
2. Tzoulaki I, White IM, Hanson IM (2005) PAX6 mutations: genotype-phenotype correlations. BMC Genet 6:27. doi: 10.1186/1471-2156-6-27
3. Bamiou DE, Free SL, Sisodiya SM, et al. (2007) Auditory interhemispheric transfer deficits, hearing difficulties, and brain magnetic resonance imaging abnormalities in children with congenital aniridia due to PAX6 mutations. Arch Pediatr Adolesc Med 161:463–469. doi: 10.1001/archpedi.161.5.463
4. Bamiou DE, Musiek FE, Sisodiya SM, et al. (2004) Deficient auditory interhemispheric transfer in patients with PAX6 mutations. Ann Neurol 56:503–509. doi: 10.1002/ana.20227
5. Sisodiya SM, Free SL, Williamson KA, et al. (2001) PAX6 haploinsufficiency causes cerebral malformation and olfactory dysfunction in humans. Nat Genet 28:214–216. doi: 10.1038/90042
6. Mitchell TN, Free SL, Williamson KA, et al. (2003) Polymicrogyria and absence of pineal gland due to PAX6 mutation. Ann Neurol 53:658–663. doi: 10.1002/ana.10576
7. Abouzeid H, Youssef MA, ElShakankiri N, et al. (2009) PAX6 aniridia and interhemispheric brain anomalies. Mol Vis 15:2074–83.
8. Free SL, Mitchell TN, Williamson KA, et al. (2003) Quantitative MR image analysis in subjects with defects in the PAX6 gene. Neuroimage 20:2281–2290.
9. Yogarajah M, Matarin M, Vollmar C, et al. (2016) PAX6 , brain structure and function in

human adults: advanced MRI in aniridia. Ann Clin Transl Neurol. doi: 10.1002/acn3.297

10. Mastick GS, Davis NM, Andrew GL, Easter Jr. SS (1997) Pax-6 functions in boundary formation and axon guidance in the embryonic mouse forebrain. Development 124:1985–1997.

11. Ellison-Wright Z, Heyman I, Frampton I, et al. (2004) Heterozygous PAX6 mutation, adult brain structure and fronto-striato-thalamic function in a human family. Eur J Neurosci 19:1505–12. doi: 10.1111/j.1460-9568.2004.03236.x

12. Woodruff-Pak DS, Foy MR, Akopian GG, et al. (2010) Differential effects and rates of normal aging in cerebellum and hippocampus. Proc Natl Acad Sci U S A 107:1624–9. doi: 10.1073/pnas.0914207107

13. Piñon MC, Tuoc TC, Ashery-Padan R, et al. (2008) Altered molecular regionalization and normal thalamocortical connections in cortex-specific Pax6 knock-out mice. J Neurosci 28:8724–34. doi: 10.1523/JNEUROSCI.2565-08.2008

14. Tuoc TC, Radyushkin K, Tonchev AB, et al. (2009) Selective cortical layering abnormalities and behavioral deficits in cortex-specific Pax6 knock-out mice. J Neurosci 29:8335–49. doi: 10.1523/JNEUROSCI.5669-08.2009